

**BIOELECTROCHEMICALLY-ASSISTED ANAEROBIC
DIGESTION FOR BIOGAS UPGRADING AND ENHANCED
METHANE PRODUCTION**

A Dissertation
Presented to
The Academic Faculty

by

Zeou Dou

In Partial Fulfillment
of the Requirements for the Degree
Master of Science in Environmental Engineering in the
School of Civil and Environmental Engineering

Georgia Institute of Technology
August 2017

COPYRIGHT © 2017 BY ZEOU DOU

**BIOELECTROCHEMICALLY-ASSISTED ANAEROBIC
DIGESTION FOR BIOGAS UPGRADING AND ENHANCED
METHANE PRODUCTION**

Approved by:

Dr. Spyros G. Pavlostathis, Advisor
School of Civil and Environmental Engineering
Georgia Institute of Technology

Dr. Ching-Hua Huang
School of Civil and Environmental Engineering
Georgia Institute of Technology

Dr. Sotira Yiacoumi
School of Civil and Environmental Engineering
Georgia Institute of Technology

Date Approved: May 11, 2017

ACKNOWLEDGEMENTS

I would like to express my sincere gratitude to Dr. Spyros G. Pavlostathis for his support and guidance. He has been an enlightening and kind advisor always willing to communicate and share his experience and knowledge. I genuinely appreciate the opportunity he offered me to work with him on this research, which has been and will always be a memorable and rewarding experience for me. He cares for students not only in academic sphere but also to the extent of their self-improvement as growing individuals. I would also like to thank my thesis committee members, Dr. Ching-hua Huang and Dr. Sotira Yiaccoumi, for their time and valuable feedback.

I would like to thank Christy Dykstra for her kind help and training throughout my research. I genuinely appreciate all her effort and time spent on taking care of instrumentation and equipment in the lab. I wish I could have been of more help to her. She has been a super lab manager and co-advisor to me. I would also like to thank Dr. Guangxuan Zhu for his technical support with equipment in the lab.

Additionally, I would like to thank staffs working in the School of Civil and Environmental Engineering, Robert Simon and Jessica Brown, with whose help my graduate student life on campus has been really smooth.

Last but not least, I would like to express my gratitude to my family, without whose support and love I would not be here.

TABLE OF CONTENTS

	Page
ACKNOWLEDGEMENTS	iii
LIST OF TABLES	vi
LIST OF FIGURES	vii
SUMMARY	xi
INTRODUCTION	1
BACKGROUND	5
3.1 Anaerobic Digestion	5
3.1.1 Anaerobic Digestion Fundamentals	5
3.1.2 Biogas Upgrading	7
3.2 Bioelectrochemical Systems	9
3.2.1 Microbial Electrolysis Cells	9
3.2.2 BES-AD Integrated Systems	11
GENERAL ANALYTICAL METHODS	14
3.1 pH	14
3.2 Chemical Oxygen Demand (COD)	14
3.3 Total and Volatile Solids (TS and VS)	15
3.4 Total Gas Production	15
3.5 Gas Composition	16
3.6 Volatile Fatty Acids (VFAs)	16
3.7 Cyclic Voltammetry	17
CHARACTERIZATION OF ABIOTIC SYSTEMS	18
4.1 Introduction	18
4.2 Materials and Methods	19
4.2.1 Water Electrolysis in Abiotic Systems	19
4.2.2 CV Tests on Abiotic Systems	20
4.3 Results and Discussion	20
4.3.1 Hydrogen Evolution	20
4.3.2 CV Tests	23
4.4 Summary	25
INTEGRATED ANAEROBIC SYSTEMS FOR BIOGAS UPGRADING AND ENHANCED METHANE PRODUCTION	26
5.1 Introduction	26
5.2 Materials and Methods	27
5.2.1 Ultimate Biodegradability	27

5.2.2	Anaerobic Digester Development and Operation	30
5.2.3	Gas Recirculation	31
5.2.4	Effect of Increasing Organic Loading	32
5.2.5	BES-AD Integrated System Development	32
5.2.5.1	Phase I: Application of 2.5 V on R3A	33
5.2.5.2	Phase II: Application of a range of voltages on R3B	33
5.2.5.3	Phase III: Application of 1.6, 2.0, and 2.5 V on R3C (titanium anode collector)	34
5.3	Results and Discussion	35
5.3.1	Ultimate Biodegradability	35
5.3.2	Performance of Anaerobic Digester and Integrated System	41
5.3.3	Gas Recirculation	52
5.3.4	Performance of AD and AD-Biofilm Systems Under Increasing Organic Loading	58
5.3.5	Performance of Closed Circuit BES-AD System	62
5.3.5.1	Phase I: Effect of 2.5 V on the performance of R3A	62
5.3.5.2	Phase II: Effect of a range of voltages on the performance of R3B	67
5.3.5.3	Phase III: Effect of a range of voltages on the performance of R3C	77
5.4	Summary	91
	CONCLUSIONS AND RECOMMENDATIONS	93
	REFERENCES	97

LIST OF TABLES

	Page
Table 1.1 Combustion enthalpy of different biofuels produced by fermentation of glucose	2
Table 4.1 Comparison of electrochemical properties of titanium with stainless steel ^a	19
Table 4.2 Current and H ₂ content before and after 1 hour at 1.6, 2.0, and 2.5 V in the abiotic reactor with titanium or stainless steel collectors	22
Table 4.3 Anode and cathode potential at 1.6, 2.0, and 2.5 V cell voltage using titanium as anode collector and stainless steel as cathode collector	22
Table 5.1 Composition of the anaerobic culture medium	29
Table 5.2 Composition of vitamin stock solution	29
Table 5.3 Composition of trace metals stock solution	29
Table 5.4 Results of the batch ultimate digestibility test (after seed blank correction) ^a	39
Table 5.5 TS and VS concentrations in R1 and R2 during the first 89 days of operation	49
Table 5.6 Characteristics of R1 and R2 under stable performance ^a	50
Table 5.7 pH and CO ₂ before and after CO ₂ addition to the gas phase of R1 and R2	58

LIST OF FIGURES

		Page
Figure 2.1	Schematic of a BES-AD system resulting in CH ₄ production	13
Figure 4.1	CV test on abiotic reactor with Ti-anode, Ti-cathode (A), Ti-anode, SS-cathode (B), and SS-anode, SS-cathode (C)	24
Figure 5.1	Cumulative gas production in biodegradability test batch reactor (seed blank corrected; gas data at 22°C and 1 atm)	38
Figure 5.2	Cumulative CH ₄ production in biodegradability test normalized to initial total D/P COD	38
Figure 5.3	CH ₄ _COD/Initial degradable COD versus time ($k = \text{mean estimate} \pm \text{standard error}$)	39
Figure 5.4	Fraction of degradable COD destruction in a batch reactor and a CSTR as a function of incubation time and HRT, respectively ($k = 0.133 \text{ d}^{-1}$)	40
Figure 5.5	Biogas production in R1 (A) and R2 (B) over 3-day and 4-day feeding cycles during the first 72 days of operation	43
Figure 5.6	Total COD (A), soluble COD (B), VFAs (C), and pH (D) at the end of each feeding cycle in R1 and R2 during the first 72 days of operation	44
Figure 5.7	VFA species over a 4-day feeding cycle in R1 (A) and R2 (B). Error bars represent mean values \pm one standard deviation, $n = 3$	45
Figure 5.8	Soluble COD profile (A), total biogas production (B), and CH ₄ and CO ₂ content (C) over the course of the 4-day feeding cycle after 173 days of operation. Error bars represent mean values \pm one standard deviation, $n = 3$. Standard deviations less than 1% are not shown	47

Figure 5.9	VFA species in R1 (A) and R2 (B) over the 4-day feeding cycle after 173 days of operation. Error bars represent mean values \pm one standard deviation, $n = 3$. Standard deviations less than 1% are not shown	48
Figure 5.10	Soluble COD profile (A), total biogas production (B), and CH ₄ and CO ₂ content (C) over the course of the 4-day feeding cycle under gas recirculation after 319 days of operation. Error bars represent mean values \pm one standard deviation, $n = 3$. Standard deviations less than 1% were not shown	55
Figure 5.11	VFAs profile in R1 (A) and R2 (B) over the course of the 4-day feeding cycle under gas recirculation after 319 days of operation. Error bars represent mean values \pm one standard deviation, $n = 3$. Standard deviations less than 1% were not shown	56
Figure 5.12	Volume of CO ₂ and CH ₄ over two days after CO ₂ addition to the gas phase of R1 (A), and R2 (B) (Both reactors were maintained under starvation)	57
Figure 5.13	Soluble COD profile (A), pH profile (B), and CH ₄ and CO ₂ content (C) in R1 and R2 under 1X, 2X, and 4X organic loading condition	60
Figure 5.14	VFAs profile in R1 (A) and R2 (B) under 1X, 2X, and 4X organic loading condition	61
Figure 5.15	CH ₄ production after 4X feeding over 14 days of incubation in R1 and R2	61
Figure 5.16	pH (A), total and soluble COD before and after feeding (B), and biogas production over 3-day and 4-day feeding cycles (C) in R3A from 33 to 54 days of operation (2.5 V applied on day 47)	63
Figure 5.17	VFAs in R3A during operation from day 32 to 53 (2.5 V applied on day 47). Error bars represent mean values \pm one standard deviation, $n = 3$. Standard deviations less than 1% were not shown	64
Figure 5.18	CO ₂ , CH ₄ , and H ₂ in the headspace of R3A during operation from day 36 to 65 (2.5 V applied on day 47)	66
Figure 5.19	Current profile of R3A at 2.5 V (from day 51 to 75)	66

Figure 5.20	Soluble COD (A) and CH ₄ production (B) over a 4-day feeding cycle of R3B under open circuit, 0.5 V, and 1.1 V	68
Figure 5.21	VFAs over a 4-day feeding cycle of R3B at 1.1 V. Error bars represent mean values \pm one standard deviation, n = 3. Standard deviations less than 1% were not shown	70
Figure 5.22	Current profile of R3B at 0.5 V (from day 145 to 156) and 1.1 V (from day 164 to 175)	70
Figure 5.23	pH profile in R3B at 2.0 V (day 190 to 197) and 1.6 V (day 197 to 208)	72
Figure 5.24	Soluble COD (A), biogas CH ₄ and CO ₂ content (B), and CH ₄ production (C) over two 4-day feeding cycles of R3B at 2.0 V (day 187 to 198) and one 4-day cycle at 1.6 V (day 201 to 205). Error bars represent mean values \pm one standard deviation, n = 3. Standard deviations less than 1% were not shown	75
Figure 5.25	VFAs over the second 4-day feeding cycle of R3B at 1.6 V (from day 201 to 205). Error bars represent mean values \pm one standard deviation, n = 3. Standard deviations less than 1% were not shown	76
Figure 5.26	Current profile of R3B at 2.0 V (from day 185 to 194) and 1.6 V (from 201 to 205)	76
Figure 5.27	Soluble COD (A), biogas production (B), biogas CH ₄ and CO ₂ content (C), and pH (D) in R3C at 1.6, 2.0, and 2.5 V. Error bars represent mean values \pm one standard deviation, n = 3. Standard deviations less than 1% were not shown	79
Figure 5.28	VFAs in R3C at 1.6, 2.0, and 2.5 V. Error bars represent mean values \pm one standard deviation, n = 3	80
Figure 5.29	Current profile of R3C at 1.6 V (from day 311 to 315), 2.0 V (from day 318 to 322), and 2.5 V (from day 325 to 329)	81

Figure 5.30	Soluble COD (A), biogas production (B), gas composition (C), and pH (D) in R3C before (I) and after (II) transferring out the suspended biomass, under gas recirculation (III), 2X (IV), and 4X (V) organic loading. Error bars represent mean values \pm one standard deviation, $n = 3$. Standard deviations less than 1% were not shown	86
Figure 5.31	VFAs before (I) and after (II) transferring out the suspended biomass, under gas recirculation (III), 2X (IV), and 4X organic loading (V). Error bars represent mean values \pm one standard deviation, $n = 3$	87
Figure 5.32	Current before (I) and after (II) transferring out the suspended biomass, under gas recirculation (III), 2X (IV), and 4X organic loading (V)	87
Figure 5.33	CH ₄ and CO ₂ in the headspace of R3C under starvation over two days after 650 mL of CO ₂ was introduced to its headspace	88
Figure 5.34	CV runs on R3C after 1 (A), 2 (B), and 3 (C) days of incubation under conditions of normal (i.e., 1X) organic loading	90

SUMMARY

Biogas produced by anaerobic digestion (AD) is a promising renewable alternative energy source, which may lead to the realization of carbon neutral, zero net energy wastewater treatment plants (WWTP). Upgrading is necessary to increase the biogas methane (CH_4) content for its use in commercial and industrial applications. Bioelectrochemically assisted anaerobic digestion (BES-AD) is an emerging technology capable of increasing CH_4 production through biogas upgrading by converting carbon dioxide (CO_2) to CH_4 . Although BES-AD technology for in situ biogas upgrading is receiving increasing attention due to its small footprint and low capital cost, little is known about the role of electrode-attached biofilm in BES-AD systems relative to the production of CH_4 . Moreover, the relation between the biofilm and externally added voltage, which is critical for successful start-up and operation of BES-AD systems, remains unclear. The overall goal of this research was to upgrade the biogas produced from anaerobic digestion through integration with BES and to improve the understanding of limiting factors on the performance of BES-AD integrated systems. The specific objectives of this research were to:

1. Improve the CH_4 content in the biogas produced from anaerobic digestion by adding electrodes and voltage.
2. Demonstrate the effect of biofilm on anaerobic digestion in the integrated AD system.
3. Investigate the significance of CO_2 mass transfer in biogas upgrading using the BES-AD system.

4. Investigate the relation between applied voltage and biofilm development in the BES-AD system.
5. Assess the resilience of integrated AD reactors to shock, high organic loading.

To demonstrate the effect of biofilm on anaerobic digestion, one conventional AD (R1) and one AD with two electrodes for biofilm formation (R2) were developed and operated throughout the study. After both reactors reached stable performance, the COD consumption and CH₄ production in R2 were occurring at a much higher rate than in R1, which was attributed to the efficient interspecies substrate transfer through the network of diverse microorganisms in the biofilm. Gas recirculation was applied to both reactors to improve the mass transfer of CO₂ in order to provide more HCO₃⁻ for hydrogenotrophic methanogens to produce CH₄. The CH₄ content in the headspace of both reactors increased, while only in R2 the net CH₄ production was higher compared to when gas recirculation was not applied. Combining with the results of external CO₂ addition conducted later, the increase of CH₄ content in the headspace of R1 was attributed to the dissolution of CO₂ resulting from enhanced contact area and time between gas and liquid phase under gas recirculation. In contrast, within the biofilm of R2 hydrogenotrophic methanogens effectively utilized H₂ through interspecies syntrophic interactions, converting available carbonate species (i.e., HCO₃⁻) to extra CH₄ even under starvation, which was demonstrated by the CO₂ addition/dissolution test. Thus, CO₂ transfer is critical for the biogas upgrading process taking place in the BES-AD reactor. To assess the resilience of the AD reactors to shock, high organic loading, double (2X) and four times (4X) of organic loading was applied to R1 and R2. With the biofilm providing efficient oxidation of organic matter through mechanisms described above, accumulation of volatile fatty acids (VFAs)

leading to acidification observed in R1 did not occur in R2. Therefore, biofilm contributes significantly to the resilience of hybrid (i.e., suspended- and attached-biomass) anaerobic digestion systems to sudden increases in high organic loadings (i.e., shock loads).

To investigate the relation between biofilm development and applied voltage, start-up and operation of a third BES-AD reactor (R3) were conducted in three phases (reactor notation R3A, R3B, R3C, respectively). In phase I, voltage of 2.5 V was applied to R3A, which severely inhibited the metabolism of the mixed microbial community biofilm. An increase in pH above 8.0 and significant H₂ evolution were observed in R3A. Moreover, corrosion of the stainless steel anode collector at the gas/liquid interface led to the failure of R3A. Lower voltages were applied to R3B in phase II. No CH₄ production improvement was observed in R3B at low voltages of 0.5 and 1.1 V, probably due to the low electron capture efficiency at the cathode by methanogens and the limited electrons transferred to the cathode. Voltage of 2.0 V improved both the CH₄ production and the CH₄ content in the produced biogas in R3B through electromethanogenesis directly utilizing electrons and through hydrogenotrophic methanogenesis using H₂ produced from water electrolysis. However, corrosion of the stainless steel anode collector occurred again. Iron from the stainless steel collector was leached into the medium of the BES-AD reactor, which might have exerted a positive effect on anaerobic digestion.

In contrast to R3A and R3B, R3C was developed from the beginning at a constant voltage of 1.1 V to investigate the effect of voltage on biofilm development. Compared with the performance of R3B at a voltage of 1.1 V, the net CH₄ production of R3C was lower and the extra CH₄ production observed in R2 during the external CO₂ addition/dissolution test was not observed in R3C, indicating compromised biofilm

development in R3C under the influence of voltage. Considering the advantages of the biofilm in the BES-AD system and the inhibitive effect of voltage on biofilm formation on the electrodes, applying voltage after the system has obtained substantial biomass on its electrodes or using pre-inoculated and enriched bioelectrodes is a preferable procedure for a successful start-up and operation of BES-AD systems.

Given the results of water electrolysis and cyclic voltammetry (CV) tests run on an abiotic reactor, 2.0 V and titanium anode collector and stainless steel cathode collector were determined as the best combination for the operation of the BES-AD reactor used in this study. In this configuration, the CH₄ production was remarkably increased, while significant biogas upgrading was not observed in R3C, which was attributed to the absence of water electrolysis constantly providing H₂ for the conversion of CO₂ to CH₄ through hydrogenotrophic methanogenesis in the biotic system (R3C). R3C returned to its stable performance shortly after acidification caused by a shock organic load.

This research improves our understanding of the role of biofilm and voltage in bioelectrochemical processes. In BES-AD systems, the applied external voltage results in water electrolysis providing H₂ for hydrogenotrophic methanogenesis and promotes electromethanogenesis utilizing electrons and CO₂ to produce CH₄ leading to biogas upgrading. Meanwhile, the biofilm attached to the conductive electrodes provides effective interspecies substrate and electron transfer through syntrophic interactions between fermentative and electroactive microorganisms stimulated by the applied voltage. Such conditions may result in a higher extent of fermentation and acidogenesis leading to enhanced CH₄ production. However, due to the inhibitive effect of voltage on the development and metabolism of the biofilm, specific start-up and operation protocols are

needed for BES-AD systems. This study also demonstrates the significance of CO₂ mass transfer for biogas upgrading in BES-AD systems, for which biogas recirculation may be necessary. Overall, this study provides insights into the relation between biofilm and voltage in BES-AD systems, which is essential for successful start-up and operation of BES-AD systems aiming in the production of enhanced biogas production with a high CH₄ content.

CHAPTER 1

INTRODUCTION

The increasing demand for energy and the draining of traditional fossil fuel drive the development of renewable energy technologies. Anaerobic digestion (AD), as a well-established process capable of converting organic waste into biogas (60–70% v/v CH₄) (Appels et al., 2008), appears to be preeminent among all alternatives, especially in the pursuit of self-sustainable, carbon neutral, net zero energy wastewater treatment plants (WWTP). With its advantages, including low volume of final sludge solids for disposal, low energy requirement, and energy recovery, anaerobic digestion is considered a major and essential part of a modern WWTP (Chen et al., 2008). In spite of all the benefits, the potential for further optimization of anaerobic digestion is still high, particularly in terms of energy recovery. The energy recovery in terms of heat of combustion from three alternative biofuels, i.e., CH₄, ethanol, and H₂, produced from the fermentation of glucose is shown in **Table 1.1**. Based on these heat of combustion values, H₂ and CH₄ production yield 38 and 94% of energy, respectively, compared to ethanol. In addition, the CO₂ content in the raw biogas from anaerobic digestion significantly compromises the sustainability of AD and severely restrains the commercial use of biogas, which has made biogas upgrading increasingly essential for its use in industrial, commercial, and transportation applications. Multiple methods, including chemical scrubbing, physical separation, and biological consumption have been developed to decrease the biogas CO₂ content. However, high

energy and chemical input, as well as capital cost have always been the major concerns for these typical biogas upgrading processes (Muñoz et al., 2015).

Table 1.1. Heat of combustion of different biofuels produced by fermentation of glucose

Biofuel	Stoichiometric equation	Heat of combustion ^{a,b} (kJ/mol glucose)
Methane	$C_6H_{12}O_6 \rightarrow 3 CH_4 + 3 CO_2$	2407
Ethanol	$C_6H_{12}O_6 \rightarrow 2 C_2H_6O + 2 CO_2$	2555
Hydrogen	$C_6H_{12}O_6 + 2 H_2O \rightarrow 4 H_2 + 2 CO_2 + 2 CH_3COOH$	967

^a Lower heating value calculated from enthalpy of formation of combustion species (25°C and 1 atm)

^b Enthalpy values from McAllister et al., 2013

A bioelectrochemical system (BES) consists of a bioreactor equipped with anode and cathode electrodes on which exoelectrogenic and electrotrophic microorganisms colonize, respectively. The bioelectrodes with microorganisms as catalyst can act as the electron sink (anode) or donor (cathode) in redox reactions taking place in the bioreactor. The fundamental mechanism behind BES is extracellular electron transfer (EET) (Lovley and Phillips, 1988; Myers and Nealson, 1988), which allows electron flow from the anode through an external circuit to the cathode. Microbial fuel cells (MFCs) were first developed to produce moderate levels of electricity from the oxidation of organic matter in the bioanode based on the EET mechanism (Logan et al., 2006). The capability of treating wastewater and simultaneously producing electricity has made BES an emerging and promising technology, which has attracted an increasing interest. With addition of an external power supply, in other words, with the supply of extra electrons, microbial

electrolysis cells (MECs) were developed from MFCs. In MECs, the combination of microbial electrocatalysts and external power supply has helped to overcome the thermodynamic barrier of diverse redox reactions, leading to the conversion of CO₂, organics and electrical energy into various useful compounds, such as hydrogen (H₂), acetate, ethanol and butyrate (Choi et al., 2012; Jeremiasse et al., 2010; Marshall et al., 2013; Nevin et al., 2010; Rozendal et al., 2008; Steinbusch et al., 2010). CH₄ production directly from electrons, protons, and CO₂ can be realized by MECs (Cheng et al., 2009). Through this process, termed electromethanogenesis, CO₂ can be directly converted to CH₄, which matches perfectly with the objective of biogas upgrading.

Bioelectrochemically assisted anaerobic digestion (BES-AD) is a novel process, through which not only microbial metabolism and interspecies interactions in anaerobic digester could be significantly affected (Moscoviz et al., 2016), but also enhanced CH₄ production, through electromethanogenesis stimulated by BES, could become attainable at a relatively low temperature (Liu et al., 2016a). In this integrated system, biogas could be produced and upgraded simultaneously, which makes in situ biogas upgrading possible. The benefits of in situ biogas upgrading include small footprint, low capital cost and low energy demand, compared to ex situ biogas upgrading through physical and chemical processes. The BES-AD integrated system fits perfectly in the pressing need to switch from fossil fuels to sustainable and renewable energy sources. Although several studies have shown enhanced CH₄ production in BES-AD systems, limited research has been performed on long-term operation of such systems. In addition to net CH₄ production, CH₄ content is a crucial parameter determining the quality and use of biogas. Nevertheless, little has been reported on the CH₄ content in the biogas produced in BES-AD systems. It is unclear what

the relative contribution of biofilm and voltage is on the observed enhanced CH_4 production. Although CO_2 conversion is an essential process for biogas upgrading, not much is known about the effect of CO_2 transfer on the CH_4 content of the biogas produced in an integrated BES-AD system. In light of full scale application, the resilience of the BES-AD system to shock, high organic loadings is crucial.

The overall goal of this research was to upgrade the biogas produced from anaerobic digestion through integration with BES and to improve our understanding of limiting factors on long-term performance of BES-AD integrated systems. The specific objectives of this research were to:

1. Improve the CH_4 content in the biogas produced from anaerobic digestion by adding electrodes and voltage.
2. Demonstrate the effect of biofilm on anaerobic digestion in the integrated AD system.
3. Investigate the significance of CO_2 mass transfer in biogas upgrading using the BES-AD system.
4. Investigate the relation between applied voltage and biofilm development in the BES-AD system.
5. Assess the resilience of integrated AD reactors to shock, high organic loading.

CHAPTER 2

BACKGROUND

3.1 Anaerobic Digestion

3.1.1 *Anaerobic Digestion Fundamentals*

Anaerobic digestion is a process through which the electron equivalents in organic matter are channeled to CH_4 to fulfill the goal of removing biochemical oxygen demand (BOD) and simultaneously producing energy-rich biogas (Rittmann and McCarty, 2001). Anaerobic digestion processes occur when organic material is available and the redox potential is low (i.e., sufficiently negative). Anaerobic degradation is a multi-stage process of series and parallel reactions involving complex interactions between different microbial species (Henze et al., 2008). The reactions are typically grouped into four subprocesses: (1) hydrolysis, (2) acidogenesis, (3) acetogenesis, and (4) methanogenesis. The conversion of complex organic matter to CH_4 begins with the hydrolysis, or solubilization, of particulate and colloidal, polymeric organic material – such as carbohydrates, protein, and lipids – into simple carbohydrates, amino acids and long-chain fatty acids by hydrolytic and fermentative bacteria. The hydrolysis products are then fermented or anaerobically oxidized during acidogenesis. The simple carbohydrates and organic acids are utilized to fuel the growth of fermentative bacteria, producing VFAs (mainly acetate, propionate, butyrate) and H_2 as the dominant intermediate products. The VFAs other than acetate, as well as lactate, methanol, and ethanol are then partially oxidized by acetogenic bacteria to acetic acid, H_2 , and CO_2 . At last, the main substrates used by archaeal methanogens, acetate

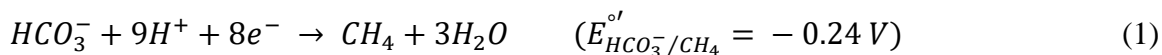
and H_2/CO_2 , are converted into CH_4 by acetate fermenters and H_2 oxidizers, respectively (Pavlostathis, 2011). Due to the greater energy yield from fermentation reactions than CH_4 production reactions, methanogens – particularly the acetate fermenters – grow relatively slowly. Therefore, the operation of anaerobic systems requires balanced quantity of hydrolytic and fermentative bacteria and methanogenic archaea. Besides proper seeding, pH and temperature are also essential for anaerobic digestion, especially for methanogenesis. The favorable pH is between 6.6 and 7.6. The optimum temperature ranges for mesophilic and thermophilic methanogens are 35 to 40°C and 55 to 65°C, respectively (Rittmann and McCarty, 2001). Anaerobic digestion is a widely used biological treatment process for the stabilization of municipal wastewater sludges and municipal solid wastes. High-strength industrial wastewaters anaerobic fermentation for CH_4 production is also a well-practiced process. Compared with aerobic treatment, the anaerobic treatment process has several advantages. (1) Low sludge production for disposal and low nutrient requirements, due to the low energy yield from methanation and slow biomass growth rate; (2) lower energy input and energy rich biogas from methanogenesis; and (3) higher organic loading and smaller footprint. Although initially focused on sludge reduction and stabilization, anaerobic digestion capable of net energy production has received increasing interest in light of self-sustainable, energy neutral WWTP. However, the energy content (i.e., CH_4) of the biogas is fixed by the mean oxidation state of the substrate carbon, which in most cases results in biogas containing 60-70% CH_4 (Gujer and Zehnder, 1983).

3.1.2 *Biogas Upgrading*

The process in which biogas contaminants are removed to increase its CH₄ content is referred to as biogas upgrading. CO₂ is the major contaminant of biogas produced by anaerobic digestion which decreases its specific calorific value and therefore its potential as an alternative to fossil fuels for on-site heat and electricity generation in industry, as a substitute of natural gas for domestic and industrial use prior to injection into natural gas grids and as a transportation fuel (Andriani et al. 2014; Thran et al., 2014). To fully exploit the potential of biogas as renewable energy source for WWTP, biogas upgrading has been practiced. Conventional physical/chemical biogas upgrading usually involves high energy or chemical use, which makes it less environmentally friendly and cost effective. In this context, biological biogas upgrading has been rapidly developed based on economic and environmental concerns (Muñoz et al., 2015). Although energy and chemical intensive, physical/chemical CO₂ removal processes are well established and used because of their reliability and maturity. Typical physical biogas upgrading technologies include water scrubbing, which is considered less susceptible to biogas contaminants (Thran et al., 2014); scrubbing using polyethylene glycol-based absorbents with higher affinity for CO₂ than water (Tock et al., 2010); pressure swing adsorption using adsorbents with high specific area such as activated carbon (Patterson et al., 2011); and membrane separation through a semi-permeable membrane (Bauer et al., 2013). Multiple pathways of CO₂ removal through biological processes have been studied. Chemoautotrophic processes utilizing hydrogenotrophic methanogens to convert the CO₂ with externally applied H₂ to CH₄ has been used in the electronic industry (Ju et al., 2008; Kim et al., 2013). Another typical biological biogas upgrading process relies on photosynthesis using microalgae capable of

utilizing the CO₂ present in the biogas for biomass growth. Electrons released during water photolysis are steered to CO₂ to synthesize biomass (López et al., 2013).

The premise of biological consumption of CO₂ relies on an efficient mass transfer of CO₂ from the biogas to the microbial cells, which means CO₂ dissolution and mass transport of carbonate species are essential for biological biogas upgrading. Increasing gas recirculation rate enhanced the biogas upgrading efficiency of an ex situ process using hydrogenotrophic methanogens to convert externally provided H₂ and CO₂ to CH₄ (Kougias et al., 2017). Biogas recirculation transferring produced CO₂ from the gas phase back into the liquid phase improves the dissolution of CO₂ for better biological conversion by increasing the gas retention time and gas-liquid exchange area. The dissolution of a gas into a liquid approaches equilibrium at which the ratio of the gas partial pressure to its aqueous concentration is converted by Henry's Law. Dissolved CO₂ is distributed through dynamic equilibria between carbonic acid/dissolved gaseous CO₂ (i.e., H₂CO₃^{*}), bicarbonate (HCO₃⁻) and carbonate (CO₃²⁻), which are strongly affected by the pH of the liquid; at circumneutral pH, HCO₃⁻ is the predominant liquid-phase carbon species available for CO₂ consuming microorganism such as hydrogenotrophic methanogens. The half reaction for HCO₃⁻ reduction to CH₄ is as follows (Geppert et al., 2016):



It has been reported that gaseous carbon transport has a significant effect on CH₄ production in a bioelectrochemical system (BES) used for biogas upgrading (Dykstra and Pavlostathis, 2017).

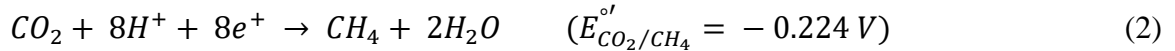
3.2 Bioelectrochemical Systems

3.2.1 Microbial Electrolysis Cells

Microbial electrolysis cell (MEC) is an emerging bioelectrochemical technology capable of recovering substantial energy from cellulosic biomass, salinity gradient, and wastewater organic matter (Logan and Elimelech, 2012; Logan and Rabaey, 2012; Zeng et al., 2015) by directing electrons from organic matter to various electron acceptors to produce a variety of energy-rich compounds such as H₂, ethanol, and CH₄ by externally supplying a relatively small voltage. The essential component of this process is the exoelectrogens having the ability to transfer electrons extracellularly to insoluble electron acceptors, such as the anode in bioelectrochemical systems. This extracellular electron transfer ability was first found in *Geobacter* and *Shewanella* spp. (Lovley and Phillips, 1988; Myers and Nealson, 1988). Subsequently, exoelectrogenic ability has been found to be prevalent in microorganisms, even between different species (Rotaru et al., 2014). Electrons can be transferred indirectly through electron shuttles such as flavins and phenazines between electron donors and acceptors (Marsili et al., 2008; Pham et al., 2008; Canstein et al., 2008). Through direct contact electrons can also be transferred using outer membrane proteins (Myers and Myers, 2001). Sometimes, these microorganisms can produce conductive pili called nanowires to complete electron transfer (Gorby et al., 2006; Reguera, 2005). The microorganisms capable of transferring electrons directly or indirectly into the cell are called electrotrophs (Gregory et al., 2004).

In a MEC, exoelectrogens transfer electrons from the oxidation of organic matter to the anode, then through an external circuit passing through the power supply, electrons

are transferred to the cathode, where valuable compounds can be produced from various electron acceptors. H₂, because of its high calorific value was first produced in MECs using protons as the electron acceptor. H₂ production and COD removal have been reported to be achieved simultaneously in a MEC at a scale of 10 L (Gil-Carrera et al., 2013). Nevertheless, a precious metal catalyst, such as platinum, is usually used on the cathode end of the MEC producing H₂ and the transport and storage of explosive H₂ can be problematic. Electromethanogenesis, which is directly producing CH₄ from CO₂, electrons, and protons using a biocathode colonized by methanogens, provided a promising alternative for energy recovery and CO₂ capture. The cathodic reaction for electromethanogenesis is as follows (Cheng et al., 2009):



Through producing CH₄ and converting CO₂ at the same time, a CH₄-producing MEC can increase the fuel yield per hectare of land area (Van Eerten-Jansen et al., 2012), providing the possibility of a biogas-producing and upgrading treatment plant with a small footprint and low energy input. Because wastewater organic matter can be utilized as the carbon source and electron donor and the small power input can be fulfilled by the energy generation using CH₄ produced in the MEC, bioelectrochemical technology can lead to self-sustainable, energy neutral or even energy positive WWTP. It has been reported that in a two-chamber MEC, 94% influent acetate COD was oxidized resulting in CH₄ production with 79% electron capture efficiency (Villano et al., 2013). Based on capital cost considerations, one-chamber membraneless MEC for domestic wastewater treatment and CH₄ production was investigated for low-strength wastewater treatment (Moreno et al.,

2016). Besides lowering the capital cost, membraneless MEC can also minimize the pH gradient between anode and cathode saving on pH adjustment costs (Clauwaert and Verstraete, 2009).

3.2.2 *BES-AD Integrated Systems*

Bioelectrochemically assisted anaerobic digester (BES-AD) is an integrated system utilizing the microbial electrocatalysts and power supply of bioelectrochemical systems to enhance the CH₄ production from anaerobic digestion (**Figure 2.1**). BES-AD system is the combination of a one-chamber MEC and an anaerobic digester. With bioelectrodes and electrical energy input, advantages of MECs can be attained in AD. The catalytic bioelectrodes as either electron sinks or sources and voltage application can mediate unbalanced fermentation and change the redox balance in the medium. Bioelectrochemical systems have complex and intertwined effects on mixed cultures in AD, in terms of microbial metabolism, interspecies interaction, as well as enrichment and selection of microbial communities (Moscoviz et al., 2016). Through the effective EET between electrodes and electroactive microorganisms forming electrode-attached biofilms, interspecies cooperation between fermenters and methanogens can be improved to convert complex organic matter to CH₄. Through the effective interspecies interactions, acidogenesis and methanogenesis can be balanced, which keeps the system from acidification without pH adjustment. Syntrophic interactions between mixed cultures of fermenters and electroactive bacteria can convert substrates into metabolites favorable for electroactive bacteria and in turn, channel the electrons from the substrate through an external circuit to the cathode, where archaeal methanogens utilize the electrons, protons, and CO₂ to produce CH₄ (Ishii et al., 2015; Kiely et al., 2011; Kouzuma et al., 2015;

Parameswaran et al., 2009). Through these mechanisms, growth of electroactive bacteria and fermenters in association with them in the biofilm may be favored, which would also affect the distribution of the fermentation products (Dennis et al., 2013; Xafenias et al., 2015; Zhou et al., 2015). It has been reported that integrating BES with AD led to the enrichment of *Geobacter* species in the suspended biomass phase and the anodic biofilm. Interspecies electron transfer between *Geobacter* and *Methanosaeta* species was proposed as an alternative to the mechanism in which H₂ is the primary interspecies electron carrier in methanogenesis (Zhao et al., 2015). Microbial electrolysis occurring in BES-AD systems can accelerate the conversion of complex organic matter to H₂, which can then be utilized by hydrogenotrophic methanogens to enhance CH₄ production (Bo et al., 2014; Liu et al., 2016b). By manipulating of voltage input, water electrolysis can occur in the BES-AD system, which facilitated the hydrolysis of a synthetic wastewater and reduced the hydrogen sulfide (H₂S) production by creating micro-aerobic conditions (Tartakovsky et al., 2011).

The BES-AD system is a promising technology for in situ biogas upgrading involving low energy consumption and capital cost. However, the exact effect of electrical energy input on the microbial metabolism of mixed cultures in the electrode-attached biofilm and suspended biomass remains unclear, which severely compromises the reliability of BES-AD integrated systems. Long-term testing is pressing needed to demonstrate the potential limiting factors for the performance of bioelectrochemical systems in terms of COD removal and CH₄ production. A well-established procedure for the successful start-up and operation of integrated BES-AD systems is yet to be developed.

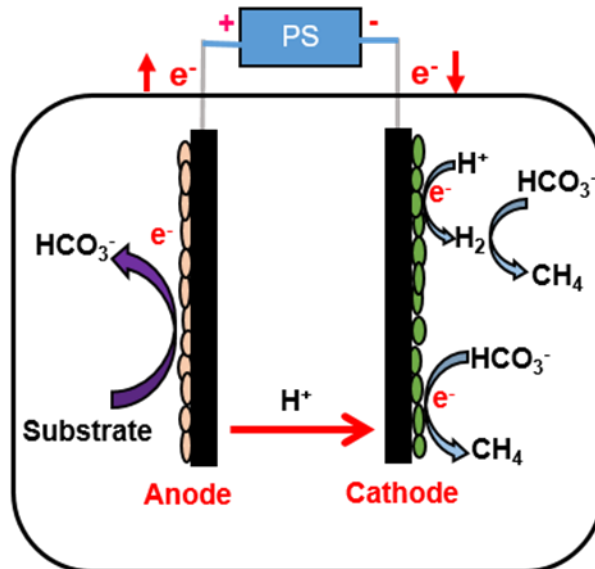


Figure 2.1. Schematic of a BES-AD system resulting in CH_4 production

CHAPTER 3

GENERAL ANALYTICAL METHODS

3.1 pH

All pH measurements were performed using the potentiometric method with an ATI Orion Model 370 digital pH meter (Orion Research Inc., Boston, MA) and a gel-filled combination pH electrode (VWR International, West Chester, PA). The meter was calibrated weekly with pH 4.0, 7.0, and 10.0 standard buffer solutions (Fisher Scientific, Pittsburg, PA).

3.2 Chemical Oxygen Demand (COD)

COD was measured using the closed reflux, colorimetric method as described in Standard Methods (Eaton et al., 2005). An aliquot of 2 mL of sample was added to the vial containing 3 mL pre-made digestion solution composed of 4.9 g $\text{K}_2\text{Cr}_2\text{O}_7$, 6 g HgSO_4 , 6 g Ag_2SO_4 and 500 mL H_2SO_4 (HACH Company, Loveland, CO). After tumbling the vial for 4-8 times, the content in the vials was digested at 150°C for 2 hours and then cooled down to room temperature. The absorbance was measured at 620 nm with a spectrophotometer (DR3900, HACH Company, Loveland, CO). Samples were centrifuged and filtered through a 0.45 μm polypropylene membrane filter if the soluble COD was measured, otherwise well-mixed samples were used after appropriate dilution for total COD measurements. All samples were prepared in triplicates.

3.3 Total and Volatile Solids (TS and VS)

Total solids content of samples was determined according to procedures outlined in Standard Methods (Eaton et al., 2005). Samples were weighed in pre-ignited (550°C) and cooled ceramic crucibles using a PG503-S balance (METTLER TOLEDO, Columbus, OH). The samples were then dried at 105°C for 24 hours in a Fisher Isotemp Model 750G oven. After drying, the crucibles were transferred to a desiccator until cooled, and then the dry weight was measured. If VS were to be determined, the crucibles were transferred to a Fisher Isotemp Model 550-126 muffle furnace and ignited at 550°C for 20 minutes. After ignition, the samples were cooled in a desiccator and the remaining solids weight was measured. TS were calculated as the difference between the weight of the crucible after the sample was dried at 105°C and the tare weight of the crucible divided by the sample volume. VS were calculated as the difference between the weight of the crucible after the sample was dried at 105°C and the weight of the crucible after the sample was combusted at 550°C divided by the sample volume.

3.4 Total Gas Production

Total gas production in closed assay bottles and large volume reactors was measured by either the gas-liquid displacement method or with a wide range pressure meter and PS-100 transducer (Sper Scientific, Scottsdale, AZ). Unless otherwise stated, gas data reported throughout this work are at 22°C and 1 atm.

3.5 Gas Composition

The gas composition was determined by a gas chromatography (GC) unit (Agilent Technologies, Model 6890N; Agilent Technologies, Inc., Palo Alto, CA) equipped with two columns and two thermal conductivity detectors. CH₄ and H₂ were separated with a 15 m HP-Molesieve fused silica, 0.53 mm i.d. column (Agilent Technologies, Inc.)(front column). CO₂ and H₂S were separated with a 25 m Chrompac PoraPLOT Q fused silica, 0.53 mm i.d. column (Varian, Inc., Palo Alto, CA)(back column). Nitrogen and helium were used as the carrier gas for the front and back column, respectively, at a constant flow rate of 6 mL/min. The 10:1 split injector was maintained at 150°C, the oven was set at 40°C and the detector temperature was set at 150°C. All gas analyses were performed by injecting a 100 µL gas sample. The minimum detection limits for CH₄, H₂, CO₂, and H₂S were 500, 100, 800, and 100 ppmv, respectively.

3.6 Volatile Fatty Acids (VFAs)

VFAs (C₂ to C₇; i.e., acetic, propionic, iso-butyric, n-butyric, iso-valeric, n-valeric, iso-caproic, n-caproic, and heptanoic acids) were measured after acidification of centrifuged and filtered samples with a 5% H₃PO₄ (sample:acid, 2:1 volume ratio) using an Agilent 6890 Series GC unit equipped with a flame ionization detector and a Nukol capillary 30 m × 0.32 mm I.D. column (Supelco, Bellefonte, PA). Injections were performed with a 1:1 split ratio. Injection volume was 4 µL. Samples used for the measurement of VFAs were prepared by centrifugation at 4000 rpm for 30 minutes and filtration through 0.2-µm polycarbonate membrane filters (Whatman, Maidstone, United

Kingdom) before acidification. The minimum detection limit for each acid mentioned above was 0.13, 0.06, 0.09, 0.06, 0.08, 0.06, 0.07, 0.07, 0.07 mM, respectively.

3.7 Cyclic Voltammetry

Cyclic voltammetry (CV) is a widely used technique to investigate the electrochemical reactivity of chemical species. It measures the current that develops in an electrochemical cell under conditions where voltage is in excess of that predicted by the Nernst equation. The CV of abiotic and biotic cathodes was performed by using a 6 mm diameter Ag/AgCl reference electrode (0.199 V SHE; BASi, West Lafayette, IN) immersed in the medium close to the cathode electrode. The potentiostat (Interface 1000, Gamry Instruments, Warminster, PA) was connected to the reactor in a three-electrode setup. The working electrode lead was connected to the cathode, the counter electrode lead connected to the anode, and the reference electrode lead connected to the Ag/AgCl electrode. The medium was not mixed during the cyclic voltammetric test. The potential was scanned positively to introduce oxidation first then cycled back negatively to trigger reduction. The specific scanning ranges and rates for different tests are described in CV tests performed on abiotic systems (see Section 4.2.2, below). Gamry PHE200 Physical Electrochemistry Software version 6.21.2719 was used for CV test and collecting and plotting the data.

CHAPTER 4

CHARACTERIZATION OF ABIOTIC SYSTEMS

4.1 Introduction

The performance of bioelectrochemical systems is related to the internal resistance, over potential of electrodes, and conductivity or ion strength of the medium in which redox reactions take place. All these factors can vary from one bioreactor to another depending on configuration as well as material used. Therefore, the characterization of an abiotic system as a control for the biotic reactors is necessary for the appropriate operation and performance interpretation of bioelectrochemical systems.

Water electrolysis involving O_2 and H_2 evolution is critical for the performance of bioelectrochemical systems, especially in BES-AD systems, due to the creation of micro-aerobic conditions as well as the production of additional H_2 (Tartakovsky et al., 2011). Accordingly, the voltage needed for the abiotic system to trigger water electrolysis can be used as a reference for the biotic system. In addition, to avoid stainless steel collector sacrificial corrosion which took place at the anode at relatively high voltages (1.6, 2.0 V), titanium was considered as a substitute for stainless steel (see Section 5.2.5, below). Titanium was chosen based on its similar electrical properties and higher corrosion resistance compared to stainless steel (**Table 4.1**). The characteristics of the abiotic system with different collectors are useful for a better understanding of the performance of the BES-AD integrated system. Therefore, the objective of this part of the study was to determine the minimum voltage needed for water electrolysis to take place in the abiotic

system with stainless steel and/or titanium collectors and evaluate the compatibility of stainless steel and titanium as the anode and cathode collectors through CV testing.

Table 4.1. Comparison of electrochemical properties of titanium with stainless steel^a

Property	Titanium	Stainless steel
Specific electrical resistance ($\mu\text{Ohm-cm}$)	55	72
Electrical conductivity (%IACA)	3.1	2.4

^a Modified from Azo Materials

4.2 Materials and Methods

4.2.1 Water Electrolysis in Abiotic Systems

Water electrolysis involving H_2 and O_2 evolution could be critical to the BES-AD system used in this study (i.e., R3; see Section 5.2.5, below). To determine the voltage needed for water electrolysis in an abiotic control as the reference for the biotic R3, an abiotic reactor was constructed in the same configuration as R3 (see Section 5.2.5, below), except it was not connected to the gas collection cylinder and was not inoculated. The electrodes were made by bonding 4 pieces of carbon felt (Alfa Aesar, Ward Hill, MA; 6×1×1 inch each) to a 6 mm diameter stainless steel rod (Alfa Aesar, Ward Hill, MA) or titanium rod (ATI, Pittsburgh, PA) used as the collector. The reactor headspace volume was 500 mL. A series of voltages of 1.6, 2.0, and 2.5 V was applied on the abiotic reactor for 1 hour at each voltage using a DC power supply (XINYUJIE Electronics, China). To compare the electrical properties of stainless steel and titanium rod as the electrode collector, the same voltages were applied on the cell of the abiotic reactor with three

combinations of collectors: 1) titanium-anode, stainless steel-cathode (Ti-SS); 2) titanium-anode, titanium-cathode (Ti-Ti); and 3) stainless steel-anode, stainless steel-cathode (SS-SS). Anode and cathode potentials, current, as well as gas production and composition were measured throughout the abiotic test. Current was measured using a multimeter (RadioShack, Fort Worth, TX).

4.2.2 CV Tests on Abiotic Systems

In order to compare the electrical performance of the three combinations of collectors and determine the scan range for the abiotic CV tests, a cathode CV was conducted at a wide potential scan range from -1.5 V to approximately $+1.5$ V (vs. Ag/AgCl), using abiotic carbon felt cathode with titanium and stainless steel as collector, submerged in only medium. The abiotic reactor with the three combinations of collectors was scanned at a rate of 50 mV/s. Details on the CV tests are provided in Section 3.7, above.

4.3 Results and Discussion

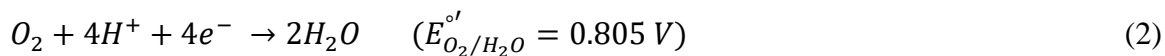
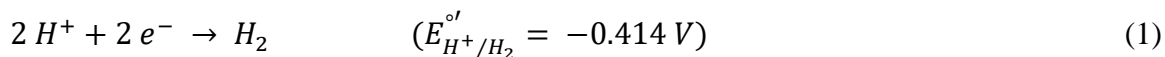
4.3.1 Hydrogen Evolution

Voltage of 1.6 , 2.0 , and 2.5 V, which were the typical values applied on the BES-AD integrated reactor (R3; see Section 5.2.5, below), were applied in sequence on the abiotic reactor with three different combinations of collectors.

The initial current upon the application of voltage was higher than the current after 1 hour with voltage applied (**Table 4.2**), which may be attributed to the relatively low resistance. The current profile under increasing voltage was about the same for the three combinations of collectors, except that the current at 1.6 V in the abiotic reactor with SS-

anode and SS-cathode was lower than that with the other two combinations of collectors. Thus, the intrinsic resistance of titanium and stainless steel rods is comparable. Assuming the initially detected H_2 (0.1% v/v) was negligible, the onset of water electrolysis in the abiotic reactor with titanium or stainless steel as anode collector and stainless steel as cathode collector was at 2.0 V. No H_2 was detected in the reactor below 2.5 V when using titanium as the cathode collector. Because the H_2 production was low and the reactor headspace pressure did not change significantly (less than 0.02 atm) during the abiotic test, the volume of the total gas in the reactor headspace was assumed to be the same over the test period (i.e., 500 mL). Based on this assumption, the rate of H_2 production from water electrolysis was about 3.5 mL/h in the abiotic system (**Table 4.2**). The higher voltage needed for water electrolysis to take place in the system with titanium as the cathode collector may be attributed to an oxide layer predominantly consisting of TiO_2 covering the titanium rod, which acted as an electron acceptor instead of protons. The oxidation of titanium was observed during the CV test on the system using titanium as the cathode collector (see Section 4.3.2, below). The oxidation of titanium and reduction of its oxide layer could be affecting its performance as a collector in electrochemical systems.

The half reactions for water electrolysis are as follows:



The standard reduction potential values are obtained under standard conditions of 25°C, 1 bar, pH 7.0 (Atkins, 1997). Therefore, the anode potential needs to be higher than 0.805 V

and the cathode potential is required to be lower than -0.414 V for water electrolysis to occur under ideal conditions. At 2.0 V, when H_2 was first detected in the abiotic system with SS-SS and Ti-SS collectors, the anode potential was 0.952 and 0.979 V, respectively, which is higher than the above-mentioned value of 0.805 V. Based on the anode and cathode potential values at increasing cell voltage, the anode potential seems to be the thermodynamic threshold for water electrolysis (**Table 4.3**). Due to the energy loss and over potential of the electrodes under realistic application conditions, a voltage input greater than 1.7 V is normally needed for abiotic water electrolysis (Logan and Rabaey, 2012).

Table 4.2. Current and H_2 content before and after 1 hour at 1.6 , 2.0 , and 2.5 V in the abiotic reactor with titanium or stainless steel collectors

Time (h)	Cell Voltage (V)	Ti-Anode Ti-Cathode		Ti-Anode SS-Cathode		SS-Anode SS-Cathode	
		Current (mA)	H_2 (% v/v)	Current (mA)	H_2 (% v/v)	Current (mA)	H_2 (% v/v)
0	1.6	20	-	20	-	12	-
1	1.6	12	-	8.3	0.1	7.3	-
1	2.0	22	-	21	0.1	17	-
2	2.0	20	-	18	0.5	18	0.7
2	2.5	41	-	38	0.5	37	0.7
3	2.5	28	0.7	33	1.6	31	1.4

Table 4.3. Anode and cathode potential at 1.6 , 2.0 , and 2.5 V cell voltage using titanium as anode collector and stainless steel as cathode collector

Cell Voltage (V)	Anode potential (V)	Cathode potential (V)
1.6	0.647	-0.962
2.0	0.979	-1.026
2.5	1.418	-1.095

4.3.2 CV Tests

To demonstrate the electrochemical characteristics of titanium and stainless steel as collectors and to determine the scan range for the biofilm-attached cathode in R3, a wide range CV test from -1.5 to approximately $+1.5$ V was run on the abiotic reactor with the three combinations of collectors. For all the three combinations of collectors, water electrolysis was observed at > 1.1 V (O_2 evolution) and < -0.8 V (H_2 evolution) (**Figure 4.1**). The current peak for O_2 evolution was steeper when using stainless steel as the cathode collector than that when using titanium. The ending current was about 0.3 mA for the Ti-cathode, and approximately 0.6 mA for the SS-cathode, which may be attributed to the oxidation of titanium at around 0.25 V, increasing the resistance of the titanium collector. The ending current of the reduction phase of the CV test was about 0.3 mA for titanium, which was higher than that when using stainless steel as the cathode collector. The higher reduction current could be attributed to additional electrons from the reduction of the oxide layer covering the titanium collector. Overall, due to the shift between different oxidation states and the oxide layer, titanium is not as good as stainless steel as a cathode collector.

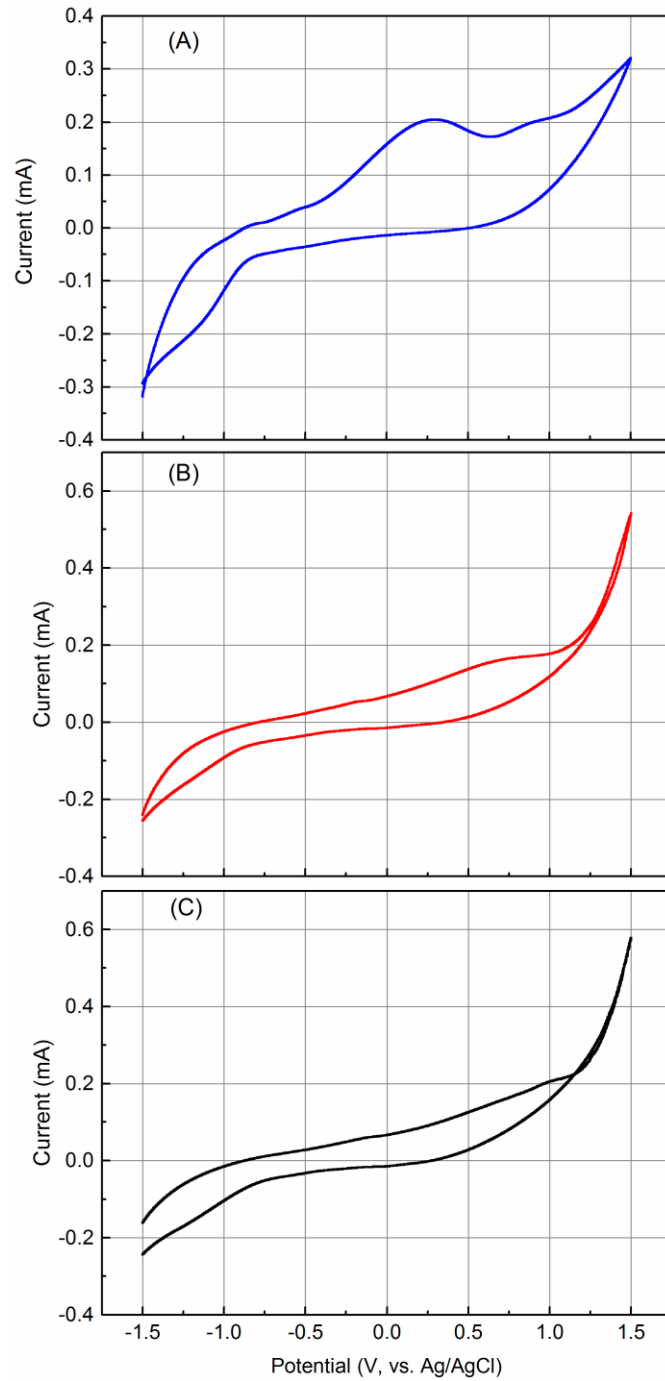


Figure 4.1. CV test on abiotic reactor with Ti-anode, Ti-cathode (A), Ti-anode, SS-cathode (B), and SS-anode, SS-cathode (C)

4.4 Summary

The performance of stainless steel and titanium rods as the collector for anode and cathode in the abiotic reactor was compared through CV tests, with reference to the conditions leading to water electrolysis. The intrinsic resistance or conductivity of these two materials is analogous. The main difference between the two materials is the oxide layer on the surface of the titanium, which could act as the electron acceptor competing with protons (and methanogens in biotic MECs producing CH₄). Moreover, the oxidation of the titanium collector at the cathode could result in a higher resistance. Consequently, stainless steel is more favorable as the cathode collector. However, the advantage of the oxide layer covering the titanium is higher resistance to corrosion compared to stainless steel, which can effectively avoid sacrificial corrosion of the bioelectrochemical system anode (see Section 0, below). Overall, titanium anode collector and stainless steel cathode collector was determined to be the best combination for the bioelectrochemical system used in this study.

CHAPTER 5

INTEGRATED ANAEROBIC SYSTEMS FOR BIOGAS UPGRADING AND ENHANCED METHANE PRODUCTION

5.1 Introduction

Biogas as a promising renewable alternative to conventional fossil fuels is becoming increasingly essential for the sustainability of WWTPs. Anaerobic digestion is a well-established process for simultaneous COD destruction and biogas production from organic material. To exploit the energy value of biogas and provide a renewable source of energy for self-sustainable WWTPs, biogas upgrading, through which the biogas CH_4 content is elevated, is necessary. In pursuit of environmentally friendly biogas upgrading processes at a low capital cost, the BES-AD integrated system appears to be a prominent technology.

In a BES-AD reactor with electroactive microorganisms serving as catalysts and a small electrical energy input, organic matter can be oxidized efficiently through the network of mixed species in biofilms attached on the bioelectrodes to provide electrons through an external circuit to exoelectrotrophic methanogens, which produce CH_4 in the biocathode through either electromethanogenesis or hydrogenotrophic methanogenesis. In this way, CO_2 can be converted to CH_4 in situ, thus contributing to biogas upgrading. However, as an emerging technology, little is known about the long-term integrated system performance. Specifically, the relation between the biofilm contribution and applied

voltage, the effect of CO₂ transfer on its conversion to CH₄, and the resilience of integrated systems to shock high organic loading are not well understood. Therefore, the objective of this study was to: 1) develop and operate BES-AD reactors to improve CH₄ production from anaerobic digestion under various conditions; 2) demonstrate the biofilm contribution to CH₄ production; 3) investigate the significance of CO₂ mass transfer for biogas upgrading in BES; 4) investigate the relation between applied voltage and biofilm development; and 5) assess the resilience of biofilm/voltage integrated digesters to shock high organic loading.

5.2 Materials and Methods

5.2.1 Ultimate Biodegradability

The kinetics and extent of the anaerobic biodegradability of a complex substrate mixture (dextrin/peptone; D/P) by a mixed microbial community at room temperature (20-22 °C) is useful for a better understanding of the metabolism of microbial communities in the anaerobic digesters used in this study (Section 5.2.2, below). The objective of this test was to determine the ultimate anaerobic biodegradability and kinetics of the D/P mixture in a batch system at room temperature. The biodegradability test was conducted using two 500-mL glass bottles, one serving as a seed blank control, and the other as a D/P-amended series. An aliquot of 40 mL deionized water and 40 mL D/P stock solution (12 g/L dextrin, 6 g/L peptone) were transferred to the seed blank bottle and the D/P bottle (total initial COD 1.8 g/L), respectively. Then, the bottles were sealed with rubber stoppers and flushed for 15 minutes with nitrogen gas at a pressure of 10 psi. An aliquot of 160 mL of medium (4.1±0.07 g TS/L; 0.5 g VS/L) was transferred anaerobically to each bottle (**Table 5.1**)

(Beydilli and Pavlostathis, 2005). In the same way, an aliquot of 200 mL seed culture (5.4 ± 0.08 g TS/L; 1.8 ± 0.12 g VS/L) obtained from the anaerobic digester (R1; see Section 5.2.2, below), initially kept at 22°C in the laboratory for two weeks without feeding (i.e., no more than a 5% daily increase in gas production), was last transferred to each bottle. Excess gas pressure was released from the bottles to equilibrate their headspace to atmospheric pressure. The initial pH, total COD (tCOD), soluble COD (sCOD), and VFAs were measured for both the seed blank control and the D/P series. The initial TS and VS in both bottles were obtained by calculation based on the TS and VS concentration of the medium and the seed culture. Incubation was carried out at 22°C and the bottles were shaken manually once a day. Throughout the incubation period, total gas production and gas composition were measured at appropriate time intervals. Total gas production was measured by liquid displacement (see Section 3.4, above). At the end of the test, the bottles were opened and the pH, TS, VS, tCOD, sCOD, and VFAs were measured.

Table 5.1. Composition of the anaerobic culture medium

Compound	Concentration
K ₂ HPO ₄	0.9 g/L
KH ₂ PO ₄	0.5 g/L
CaCl ₂ ·2H ₂ O	0.1 g/L
MgCl ₂ ·6H ₂ O	0.2 g/L
FeCl ₂ ·4H ₂ O	0.1 g/L
NH ₄ Cl	0.5 g/L
Na ₂ S·9H ₂ O	0.5 g/L
NaHCO ₃	3.5 g/L
1 g/L Resazurin Stock	2.0 mL/L
Vitamin Stock ^a	1.0 mL/L
Trace Metal Stock ^b	1.0 mL/L

^a Vitamin stock solution composition described in Table 5.2

^b Trace metal stock solution composition described in Table 5.3

Table 5.2. Composition of vitamin stock solution

Vitamin	Concentration (g/L)
Biotin	0.2
Folic Acid	0.2
Pyridoxine hydrochloride	1.0
Riboflavin	0.5
Thiamine	0.5
Nicotinic Acid	0.5
Pantothenic Acid	0.5
Vitamin B12	0.01
p-Aminobenzoic Acid	0.5
Thioctic Acid	0.5

Table 5.3. Composition of trace metals stock solution

Chemical	Concentration (g/L)
ZnCl ₂	0.5
MnCl ₂ ·4H ₂ O	0.3
H ₃ BO ₃	3.0
CoCl ₂ ·6H ₂ O	2.0
CuCl ₂ ·2H ₂ O	0.1
NiSO ₄ ·6H ₂ O	0.2
Na ₂ MoO ₄ ·2H ₂ O	0.3

5.2.2 *Anaerobic Digester Development and Operation*

The stock mixed methanogenic culture used in this study was developed initially with inoculum from a mesophilic, municipal anaerobic digester, fed with a mixture of dextrin and peptone and maintained at 35°C for several years (Misiti et al., 2013; Tugtas, 2007). To acclimate the mesophilic methanogenic culture to room temperature ($22 \pm 1^\circ\text{C}$) and further demonstrate the effect of biofilm on anaerobic digestion and CH_4 production, two reactors were developed and maintained: a conventional anaerobic digester with suspended-growth biomass (R1) and a hybrid (i.e., suspended and biofilm biomass), open circuit digester with bioelectrodes (R2). The two digesters were developed using two 2.8 L Spinner cell flasks (Bellco Glass, Inc., Vineland, NJ) with a total liquid volume of 2.1 L. The electrodes in R2 were made by bonding 4 pieces of carbon felt (Alfa Aesar, Ward Hill, MA; 6×1×1 inch) to a 6 mm diameter stainless steel rod (Alfa Aesar, Ward Hill, MA) used as the collector. The reactors' headspace was connected to graduated cylinders containing an acid brine solution (10% NaCl w/v and 2% H_2SO_4 v/v) for gas collection and measurement by liquid displacement. An aliquot of 0.6 L stock mixed methanogenic culture and 1.5 L anaerobic medium (see **Table 5.1** for the composition) were anaerobically transferred to R1 and R2 by pressure, after flushing the reactors and the gas lines with N_2 three times for about 15 minutes. The headspace was 700 mL in R1 and 500 mL in R2, with each electrode taking up about 100 mL of volume. The reactors were continuously mixed using magnetic bars-bearing impeller assemblies (Bellco Glass, Inc., Vineland, NJ) magnetically driven by Isotemp stir plates (Fisher Scientific, Waltham; MA). Both reactors were batch-fed every 3 and 4 days with a mixture of dextrin/peptone (48 g dextrin/L, 24 g peptone/L; initial D/P concentration upon feeding, 1030 and 1370 mg COD/L, respectively;

mean organic loading, 343 mg COD/L-day). Both reactors were maintained at room temperature ($22\pm 2^{\circ}\text{C}$) with a hydraulic retention time (HRT) of 21 days. To demonstrate the effect of the biofilm contribution to biogas production in R2, on day 180 of the run, suspended biomass was anaerobically transferred out from R2 and stored. Then, medium was added to R2 to the normal liquid volume of 2.1 L. During this phase of the study, pH, gas production and composition, soluble COD, VFAs and TS/VS were periodically measured for both reactors.

5.2.3 *Gas Recirculation*

On day 319, to improve the mass transfer of CO_2 in the liquid phase, biogas recirculation was applied on R1 and R2. The produced biogas collected in the graduated gas cylinder was pumped out from the top, then transferred back into the reactors at the bottom using a dual-head MaterFlex pump (Model 7523-30, Cole-Parmer Instrument, Vernon Hills, IL), so that the gas was bubbled through the liquid phase to improve CO_2 dissolution. The gas recirculation rate was 10 mL/min. The total headspace (reactors headspace and gas space in the gas collection cylinders) was 1600 and 1400 mL for R1 and R2, respectively. Thus, the gas residence time was 160 and 140 min for R1 and R2, respectively. pH, soluble COD, VFAs, and gas composition were measured daily.

To investigate the fate of dissolved CO_2 , after the high organic loading test (Section 5.2.4, below), 650 mL of CO_2 (calculated based on CO_2 partial pressure vs. bicarbonate alkalinity vs. pH chart to make sure the pH remains above 7.0; Rittmann and McCarty, 2001) was introduced from the top of the gas collection cylinder into the headspace of R1 and R2, which were under starvation (extremely low gas production for over 30 days).

Externally added CO₂ dissolved into the liquid phase under gas recirculation. Total biogas volume and gas composition were measured at certain time intervals during this test period.

5.2.4 Effect of Increasing Organic Loading

To test the response of R1 and R2 to a higher organic loading, two (2X) and four times (4X) of the organic loading was applied in sequence to both reactors, corresponding to an initial reactor COD of 2740 and 5490 mg/L, respectively, immediately after feeding. Both reactors were fed twice with a 2X organic loading and monitored for one week. Then, both reactors were fed once at a 4X organic loading and were left unfed for the next two weeks (starvation period). pH, soluble COD, VFAs, and gas composition were measured daily during this test period.

5.2.5 BES-AD Integrated System Development

To investigate the effect of electrical energy input on anaerobic digestion of the dextrin/peptone mixture by the mixed methanogenic community, the BES-AD integrated reactor (R3) was developed similarly to R2 (see Section 5.2.2, above). A 6 mm diameter Ag/AgCl reference electrode (0.199 V SHE; BASi, West Lafayette, IN) was inserted and submerged in the medium on the cathode side. The effect of external voltage application was assessed in three phases, corresponding to three operational stages of reactor R3 (R3A, R3B, and R3C) as described below.

5.2.5.1 Phase I: Application of 2.5 V on R3A

R3A was developed and operated identically to R1 and R2 (see Section 5.2.2, above) for 47 days. Then, a voltage of 2.5 V was applied on the R3A to result in a cathode potential of 1.0 V using a DC power supply (XINYUJIE Electronics, China) connected to the anode and cathode through the external circuit. pH, total and soluble COD, biogas production, gas composition, and VFAs were measured before and after feeding R3A during the incubation period. After 25 days of operation under the continuous supply of 2.5 V, the stainless steel anode collector broke because of sacrificial corrosion at the liquid/gas interface.

5.2.5.2 Phase II: Application of a range of voltages on R3B

On day 82, after the corrosion of the anode collector, R3B was developed by replacing both the anode and the cathode with new carbon felt electrodes in R3A. An aliquot of 0.6 L culture from R1 used as the inoculum and 1.5 L medium were anaerobically transferred to R3B as described above (Section 5.2.2). On day 145 and 166 (63 and 84 days of operation, corresponding to 3 and 4 retention times), after R3B reached a stable performance producing comparable biogas to that of R1 and R2, 0.5 and 1.1 V were applied on R3B in sequence. Then, to assess the effect of voltage on the biofilm attached on the electrodes, suspended biomass was transferred out of R3B on day 177 (95 days of operation, corresponding to 4.5 retention times) as described in Section 5.2.2, above. On day 187, 2.0 V was applied on R3B and maintained for 10 days before the anode collector broke due to sacrificial corrosion. The suspended biomass was transferred out anaerobically to a N₂ pre-flushed glass bottle for temporarily storage before opening R3B and replacing the anode

collector. The reactor and gas lines were flushed again with N₂ before transferring back the suspended biomass. Then, 1.6 V was applied on R3B and maintained for 10 days before the anode collector broke again. pH, gas production and composition, soluble COD, and VFAs were measured throughout this phase of R3B operation.

5.2.5.3 Phase III: Application of 1.6, 2.0, and 2.5 V on R3C (titanium anode collector)

To compare the performance of BES-AD systems with different electrode collectors, on day 218 a new BES-AD reactor, R3C, was developed. However, instead of applying voltage after the system had reached a stable performance, a voltage of 1.1 V was applied on R3C from the beginning of its operation. On day 313 (95 days of operation, corresponding to 4.5 retention times), before an increase of the applied voltage and in order to avoid the sacrificial corrosion of the anode collector, the anode and cathode stainless steel collectors were replaced with titanium collectors as described in Section 5.2.5.2, above. Subsequently, 1.6, 2.0, and 2.5 V were applied in sequence on R3C for one week at each voltage. Based on the observed water electrolysis and the CV tests described in Section 4.2.1 and 4.2.2, above, 2.0 V and with titanium anode collector and stainless steel cathode collector were determined to be the best conditions for the BES-AD reactor in this study. Therefore, on day 333 (105 days of operation, corresponding to 5.5 retention times; 20 days after the titanium collectors replacement), the titanium cathode collector was replaced with a stainless steel rod. On day 347, 14 days after the transition to the Ti-anode, SS-cathode configuration, similarly to R2 and R3B, suspended biomass was transferred out of R3C to assess the biofilm contribution on the BES-AD system. After one week of operation, biogas recirculation was applied to R3C. On day 361, the organic loading to R3C was increased to 2X and 4X using the procedure employed for both R1 and R2 (see

Section 5.2.4, above). pH, gas composition, soluble COD, and VFAs were measured over the operation of R3C.

After 14 days of R3C operation following the 4X shock load during which period a very low biogas production was observed, a CO₂ addition/dissolution test was conducted. Similarly to R1 and R2, 650 mL of CO₂ was introduced to the headspace of R3C following the procedure described in Section 5.2.3, above. Total gas volume and composition in the headspace were measured over the following two days.

A CV test was run on R3C daily in the first three days of a 4-day feeding cycle with the normal 1X organic loading to probe into the redox reactions taking place in the BES-AD reactor used in this study over the feeding cycle. During the biotic CV test, the potential was initially scanned under open circuit conditions, then decreased to -0.8 V, after which was increased up to +1.1 V; the scanning rate was 5 mV/s. Details on the CV test are described in Section 3.7, above.

5.3 Results and Discussion

5.3.1 Ultimate Biodegradability

Incubation for the batch ultimate biodegradability test lasted for 70 days. The initial and final parameters in the D/P series and the main results of the biodegradability test are summarized in **Table 5.4**. The pH in the seed blank control remained constant at around 7.47, while the pH in the D/P series decreased from 7.42 to 6.95. The initial sCOD in the D/P series was 1136±21 mg/L (seed blank corrected), representing 63% of the initial tCOD (1800 mg/L), indicating that a significant portion of the D/P mixture was not soluble. The

VFAs concentration was very low in both the seed blank control and the D/P series at the end of the 70-d incubation period. The VS increased by about 0.4 g/L. **Figure 5.1** shows the cumulative total biogas, CH₄ and CO₂ production over the entire incubation period (corrected for the seed blank contribution). Due to the starved anaerobic culture obtained from the R1 digester used as the seed for this test, the biogas production by the seed blank control was very low (32 mL at 22°C). Seed blank correction was applied to all the data reported in this section. The final CH₄ content in the D/P series was 68.6% (normalized to the sum of CH₄ and CO₂ biogas contents to 100%), which was comparable to that observed in the R1 digester (Section 5.3.2, below). The CH₄ production in the D/P series was 412 mL CH₄ at 22°C/g COD destroyed, which is higher than the theoretical value of 378 mL CH₄ at 22°C/g COD destroyed. This means more CH₄_COD was produced than the COD destroyed, which explains the negative value of the COD balance ($((tCOD_{in} - tCOD_{final} - CH_4_COD)/tCOD_{in})$) (see **Table 5.4**). This discrepancy may be attributed to experimental error in either the biogas production or COD measurements. To give a more direct visual of how the substrate was degraded over time, the CH₄ production was normalized to the initial total D/P mixture COD and **Figure 5.2** shows the result. The gas production rate decreased significantly after about 30 days of incubation. The net VS increase in the D/P series was converted to COD equivalents by using a COD:VS ratio value of 1.42 g COD/g VS (Rittmann and McCarty, 2001) to represent the COD used for biomass growth. The total degradable COD was 1710 mg/L (COD converted to CH₄ + biomass COD). Based on the above, the ultimate biodegradability of the D/P mixture was 97.3%.

Anaerobic digestion of complex and partially soluble organic matter proceeds in several stages, which can be typically sorted into four processes: hydrolysis, acidogenesis,

acetogenesis, and methanogenesis (Batstone et al., 2002; Pavlostathis, 2011; Tezel et al., 2011). A wide range of models from relatively simple ones based on the rate-limiting approach, to complex, structured models have been applied to describe the kinetics of anaerobic digestion (Batstone et al., 2002; Pavlostathis and Giraldo - Gomez, 1991). The kinetics of anaerobic digestion of D/P mixture was determined based on the experimental CH₄ production data obtained from the ultimate biodegradability test assuming pseudo first-order kinetics for the overall digestion process as follows:

$$\frac{S_t}{S_u} = 1 - e^{-kt} \quad (1)$$

where, S_t is the CH₄ production converted to COD (CH₄_COD mg) at time t ; S_u is the ultimately degradable total COD (mg); k is the pseudo first-order rate constant (d⁻¹); and t is the incubation time (d). The pseudo first-order rate constant value was estimated by applying non-linear regression fit of the CH₄_COD experimental data to Eq. (1) using SigmaPlot Version 10 software (Systat Software Inc., San Jose, CA, USA). **Figure 5.3** shows the actual S_t/S_u experimental data, fitting curve, 95% confidence band and the rate constant value (k) for the D/P mixture over the incubation period. The reported rate constant value was estimated based on CH₄ production, thus describing the overall rate of conversion of degradable COD to CH₄.

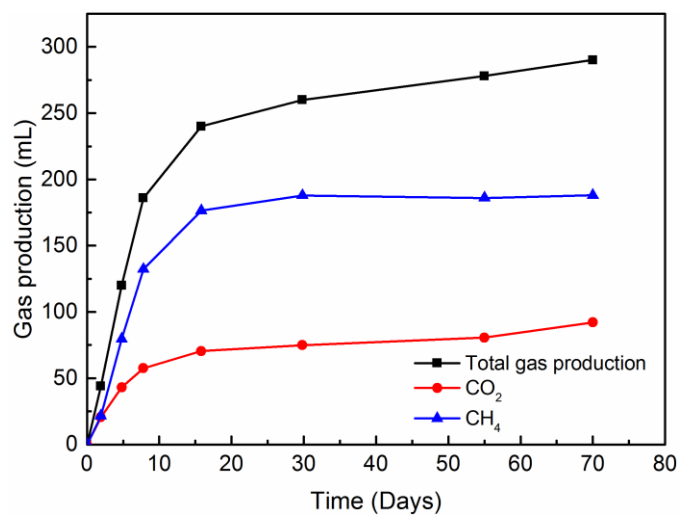


Figure 5.1. Cumulative gas production in biodegradability test batch reactor (seed blank corrected; gas data at 22°C and 1 atm)

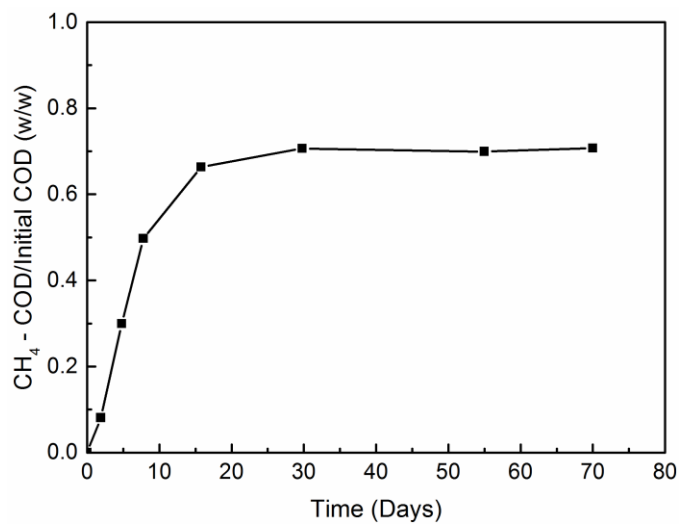


Figure 5.2. Cumulative CH₄ production in biodegradability test normalized to initial total D/P COD

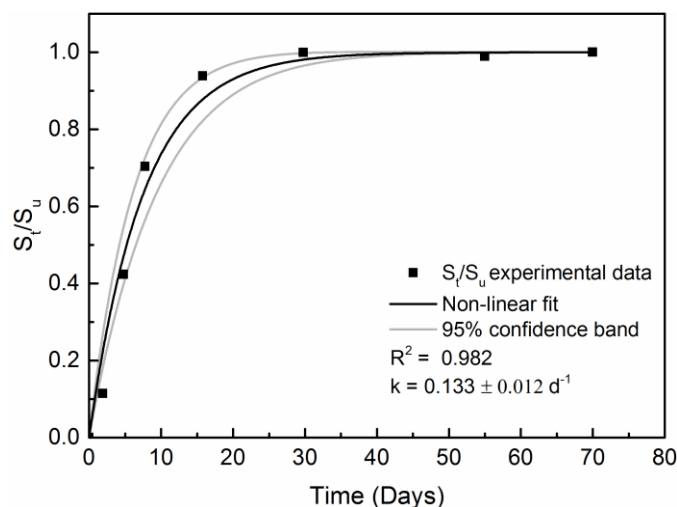


Figure 5.3. CH₄_COD/Initial degradable COD versus time (k = mean estimate \pm standard error)

Table 5.4. Results of the batch ultimate digestibility test (after seed blank correction)^a

Parameter	Seed blank	Dextrin/Peptone
Initial tCOD (mg/L)	1411.7 \pm 98.9 ^b	3170 \pm 12.2
Final tCOD (mg/L)	1036.5 \pm 0.5	1652 \pm 62
Initial sCOD (mg/L)	221 \pm 0.8	1356.7 \pm 20.1
Final sCOD (mg/L)	221.5 \pm 2.5	290 \pm 1
Initial total VFAs (mg COD/L)	38.3 \pm 3.2	474.5 \pm 25.2
Final total VFAs (mg COD/L)	43.1 \pm 0.8	40.2 \pm 0.2
Initial TS (g/L)	4.3 \pm 0.03	4.3 \pm 0.03
Final TS (g/L)	4.2 \pm 0.23	4.7 \pm 0.03
Initial VS (g/L)	1.1 \pm 0.03	1.1 \pm 0.03
Final VS (g/L)	1.1 \pm 0.08	1.5 \pm 0.14
Initial pH	7.47	7.42
Final pH	7.46	6.95
Total COD destruction (%)		65 \pm 6.2
CH ₄ production (mL)		188
Final CH ₄ content (%)		68.6
CH ₄ _COD/Initial COD (%)		70.7
CH ₄ /COD destroyed (mL@22 °C/g)		412
COD Balance (%)		-5.8

^a Gas data at 22°C and 1 atm

^b Mean \pm standard deviation ($n = 3$)

The degradable COD degradation kinetics and its conversion to CH₄ during the batch ultimate biodegradability test could be utilized to estimate the degradable COD conversion to CH₄ in a CSTR (R1; see Section 5.2.2, below). Assuming pseudo first-order kinetics for the overall anaerobic digestion process, the fraction of the degradable COD destruction as a function of a CSTR HRT is obtained from mass balance as follows:

$$\frac{S_{\theta}}{S_{in}} = 1 - \frac{1}{1+k\theta} \quad (2)$$

where, S_{θ} is the substrate degradable COD concentration converted to CH₄ (mg COD/L) at a reactor retention time θ ; S_{in} is the ultimately degradable influent substrate concentration converted to CH₄ (mg COD/L); k is the pseudo first-order rate constant (d⁻¹); and θ is the reactor retention time (d). Using the same rate constant, the fraction of degradable COD destruction at a given batch incubation time and an HRT value for a CSTR can be calculated based on Eq. (1) and Eq. (2), respectively (**Figure 5.4**).

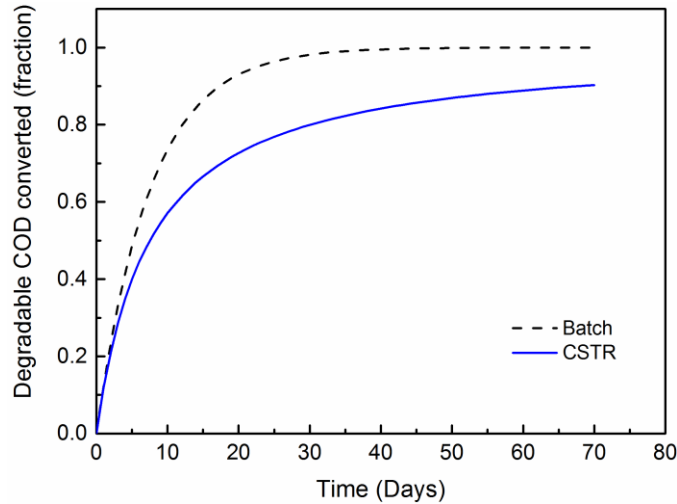


Figure 5.4. Fraction of degradable COD destruction in a batch reactor and a CSTR as a function of incubation time and HRT, respectively ($k = 0.133 \text{ d}^{-1}$)

5.3.2 Performance of Anaerobic Digester and Integrated System

After 72 days of operation, the total biogas production of R1 and R2 over a 4-day feeding cycle reached a stable level of 1030 ± 60 and 1060 ± 53 mL ($n = 5$), respectively (**Figure 5.5**). Both the total and soluble COD concentration increased in both reactors during the initial 20 days of operation. The COD increase was higher in R1 compared to R2: 3326 mg/L of total COD and 918 mg/L of soluble COD in R1 compared to 2460 mg/L of total COD and 485 mg/L of soluble COD in R2. Although both reactors were maintained under identical feeding conditions, the total and soluble COD concentrations in R2 were significantly lower than those in R1 (**Figure 5.6 A&B**). The VFAs profile was consistent with that of the COD. The total VFAs concentration in R2 reached very low values in about 30 days (1.4 retention times), while it took 70 days (3.3 retention times) for R1 to significantly decrease the VFAs concentration (**Figure 5.6 C**). The initial pH value in both reactors was around 7.6, dropped to about 7 in 10 days and fluctuated between 6.8 and 7.1 over the feeding cycles. The pH profiles in both reactors followed a similar pattern and were at about the same level (**Figure 5.6 D**). The highest total VFAs concentration occurred on the second day of the 4-day feeding cycle and the peak VFAs concentration in R2 was remarkably lower than that in R1. Acetate and propionate were the main VFA species (**Figure 5.7**).

After around 50 days of operation, a stable biogas production was achieved by both R1 and R2. However, the biogas production in R1 over the 3-day and 4-day feeding cycles was less consistent than that in R2. In terms of COD and VFAs concentration, R1 did not reach a stable performance until day 70 (3.3 retention times), while R2 reached a relatively stable performance in about 50 days of operation. The total and soluble COD increased in

both reactors initially, which was attributed to the slow biomass growth during the initial operation period with the mesophilic mixed culture transitioning from 35°C to room temperature (22±2°C). The transition period lasted longer in R1 than in R2. Under stable performance, the VFAs concentration was very low in both reactors at the end of feeding cycles. The VFAs concentration in R2 was noticeably lower over a 4-day feeding cycle compared to R1. In the later incubation period, almost no VFAs were detected in both R1 and R2 at the end of the 4-day feeding cycles and along with the observed increasing VFAs consumption over time, only acetate and propionate could be detected in daily measurements. The pH changed along the feeding cycle, due to the batch-fed mode of operation. Acidogenesis occurs before methanogenesis; therefore, it was expected that the pH would decrease at the beginning of each feeding cycle, then increase to about 7 at the end of the feeding cycle after the VFAs were further converted leading to CH₄ production. The difference between the performance of R1 (suspended biomass) and R2 (hybrid system with suspended and biofilm biomass) is attributed to the syntrophic interactions between diverse species in the biofilm of R2, which brought about efficient substrate interspecies transfer to effectively remove the substrates and produce biogas. It is also possible that with the conductive carbon felt electrodes acting as electron mediator, interspecies electron transfer between fermentative bacteria and methanogenic archaea was improved, which led to enhancement in CH₄ production in R2. Enhanced CH₄ production in a methanogenic digester containing granular activated carbon (GAC) has been previously reported (Liu et al., 2012).

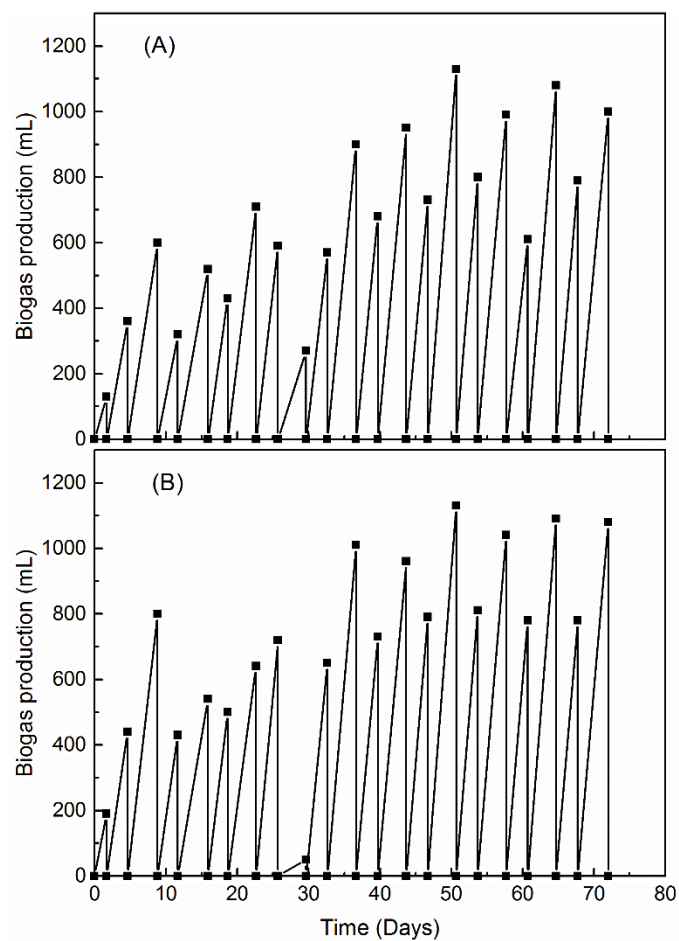


Figure 5.5. Biogas production in R1 (A) and R2 (B) over 3-day and 4-day feeding cycles during the first 72 days of operation

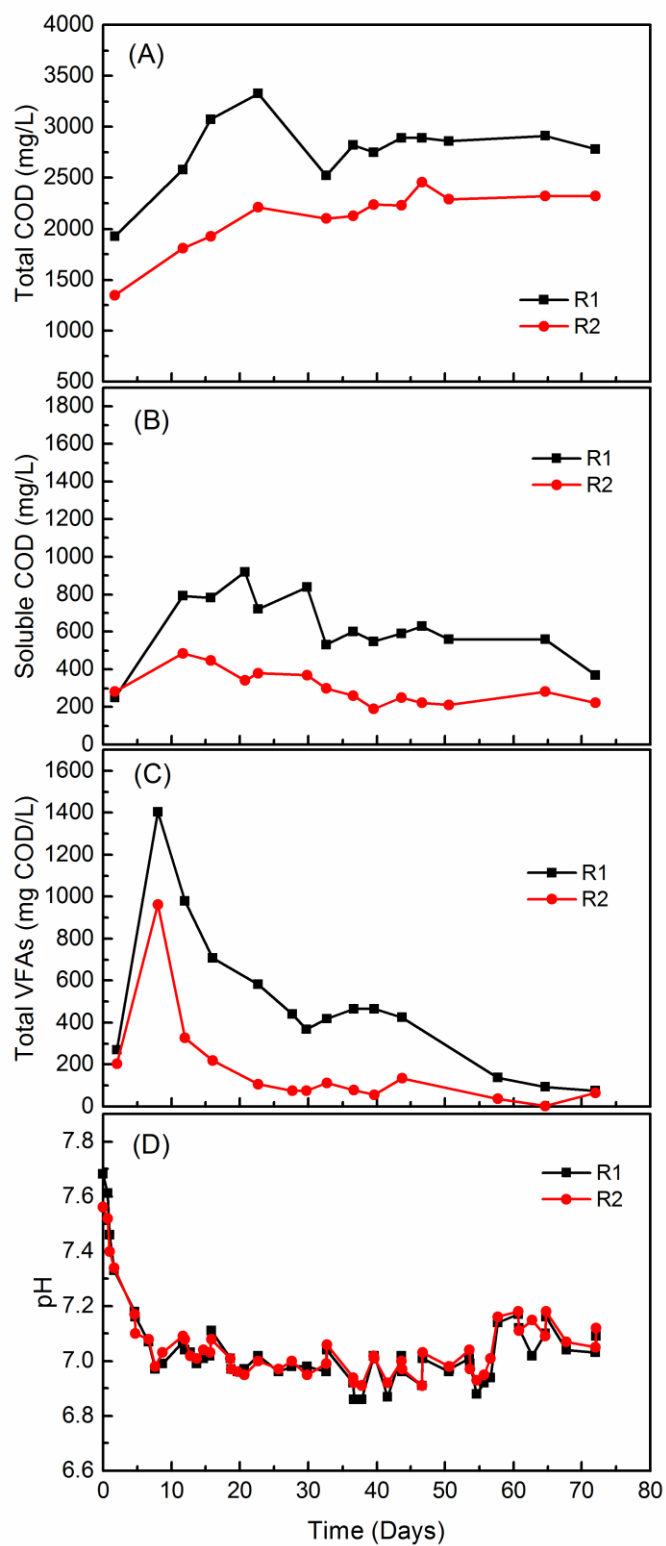


Figure 5.6. Total COD (A), soluble COD (B), VFAs (C), and pH (D) at the end of each feeding cycle in R1 and R2 during the first 72 days of operation

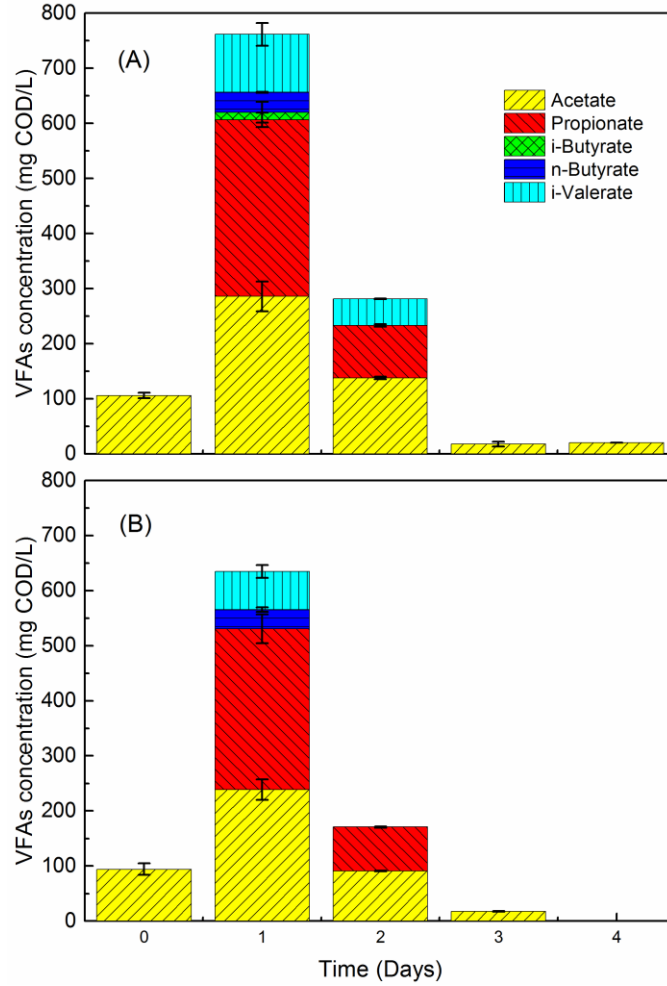


Figure 5.7. VFA species over a 4-day feeding cycle in R1 (A) and R2 (B). Error bars represent mean values \pm one standard deviation, $n = 3$ (no VFA was detected on day 4 in R2)

The performance of R1 and R2 was compared over one 4-day feeding cycle after 173 days (8.2 retention times) of operation. In R2, 57% of soluble COD was consumed within one day, while only 45% was consumed in R1. Similarly, 56% of the total biogas production over the 4-day feeding cycle was achieved in the first day in R2, which was fast compared to 46% in R1. The CH_4 content dropped and CO_2 content increased on the second day of the 4-day feeding cycle in both reactors. The ending CH_4 content in R1 and R2 was 66.3% and 68.1%, respectively (**Figure 5.8**). Although the biogas CH_4 content over the

feeding cycle was about the same in both reactors, R2 produced 331 mL of CH₄ in the first day of the 4-day feeding cycle, while only 225 mL of CH₄ was produced in R1 over the same incubation time. In the 4-day feeding cycle, following 173 days of operation, no VFA was detected in the later three days of the feeding cycle in both R1 and R2 (**Figure 5.9**). Based on the data above, R2 with biofilm could remove COD and produce biogas faster than R1 over the 4-day feeding cycle leading to higher initial CH₄ production within one day of feeding. Usually in a batch-fed anaerobic digester, fermentation and acidogenesis producing CO₂ and H₂ proceed methanogenesis, which led to the decrease of the CH₄ content in both reactors on the second day of the feeding cycle. In terms of VFAs concentration, it is possible that, at this point of operation, acidogenesis and methanogenesis were taking place effectively converting VFAs to acetate, then ultimately to CH₄, which led to undetectable VFAs left in both reactors.

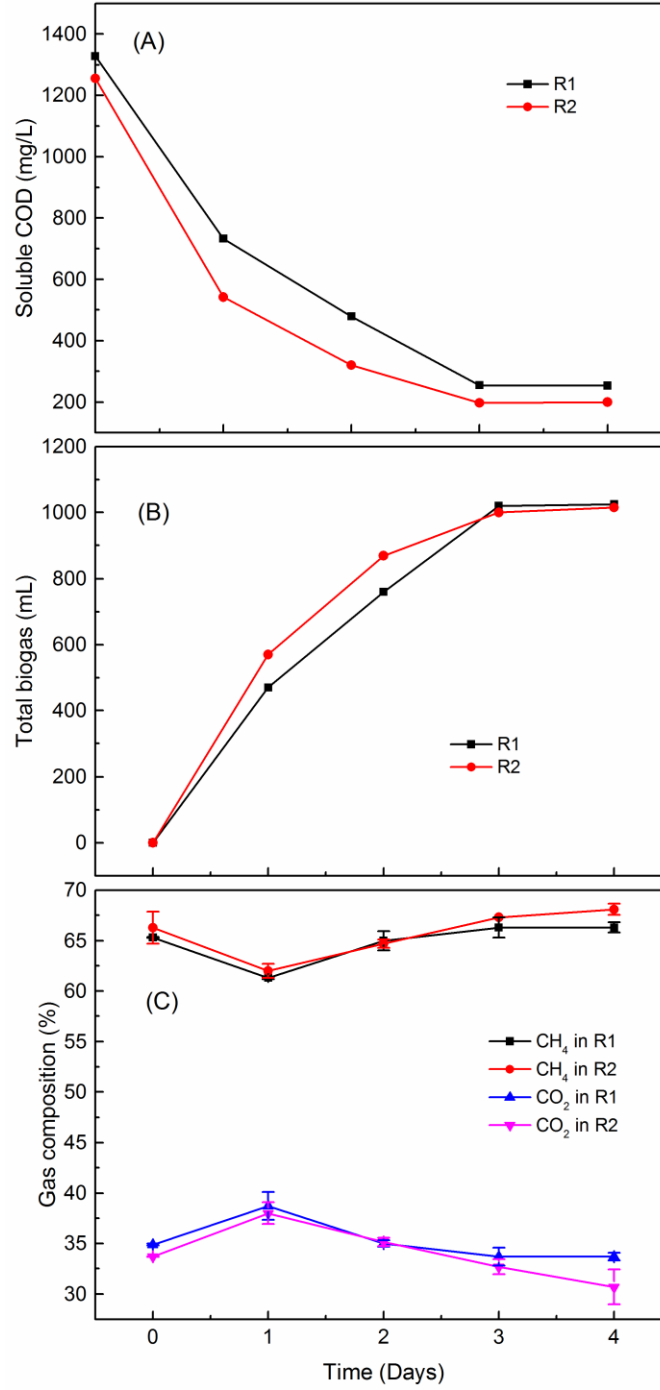


Figure 5.8. Soluble COD profile (A), total biogas production (B), and CH₄ and CO₂ content (C) over the course of the 4-day feeding cycle after 173 days of operation. Error bars represent mean values \pm one standard deviation, $n = 3$. Standard deviations less than 1% are not shown

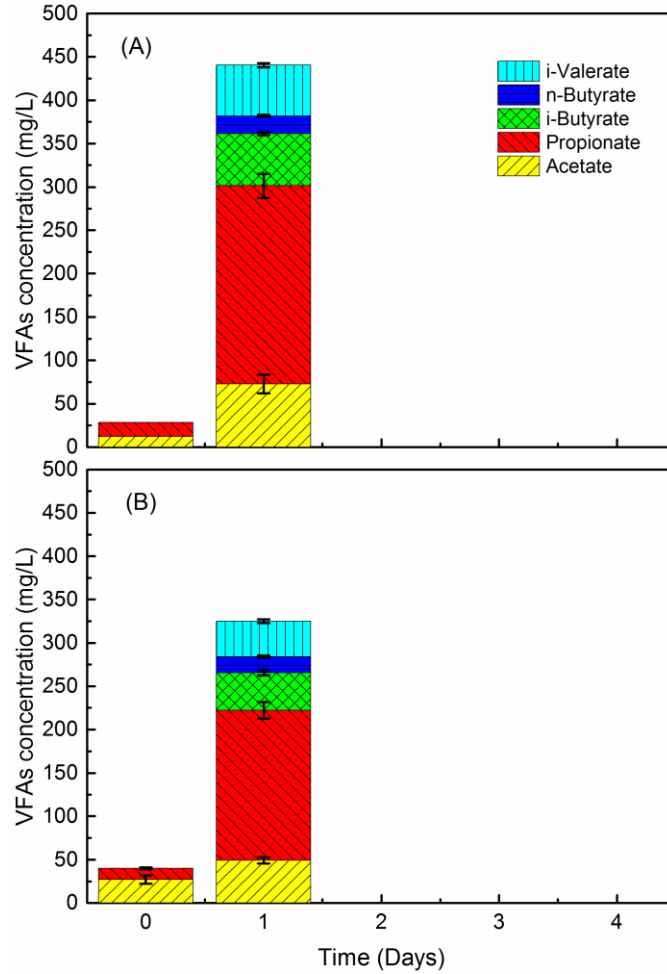


Figure 5.9. VFA species in R1 (A) and R2 (B) over the 4-day feeding cycle after 173 days of operation. Error bars represent mean values \pm one standard deviation, $n = 3$. Standard deviations less than 1% are not shown (no VFA was detected from day 2 to 4)

After 89 days of operation, the suspended biomass VS concentration decreased by 0.3 g/L in R2, while remained approximately the same in R1. Additionally, the VS concentration was always lower in R2 than in R1 over the incubation period (**Table 5.5**), all of which indicate a significant biomass retention on the two electrodes in R2.

The characteristics of R1 and R2 under stable performance are given in **Table 5.6**. Based on all of the discussion above, R2 removed soluble COD and VFAs to much lower

levels than R1, which resulted in lower VFAs accumulation in R2 initially as opposed to R1. The fraction of the total COD destruction in R1 operated with a HRT of 21 days was 0.61, which was lower than the simulated 0.73 for a CSTR based on the pseudo-first order rate constant (k) value of 0.133 d^{-1} estimated based on the batch ultimate biodegradability of dextrin/peptone (**Figure 5.4**). The discrepancy between the experimental and theoretical values is attributed to the batch-fed operation of R1 (every 3 and 4 days; see Section 5.2.2, above), as well as the difference in operational conditions (e.g., biomass concentration).

Table 5.5. TS and VS concentrations in R1 and R2 during the first 89 days of operation

Day	R1		R2	
	TS (g/L)	VS (g/L)	TS (g/L)	VS (g/L)
7	6.0 ± 0.53^a	2.6 ± 0.29	5.7 ± 0.05	2.3 ± 0.16
42	6.3 ± 0.11	2.6 ± 0.15	6.0 ± 0.11	2.3 ± 0.16
89	6.0 ± 0.25	2.7 ± 0.35	5.7 ± 0.25	2.0 ± 0.17

^aMean \pm standard deviation ($n = 3$)

Table 5.6. Characteristics of R1 and R2 under stable performance^a

Parameter	R1	R2
pH	6.98 ± 0.02 ^b	6.99 ± 0.03
Initial total COD (mg/L)	3723 ± 103	3236 ± 26
Final total COD (mg/L)	2857 ± 29	2217 ± 66
Initial Soluble COD (mg/L)	1270 ± 60	1206 ± 72
Final Soluble COD (mg/L)	315 ± 59	204 ± 7
CH ₄ content (%)	66.3 ± 0.5	68.1 ± 0.6
CH ₄ production (mL)	668 ± 13	661 ± 4
COD destruction (%) ^c	61.4 ± 1.2	60.6 ± 0.3
TS (g/L)	5.3 ± 0.31	5.3 ± 0.10
VS (g/L)	1.8 ± 0.04	1.5 ± 0.07

^a From day 159 to day 177^b Mean ± standard deviation (*n* =3)^c Calculated by CH₄_COD/Initial COD added (378 mL CH₄/g COD destroyed @22°C)

To further demonstrate the biofilm contribution to anaerobic digestion and CH₄ production, on day 180, suspended biomass was transferred out of R2 as described in Section 5.2.2, above. In the subsequent feeding cycle, the CH₄ content in R2 increased from 68.1 ± 0.6% to 74.3 ± 0.4%, and although only the biofilm biomass was left in R2, the total biogas production over the 4-day feeding cycle was 910 mL, which was 89.7% of the total biogas produced over the same incubation period when both suspended biomass and biofilm were present in R2. Based on these results, the biofilm contributed more to the biogas production in R2 than the suspended biomass. With only the biofilm, the net total CH₄ production of R2 increased from 663 to 698 mL over the 4-day feeding cycle. The observed increase in the CH₄ content of the R2 biogas gradually decreased over the next two feeding cycles when the biogas CH₄ content dropped back to 67.2 ± 0.5% and the CH₄

production decreased to 650 mL over one feeding cycle. Due to the short duration of the observed enhancement in CH₄ production, only a plausible explanation can be derived. The most likely cause could be the difference in the structure of the microbial communities of the biofilm and the suspended biomass as well as synergistic microbial interactions. With more efficient interspecies H₂ and electron transfer, the biofilm could have been dominated by methanogens, while the suspended biomass was more responsible for hydrolysis and fermentation of the complex D/P mixture. When the suspended biomass was removed, all metabolic activities took place in the biofilm. Due to a possible higher abundance of methanogens and more efficient interspecies interaction, VFAs could be converted to CH₄ efficiently without lagging behind acidogenesis. The uptake of CO₂ by hydrogenotrophic methanogens in close association with fermentative bacteria, could be enhanced within the biofilm, which may have led to the higher CH₄ content when all the biomass was concentrated in the biofilm. However, as the suspended biomass was redeveloped, most of the hydrolysis and fermentation processes may have shifted back into suspended biomass phase, which may have resulted in decreased CO₂ uptake by hydrogenotrophic methanogens, due to gas-liquid mass transfer limitations. Therefore, the biogas CH₄ content returned to its prior level. Further discussion relative to the effect of CO₂ mass transfer on CH₄ production is provided in Section 5.3.3, below. The microbial analysis of the biofilm and suspended biomass communities, which can shed light to the above discussed plausible explanation, is pending.

At the end of the operation of R1 and R2, the suspended and biofilm biomass were quantified through VS measurement. In R1, the VS in the suspended phase was 4.2 g. In R2, the suspended and biofilm biomass was 5.4 and 4 g, i.e., 57 and 43% of the total

biomass in the hybrid system, respectively. However, an exchange of biomass between the suspended phase and the biofilm during the long-term operation of R2 cannot be excluded. Molecular characterization through 16S RNA sequencing of the suspended biomass and biofilm microbial communities is pending.

5.3.3 Gas Recirculation

To improve the mass transfer of CO₂ in the liquid phase and achieve a higher conversion to CH₄, after 319 days of operation, gas recirculation was applied to both R1 and R2. Under gas recirculation, within one day of feeding, 74.6% of soluble COD was consumed in R2, while only 36.5% was consumed in R1. Similarly, 94.6% of the 4-day cycle total biogas production was achieved in one day in R2, while 50.9% of the biogas production took place in R1. In the latter feeding cycle, total produced biogas decreased from 1015 to 875 mL in R2. The CH₄ production in the first one day was 192 and 622 mL in R1 and R2, respectively. At the end of the feeding cycle before gas recirculation was applied, the CH₄ content was $67.3 \pm 1\%$ and $65.6 \pm 1.2\%$ in R1 and R2, respectively. At the end of the third feeding cycle under gas recirculation, the CH₄ content increased to $72.5 \pm 0.5\%$ and $76.3 \pm 0.7\%$ in R1 and R2, respectively. The net total CH₄ production over the 4-day feeding cycle was 661 mL in R1, which is similar to that before gas recirculation was applied, and 708 mL in R2, which is higher than the 663 mL produced without gas recirculation (**Figure 5.10**). Only acetate and propionate were detected during this feeding cycle, and the total VFAs concentration was much lower in R2 than in R1 (**Figure 5.11**). The remarkable difference between the performance of R1 and R2, in terms of both COD consumption and biogas production, is attributed to the biofilm development in R2. Under gas recirculation, produced biogas was bubbled through the liquid phase, which improved

the biogas contact time and exchange area between biogas and the medium, and in turn enhanced the CO₂ dissolution. Therefore, the volume of total biogas produced in R2 declined in the latter part of the feeding cycle, when the biogas production was very low (**Figure 5.10**). In contrast to R2 producing most of the biogas in the initial two days of the feeding cycle, significant biogas was produced at a rate higher than the dissolution of CO₂ throughout the feeding cycle in R1. Thus, biogas decline was not observed in R1. At this point of operation, a major portion of COD removal and biogas production was completed within one day of the feeding cycle in R2, indicated its ability to withstand a higher organic loading. The observed significant CH₄ production enhancement may be attributed to the biofilm developed on the electrodes in R2 promoting cooperation between diverse microbial species such as interspecies H₂ and electron transfer (Liu et al., 2012; Morita et al., 2011).

Given the CH₄ content and production data, the increase in CH₄ content in R1 is attributed to the enhanced CO₂ dissolution rather than the increase in CH₄ production. Based on the performance of R2 (hybrid system with suspended and biofilm biomass) under gas recirculation, the enhanced CH₄ production is attributed to an improvement of the gas-liquid mass transfer, especially the CO₂ transport within the biofilm. At the pH range of R2 (6.8 to 7.2), HCO₃⁻ is the predominant carbonate species available for hydrogenotrophic methanogens. The decrease in the biogas CH₄ content in R1 on the second day of the feeding cycle is attributed to the sequential nature of fermentation, acidogenesis, and methanogenesis. However, no such drop in the biogas CH₄ content in R2 was observed under gas recirculation. In contrast, in the case of R2 without gas recirculation, CO₂ content increase and CH₄ content decrease were observed on the second

day of the feeding cycle. It is possible that, with enhanced mass transfer and much higher substrate consumption and CH_4 production rate facilitated by the biofilm, the CO_2 produced by fermentation and acidogenesis was converted to CH_4 by methanogens, which contributed to the continuous increase of the biogas CH_4 content over the feeding cycle in R2.

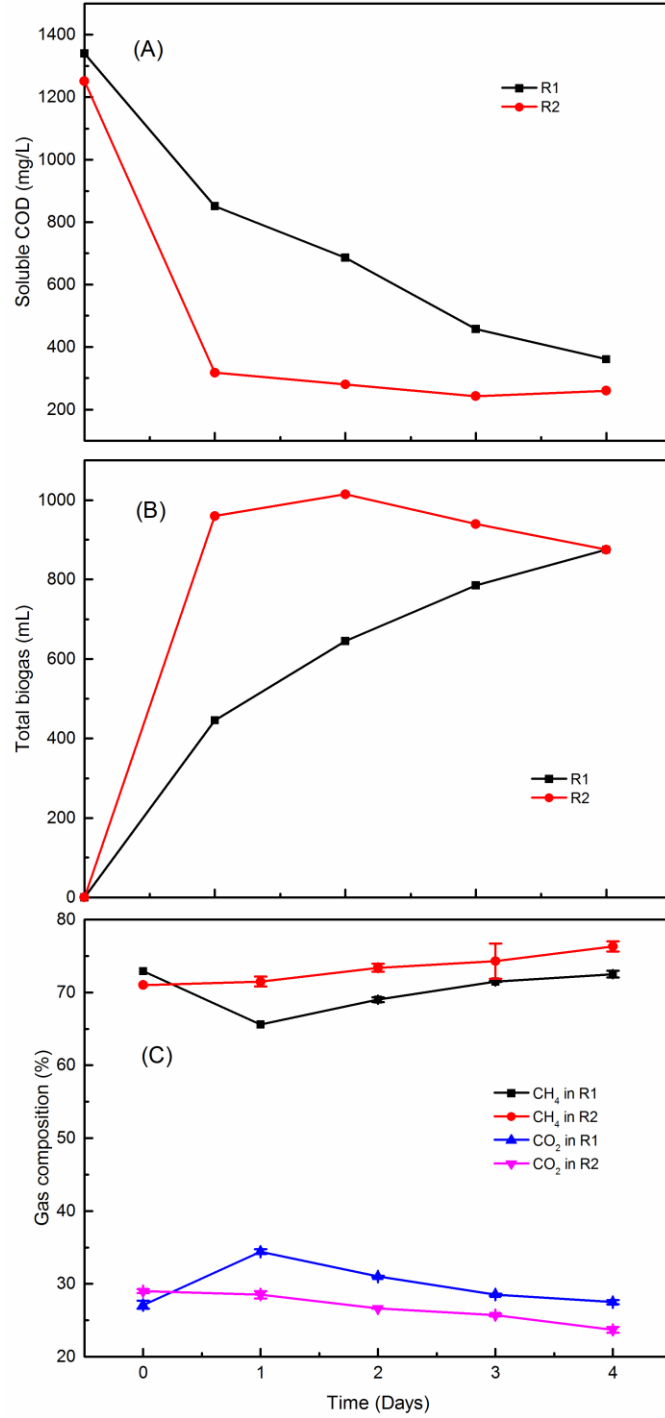


Figure 5.10. Soluble COD profile (A), total biogas production (B), and CH₄ and CO₂ content (C) over the course of the 4-day feeding cycle under gas recirculation after 319 days of operation. Error bars represent mean values \pm one standard deviation, $n = 3$. Standard deviations less than 1% were not shown

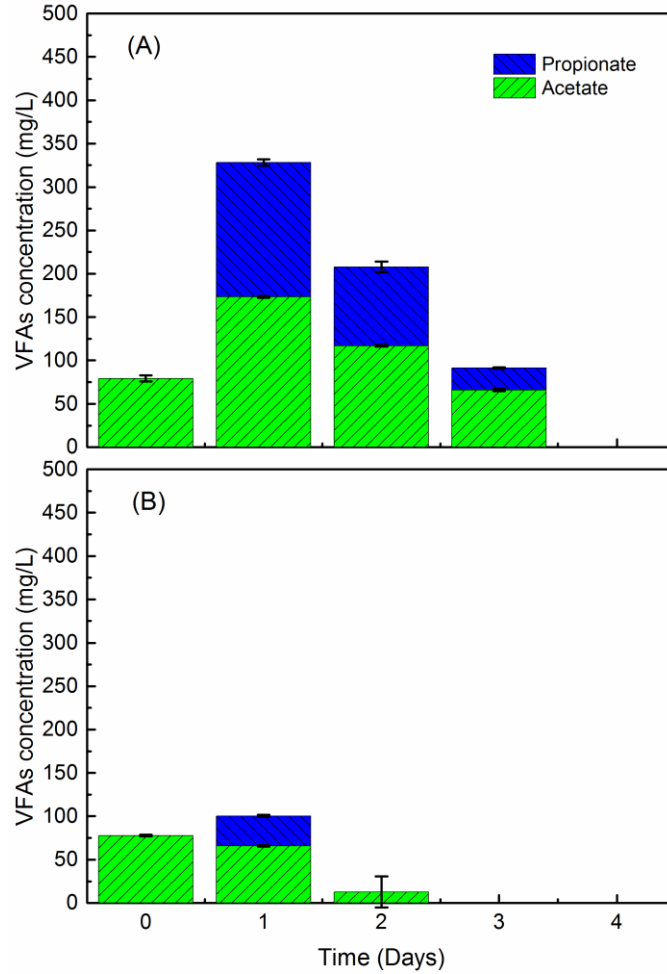


Figure 5.11. VFAs profile in R1 (A) and R2 (B) over the course of the 4-day feeding cycle under gas recirculation after 319 days of operation. Error bars represent mean values \pm one standard deviation, $n = 3$. Standard deviations less than 1% were not shown (no VFA was detected on day 4 in R1, from day 3 to 4 in R2)

In order to assess the effect of gas recirculation and CO_2 transport on CH_4 production in R1 and R2, 650 mL of CO_2 was introduced to the gas phase of R1 and R2, while both reactors were maintained under starvation (i.e., 30 and 38 days after the last feeding of R1 and R2, respectively). After two days of CO_2 dissolution and under continuous gas recirculation, 452 and 366 mL of CO_2 dissolved into the liquid phase of R1 and R2, respectively. During the first day, the volume of CO_2 decreased from 853 to 471 mL and from 811 to 404 mL in the headspace of R1 and R2, respectively. Then, the CO_2

in the R2 gas phase increased to 445 mL on the second day, which may be due to supersaturation of dissolved CO_2 . The CH_4 volume in R1 remained at the same level for two days, while it increased from 948 to 1224 mL in R2 (**Figure 5.12**). The pH and CO_2 content (CO_2 partial pressure) were about the same in R1 and R2 before and after the CO_2 addition, as well as after two days (**Table 5.7**). Externally supplied CO_2 was converted to CH_4 in R2 with the advantages of biofilm through enhanced CO_2 dissolution brought about by gas recirculation. Therefore, CO_2 mass transport is critical for biological biogas upgrading occurring in hybrid systems with both biofilm and suspended biomass.

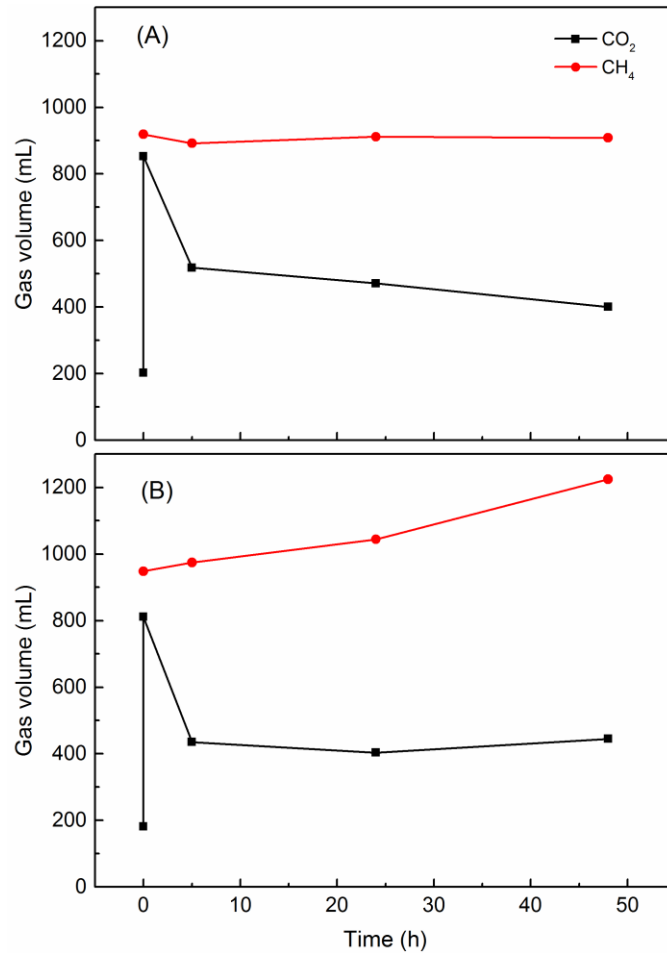


Figure 5.12. Volume of CO_2 and CH_4 over two days after CO_2 addition to the gas phase of R1 (A), and R2 (B) (Both reactors were maintained under starvation)

Table 5.7. pH and CO₂ before and after CO₂ addition to the gas phase of R1 and R2

Time (days)	R1		R2	
	pH	CO ₂ (%, v/v)	pH	CO ₂ (%, v/v)
0 (before CO ₂ addition)	7.45	13.5	7.48	14
0 (Immediately after CO ₂ addition)	-	40	-	42
2	7.21	23.6	7.12	25.5

5.3.4 Performance of AD and AD-Biofilm Systems Under Increasing Organic Loading

To assess the potential of R2 to withstand high organic loadings, on day 340 (corresponding to 16 retention times) of operation, 2X and 4X of the normal organic loading was sequentially applied to both R1 and R2.

Under double organic loading, the soluble COD at the end of the feeding cycle in R1 increased from 360 ± 5 to 945 ± 3 mg/L, while R2 consumed most of the soluble COD in two days. The pH profile had the same pattern as under normal organic loading. A CO₂ spike was observed on the second day of the 2X feeding cycle (**Figure 5.13**), which is attributed to the intensive fermentation and acidogenesis at the beginning of this feeding cycle. The concentration of VFAs increased, reaching the highest value on the second day of the feeding cycle. Similarly to the soluble COD, the VFAs concentration in R2 dropped to a low level after two days of incubation, while remained elevated in R1 (**Figure 5.14**). Under 4X organic loading, all the effects of a higher organic loading observed with a 2X feeding were also observed but at a proportionally higher level. The pH in R1 decreased sharply from 6.88 to 6.38 within two days of feeding, which required the addition of 50 mL of 1 M NaHCO₃ to adjust the pH to 6.65. The pH in R2 also dropped from 6.99 to 6.67 in the first day, but increased to 6.82 in the second day reaching a stable level of 7.02 at

the end of the feeding cycle. Most of the soluble COD was consumed in one week in R2, while it took two weeks for R1 to lower the soluble COD to a low level comparable to that in R2, which occurred after pH adjustment. A steep decrease in the CH₄ content of R1 from 68.5 to 50.5% in the first two days of the feeding cycle was observed in R1 (**Figure 5.13**), which is attributed to the transient inhibition of methanogenesis under the low pH condition. The sudden increase in the CO₂ content of the gas phase of both R1 and R2 on the second day of 4X feeding cycle is attributed to the fermentation and acidification of a large portion of substrate immediately upon feeding. Over two weeks of incubation, 3935 mL of CH₄ was produced in R2 under 4X organic loading, with most of it produced during the first week, in contrast to 3060 mL of CH₄ produced in R1 remediated by alkalinity addition (**Figure 5.15**). Therefore, the effect of the higher organic loading was far less on R2 than R1; R2 was able to recover to its stable state without any alkalinity addition, which attests to its resilience to shock organic loading. Overall, R2 as a hybrid system with both suspended biomass and biofilm had a much better capacity to withstand a shock organic loading than R1, which had only suspended biomass. Indeed, efficient COD removal in a novel anaerobic biofilm membrane bioreactor under organic loading shocks has been recently reported (Li et al., 2017).

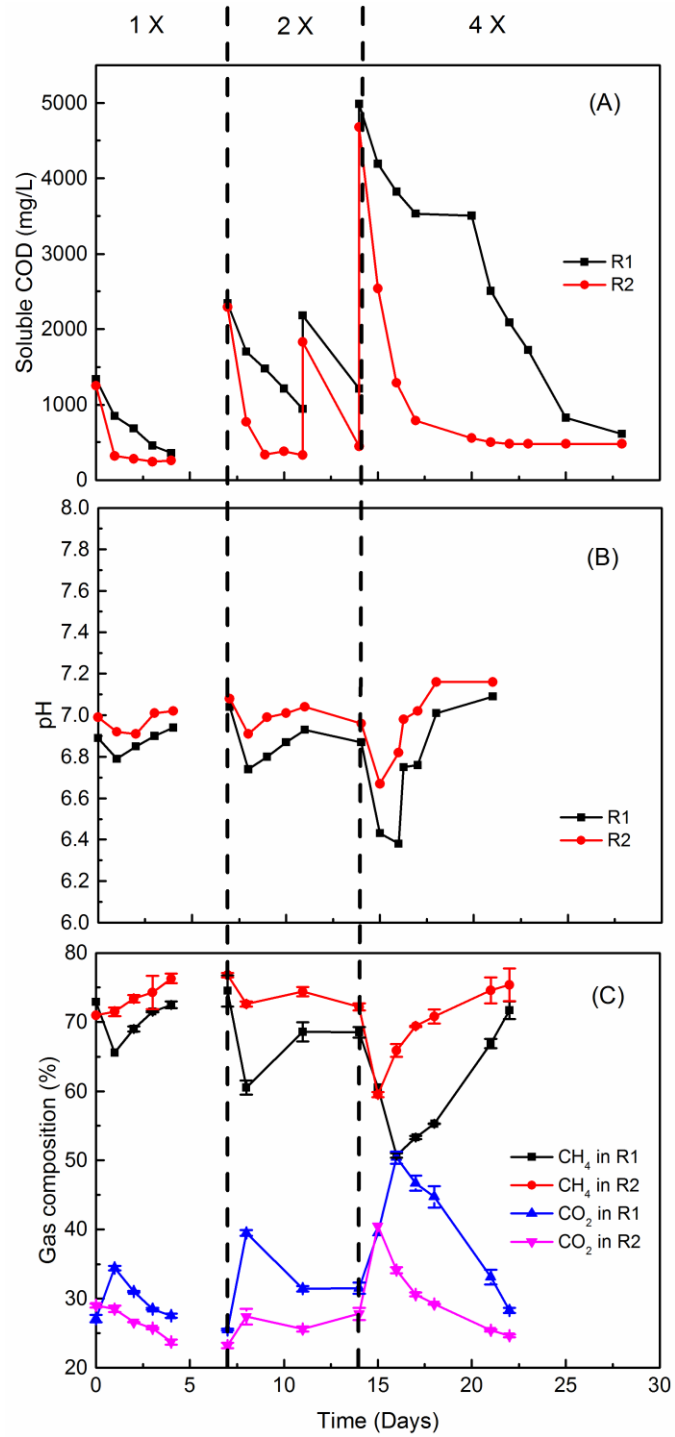


Figure 5.13. Soluble COD profile (A), pH profile (B), and CH₄ and CO₂ content (C) in R1 and R2 under 1X, 2X, and 4X organic loading condition

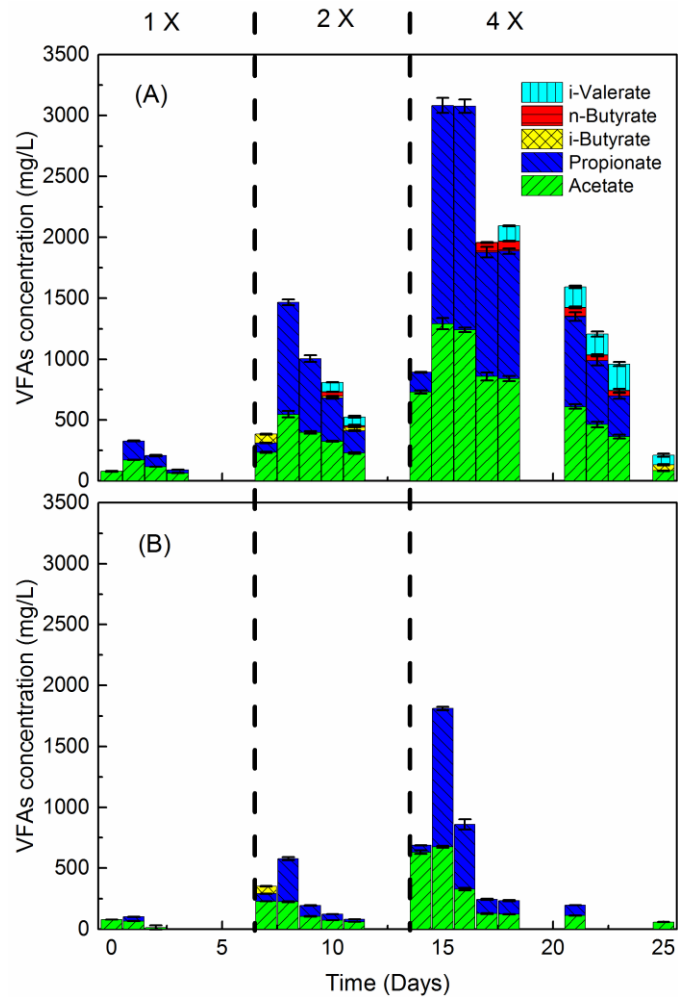


Figure 5.14. VFAs profile in R1 (A) and R2 (B) under 1X, 2X, and 4X organic loading condition

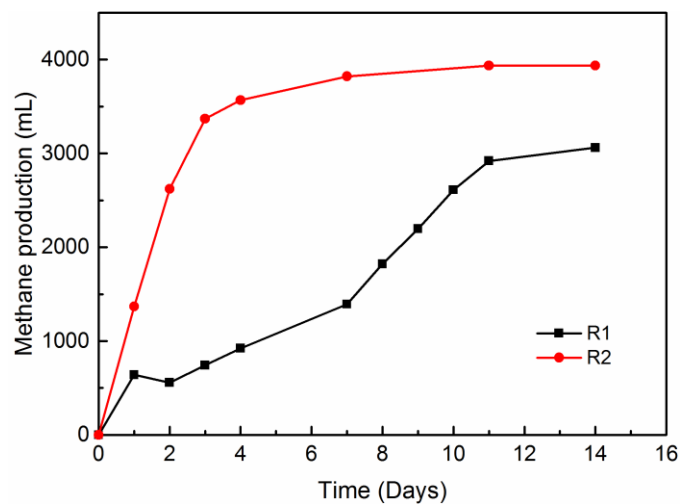


Figure 5.15. CH₄ production after 4X feeding over 14 days of incubation in R1 and R2

5.3.5 *Performance of Closed Circuit BES-AD System*

5.3.5.1 Phase I: Effect of 2.5 V on the performance of R3A

R1, R2, and R3A were developed and operated identically for 47 days. Then, 2.5 V was applied on R3A. R3A had already reached a relatively stable performance before 2.5 V was applied on day 47. With the application of 2.5 V, the pH increased sharply from 7.07 to 8.75 within 4 days, which required the addition of 8 mL of 2 N HCl on day 51 to lower the pH. The total and soluble COD at the end of a 4-day feeding cycle increased from 2310 and 210 mg/L to 3160 and 1240 mg/L, respectively. The total biogas production over a 4-day feeding cycle decreased from 1020 to 240 mL, which is consistent with the observed decrease in COD consumption (**Figure 5.16**). The total VFAs concentration at the end of the feeding cycles increased from 23 ± 0.8 to 707 ± 197 mg COD/L (**Figure 5.17**). Under the basic pH of 8.75 resulting after the application of 2.5 V, both fermentation and methanogenesis were seriously inhibited leading to the accumulation of VFAs in R3A. Propionate was the main VFA species, which accumulated in the system.

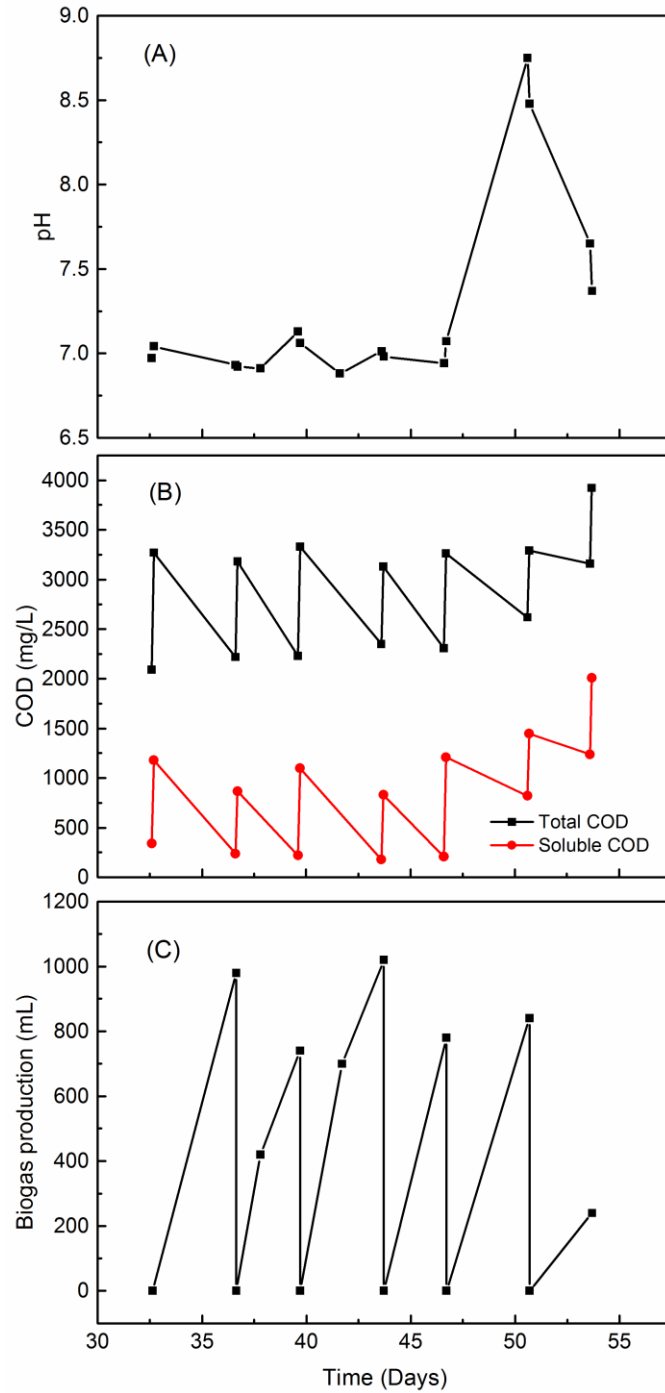


Figure 5.16. pH (A), total and soluble COD before and after feeding (B), and biogas production over 3-day and 4-day feeding cycles (C) in R3A from 33 to 54 days of operation (2.5 V applied on day 47)

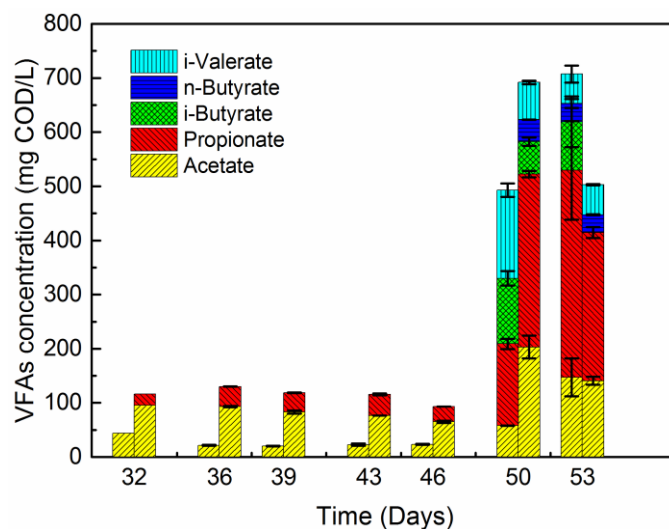


Figure 5.17. VFAs in R3A during operation from day 32 to 53 (2.5 V applied on day 47). Error bars represent mean values \pm one standard deviation, $n = 3$. Standard deviations less than 1% were not shown

Over the 4-day feeding cycle following the application of 2.5 V, the biogas CH_4 content remained at 66% and H_2 at 30% (v/v) was detected in the headspace of R3A, while the CO_2 content decreased from 34.5% to an undetectable level (**Figure 5.18**). The total gas volume in the headspace of R3A increased to 840 mL. Based on the measured gas composition and the R3A total headspace volume (720 mL), 248 mL of CO_2 were converted with H_2 produced from water electrolysis into CH_4 through hydrogenotrophic methanogenesis. At the end of the 4-day feeding cycle, 1034 mL of CH_4 and 502 mL of H_2 remained in the headspace of R3A. The net CH_4 production over these 4 days was 565 mL. The H_2 accumulation and low CH_4 production indicated a significantly hindered methanogenesis at 2.5 V, which may be attributed to the relatively high pH resulting from the continuous H_2 evolution removing protons from the medium. Moreover, the oxidizing conditions posed by the high voltage at the anode caused the stainless steel rod at the anode to undergo sacrificial corrosion. As a result, the stainless steel anode collector broke.

During the process of sacrificial corrosion, pits developed due to metal oxidation on the surface of the rod at the gas/liquid interface and the microenvironment inside the pit allowed the metal to act as an electron donor, conditions which propagated corrosion (Refaey et al., 2005). Thus, the stainless steel rod acted as a sacrificial anode during BES operation at 2.5 V, a condition previously observed for another bioelectrochemical system (Dykstra and Pavlostathis, 2017). The anodic corrosion led to iron dissolution from the stainless steel rod into the liquid phase in the BES system, which may exert a beneficial effect on VFAs oxidation during the anaerobic digestion due to the electron accepting ability of ferric iron. Zamalloa et al. (2013) observed anodic iron dissolution and precipitation of various metal salts in a bioelectrochemically-assisted anaerobic septic tank using stainless steel electrodes at 2 V applied voltage.

The initial current upon applying 2.5 V on R3A was very high at 50 mA. Then, it decreased sharply to 16 mA on the second day of the feeding cycle. Due to the anodic corrosion causing an increasing resistance, the current gradually decreased to 0 over 25 days of R3A operation at 2.5 V (**Figure 5.19**). No current increase after the feeding was observed over the cycles at 2.5 V indicating unaccountable electrons transferred through the external circuit, which may be attributed to the inhibited metabolism of the mixed cultures in the biofilm described above.

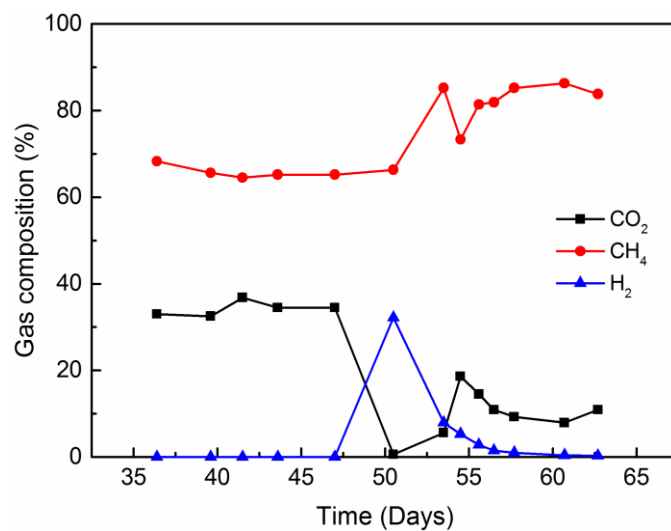


Figure 5.18. CO₂, CH₄, and H₂ in the headspace of R3A during operation from day 36 to 65 (2.5 V applied on day 47)

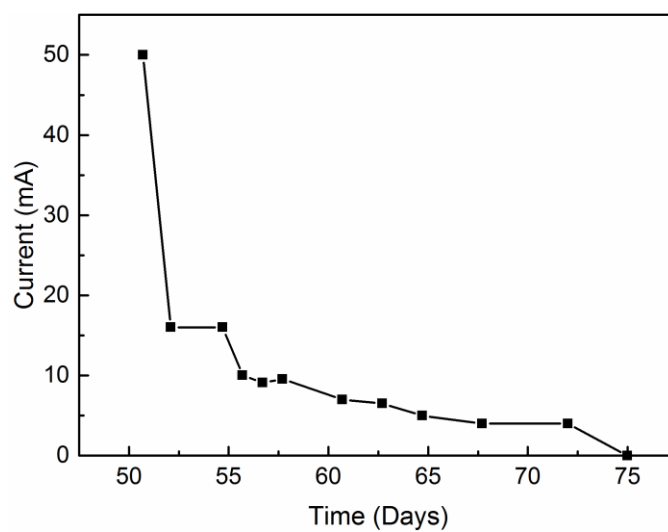


Figure 5.19. Current profile of R3A at 2.5 V (from day 51 to 75)

5.3.5.2 Phase II: Effect of a range of voltages on the performance of R3B

R3B was developed with inoculum from R1 on day 82, initially maintained similarly to R2, i.e., without any applied voltage. Then, on day 63 and 84 of operation, 0.5 V and then 1.1 V was applied on R3B, respectively. The pH remained stable at 6.9 ± 0.1 at these relatively low voltages.

The extent of soluble COD removal was 72.5, 79.8, and 79.9% under open circuit, 0.5 V, and 1.1 V operation of R3B, respectively, corresponding to a net CH₄ production was 704, 700, and 705 mL (at 22°C and 1 atm) (**Figure 5.20**). Over the three 4-day feeding cycles, the biogas CH₄ content was relatively the same at $64.4 \pm 2.1\%$. Thus, application of low voltages of 0.5 and 1.1 V could improve the soluble COD removal to a certain extent by possibly accelerating fermentation and acidogenesis resulting in the production of short-chain fatty acids, which could be easily consumed by acetoclastic methanogens. Nevertheless, no improvement in CH₄ production was observed, which implied no further total COD construction was brought about by low applied voltages.

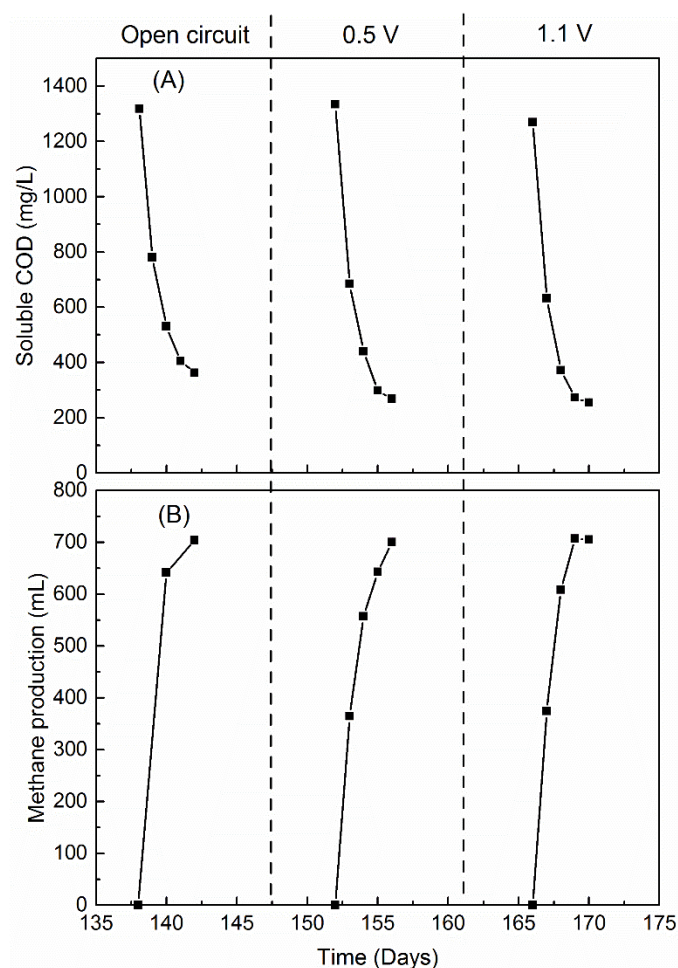


Figure 5.20. Soluble COD (A) and CH₄ production (B) over a 4-day feeding cycle of R3B under open circuit, 0.5 V, and 1.1 V

Total VFAs concentration in R3B remained at low level at the end of 4-day feeding cycles after the application of low voltages of 0.5 and 1.1 V. In contrast to R3A at 2.5 V, no evidence of VFAs accumulation was observed in R3B (**Figure 5.21**). Hence, a reasonable voltage was critical for the successful operation of BES-AD systems.

The current in R3B at 0.5 V followed the same pattern as R3A at 2.5 V: a steep decrease following a relatively high initial current. Then, the current remained stable over the feeding cycles. In contrast to 0.5 V, the current of R3B increased from 3 to 7 mA on

the second day of the second feeding cycle at 1.1 V (**Figure 5.22**). Therefore, the electrons obtained from the anodic oxidation of substrates were transferred by electroactive bacteria through the external circuit in the BES at 1.1 V. However, no CH₄ production improvement was observed, which might be attributed to the low electron capture efficiency at the cathode by methanogens and the limited electrons transferred to the cathode. In a similar study on BES-AD, applied potentials of 0.5 and 1.0 V failed to bring any improvement in CH₄ production compared to the reactor with two electrodes operated under open circuit (De Vrieze et al., 2014). Although in agreement with the result of this part of the research, the optimal voltage for a specific system to lead to an enhanced CH₄ production needs a thorough assessment. In other studies, a range of applied voltages from 0.6 to 1.0 V has been reported to be able to significantly enhance CH₄ production in BES-AD integrated systems (Liu et al., 2016a; Moreno et al., 2016; Zhang et al., 2013; Zhao et al., 2016). Therefore, a range of voltages should be investigated on a specific BES before an assertion is made.

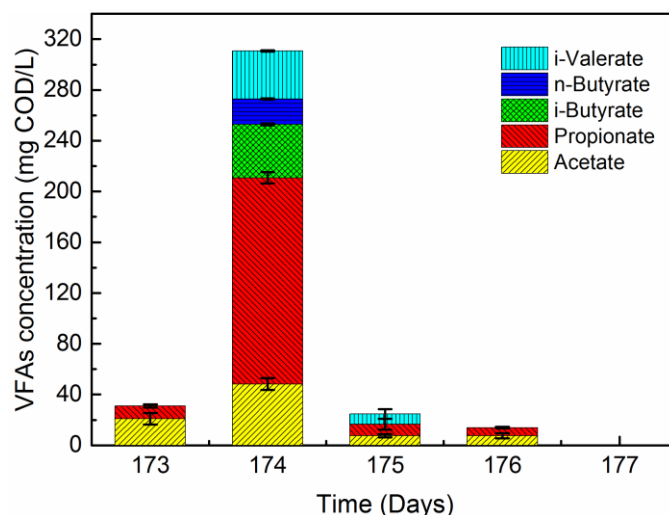


Figure 5.21. VFAs over a 4-day feeding cycle of R3B at 1.1 V. Error bars represent mean values \pm one standard deviation, $n = 3$. Standard deviations less than 1% were not shown (no VFA was detected on day 177)

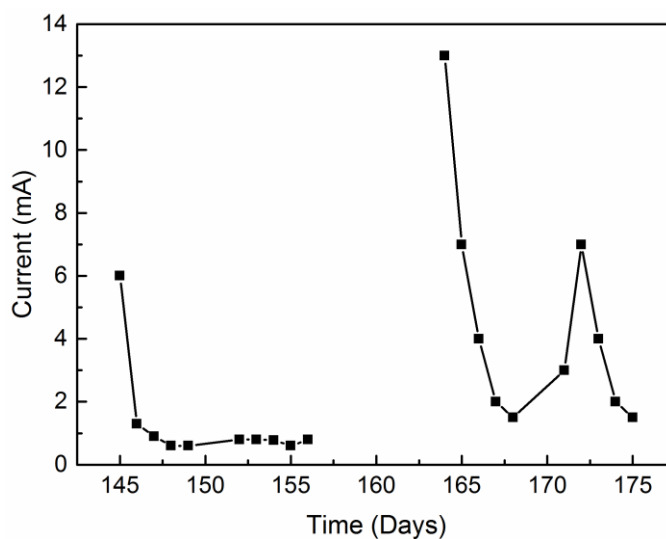


Figure 5.22. Current profile of R3B at 0.5 V (from day 145 to 156) and 1.1 V (from day 164 to 175)

To enhance the effect of electrical energy input on the biofilm attached on the bioelectrodes for the improvement in CH_4 production by electromethanogenesis, similarly to R2, suspended biomass was transferred out of R3B at 1.1 V on day 177 (95 days R3B

operation, corresponding to 4.5 retention times)(see Section 5.2.2, above). Over the 4-day feeding cycle with only biofilm in R3B, the biogas CH₄ content increased from $69.8 \pm 0.6\%$ to $74.4 \pm 1.5\%$, which is comparable to the observed CH₄ content increase in R2 when it had only biofilm biomass (see Section 5.3.2. above). In contrast to R2, the net CH₄ production over the 4-day feeding cycle decreased from 705 to 638 mL. The plausible explanation is that the biofilm in R3B at 1.1 V contained less biomass than the R2 biofilm, which led to a lower substrate consumption extent and CH₄ production after transferring out all of the suspended biomass.

Subsequently, a voltage of 2.0 and 1.6 V was applied on R3B, on day 187 and 197, respectively, both resulting in corrosion of the anode stainless steel collector after about 10 days of operation. After the anode collector broke at 2.0 V on day 197, a new stainless steel collector was immediately placed and the voltage was reduced to 1.6 V. R3B was then left unfed until day 201. When 2.0 V was applied, the pH increased from 7.19 to 7.55 over four days, requiring the addition of 4 mL 2N HCl to adjust the pH back to 7.04. After the replacement of the anode collector, the pH increased continuously to 8.08 at 1.6 V, again requiring the addition of 8 mL of 2N HCl to adjust the pH back to 7.07. At 2.0 and 1.6 V, the pH in R3B increased (**Figure 5.23**), which is similar to R3A at 2.5 V.

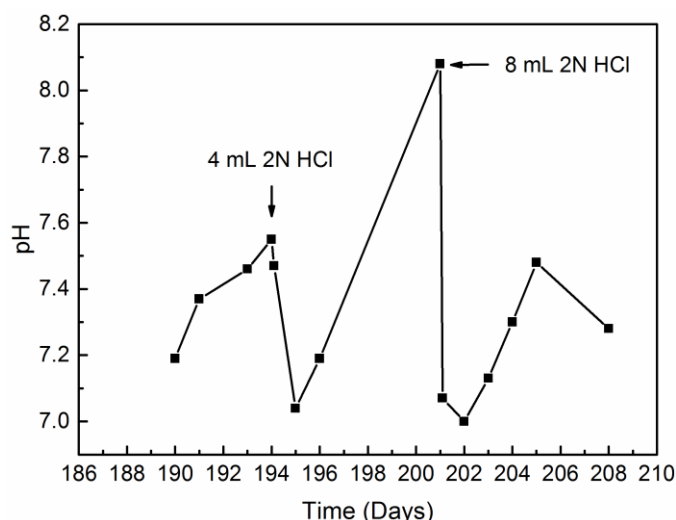


Figure 5.23. pH profile in R3B at 2.0 V (day 190 to 197) and 1.6 V (day 197 to 208)

The extent of soluble COD removal was 80.1 and 82.0% at 2.0 and 1.6 V, respectively. During the initial four days at 2.0 V, the biogas CH₄ content increased from 65 to 86%. Then, during the second 4-day feeding cycle at 2.0 V and the first 4-day cycle at 1.6 V, the biogas CH₄ content decreased during the first day then over the next three days bounced back to its former level, a pattern similar to that observed in R1 and R2 (**Figure 5.24**). H₂ at 2.2% was detected on the second day after the application of 2.0 V. No H₂ was detected over the next feeding cycles at 2.0 and 1.6 V. The net CH₄ production over the three 4-day feeding cycles at 2.0 and 1.6 V was 884, 843, and 751 mL, respectively, which was remarkably higher than that at 1.1 V (705 mL). The peak total VFAs concentration in R3B was 683 mg COD/L on the second day of the 4-day feeding cycle at 1.6 V, twice higher than at 1.1 V (**Figure 5.25**). The current in R3B increased sharply from 13 to 30 mA within two days of feeding, then dropped to its former level at the end of the feeding cycle at 2.0 V. In the second cycle at 2.0 V, the current fluctuated at a lower level.

At 1.6 V, the current was initially very high at 27 mA. After increasing to 33 mA on the second day, the current decreased to 17 mA at the end of the feeding cycle (**Figure 5.26**).

Based on the above discussed data, in spite of the observed anodic corrosion and the significant increase of pH, 2.0 V significantly enhanced both the CH₄ content and net production in R3B. The pH increase is attributed to water electrolysis occurring at relatively high voltages (see Section 5.3.5.1). The undetectable H₂ in R3B, in which water electrolysis was taking place, is attributed to the effective hydrogenotrophic methanogenesis utilizing H₂ to reduce CO₂ to CH₄ resulting in simultaneous enhanced CH₄ production as well as biogas upgrading over the first 4-day feeding cycle. However, due to the increasing internal resistance caused by the corrosion of the anode stainless steel collector, electron transfer and water electrolysis producing H₂ for biogas upgrading were interfered. Instead, the biogas CH₄ content remained at a relatively high level following the pattern attributed to the sequential nature of fermentation and methanogenesis. Voltage at 1.6 V was not high enough for water electrolysis to take place in R3B. As a result, biogas upgrading was not observed at 1.6 V. However, CH₄ production at 1.6 V was higher than that under open circuit operation, which might be attributed to the facilitated fermentation of substrates through syntrophic interactions between microbial species, with electrodes acting as electron sinks or sources in a BES (Bajracharya et al., 2016; Moscoviz et al., 2016; Schievano et al., 2016). The synergistic relation between fermenters and exoelectrogens has been demonstrated in the degradation of complex organic matter in an integrated BES-AD system (Liu et al., 2016c). Electromethanogenesis could also contribute to the enhanced CH₄ production at 2.0 and 1.6 V through directly utilizing electrons to produce CH₄, in which direct interspecies electron transfer (DIET) plays a very significant role. In

a BES-AD system, DIET has been proposed as an important pathway for enhanced CH₄ production (Zhao et al., 2015). In contrast to R3A at 2.5 V, the alkaline pH did not hinder the methanogenesis in R3B. Thus, rather than the basic pH, a voltage as high as 2.5 V was the main inhibitor of methanogenesis. The remarkable current surge in the first cycle at 2.0 V represents significant extracellular electron transfer through the external circuit promoting electromethanogenesis. Due to the corrosion, the current was limited at a lower level over the second cycle at 2.0 V. The high initial current at 1.6 V might be attributed to a higher conductivity of the medium after applying 2.0 V. A 30% higher conductivity of the sludge in a BES-AD system compared to a control digester without electrodes has been previously reported (Zhao et al., 2015). The weak initial current increase indicates declined electromethanogenesis taking place over the latter two cycles. Combining with the net CH₄ production data, the magnitude of current surge corresponds to the extent of the enhancement in CH₄ production from the BES developed in this study. Consequently, through hydrogenotrophic methanogenesis utilizing H₂ from water electrolysis and electromethanogenesis, a BES-AD system maintained within an acceptable pH and voltage range could simultaneously improve both the CH₄ production and biogas CH₄ content. Given the results of the abiotic test (see Section 4.2.1, above), 2.0 V was the optimal voltage for the BES-AD system used in this study. Additionally, because ferric iron could assume the role of electron acceptor for fermenters to enhance the oxidation of organic matter to short-chain VFAs favored by electroactive bacteria (Zhang et al., 2013) and H₂ favored by hydrogenotrophic methanogens, the dissolution of stainless steel through anodic corrosion providing ferric iron to the BES might have also benefited CH₄ production in R3B.

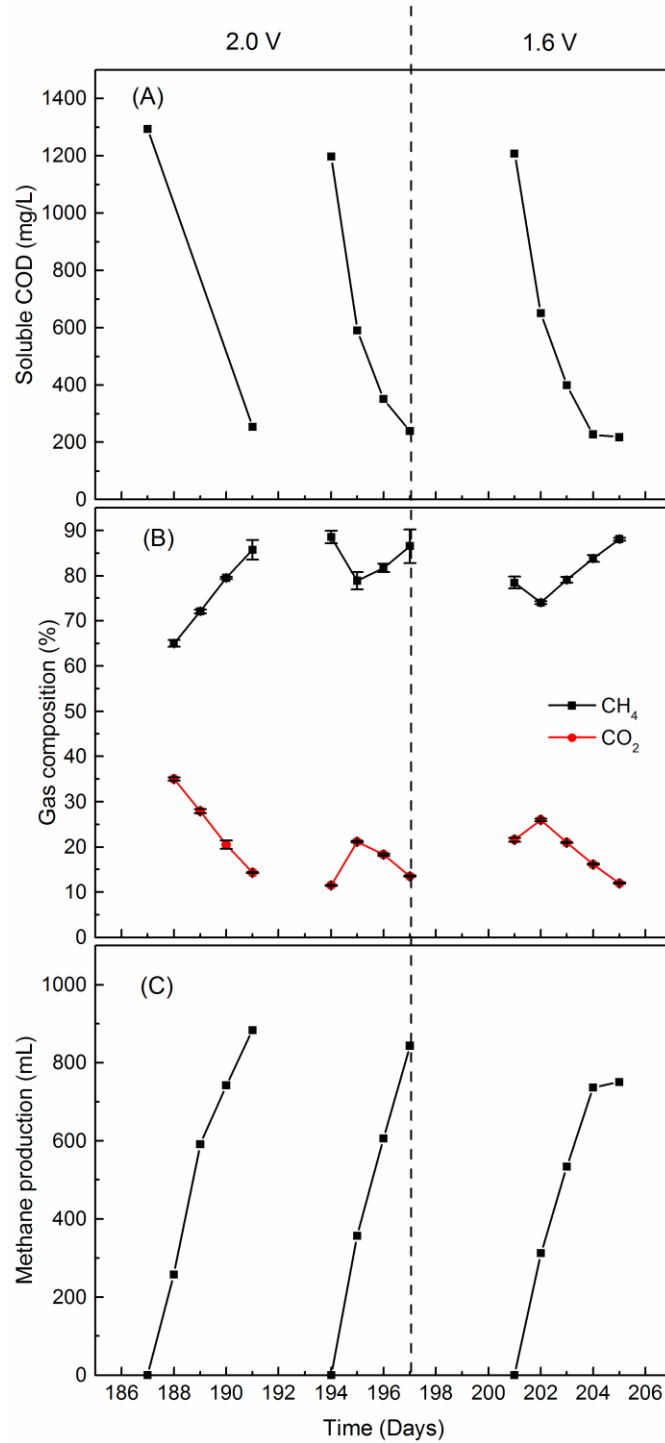


Figure 5.24. Soluble COD (A), biogas CH₄ and CO₂ content (B), and CH₄ production (C) over two 4-day feeding cycles of R3B at 2.0 V (day 187 to 197) and one 4-day cycle at 1.6 V (day 201 to 205). Error bars represent mean values \pm one standard deviation, $n = 3$. Standard deviations less than 1% were not shown

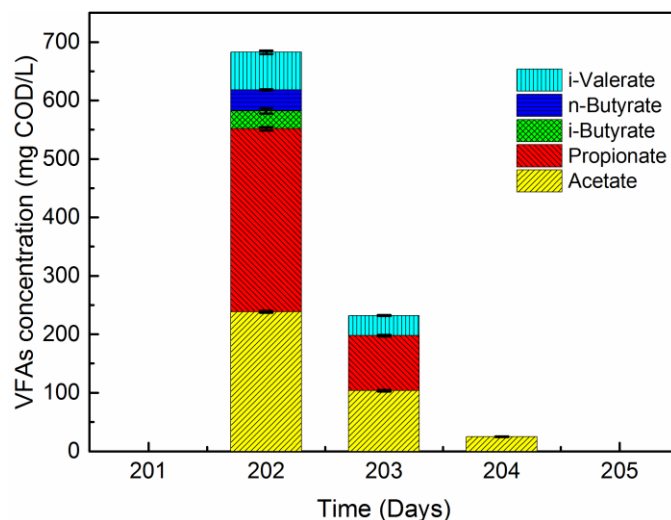


Figure 5.25. VFAs over the second 4-day feeding cycle of R3B at 1.6 V (from day 201 to 205). Error bars represent mean values \pm one standard deviation, $n = 3$. Standard deviations less than 1% were not shown (no VFA was detected on day 201 and 205)

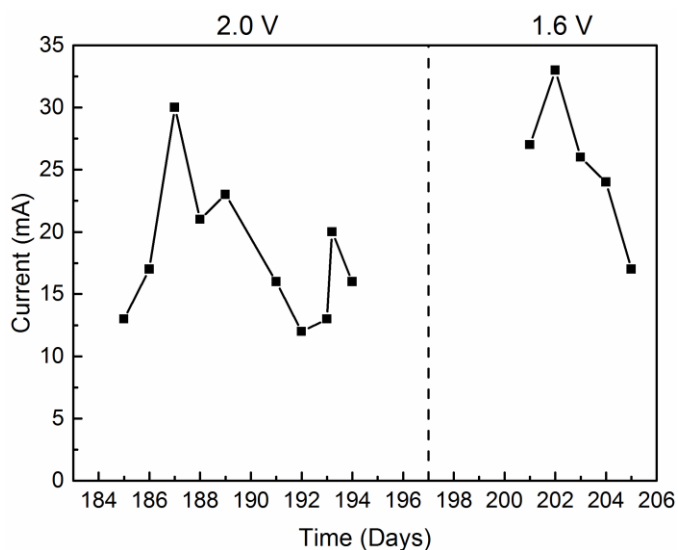


Figure 5.26. Current profile of R3B at 2.0 V (from day 185 to 194) and 1.6 V (from 201 to 205)

5.3.5.3 Phase III: Effect of a range of voltages on the performance of R3C

R3C was developed with inoculum from R1 on day 218 under closed circuit operation with 1.1 V from the very beginning (see Section 5.2.5.3, above). After about 63 days of operation (3 retention times), R3C achieved stable performance: pH, 6.95 ± 0.01 ; extent of soluble COD removal, 75.2%; biogas CH₄ content 66.5%; and a net CH₄ production over a 4-day feeding cycle, 659 mL, which is lower than that achieved by R3B at 1.1 V, applied after R3B biofilm was developed and the reactor had achieved a stable performance. The initial voltage may have negatively affected the development of biofilm on the electrodes of R3C, resulting in lower biomass in the biofilm (Werner et al., 2016), which in turn may have negatively impacted CH₄ production.

To investigate the effect of increasing voltage on CH₄ production in R3C, voltages of 1.6, 2.0, and 2.5 V were applied on R3C in which both the anode and cathode collectors were titanium rods. Titanium collectors were chosen based on the abiotic tests and physical properties of the material (see Section 4.2.1, above) to avoid the anodic corrosion took place in R3B. Operation at each voltage lasted for one week.

The pH remained stable at around 6.9 in R3C at 1.6 and 2.0 V, but decreased to 6.73 at 2.5 V. The extent of soluble COD removal was 75.1, 76.4 and 31.1% over a 4-day feeding cycle at 1.6, 2.0, and 2.5 V, respectively. Biogas production over the 4 days was 895, 965, and 775 mL in R3C at 1.6, 2.0, and 2.5 V, respectively. The CH₄ content at the end of the feeding cycles was 63.7, 67.3, and 62.5%, at 1.6, 2.0, and 2.5 V, respectively (**Figure 5.27**). Based on the CH₄ content data and the total headspace volume of R3C (1400 mL), 592, 660, and 348 mL of CH₄ was produced over the 4-day feeding cycles at 1.6, 2.0,

and 2.5 V, respectively. The relatively lower CH₄ production at 1.6 V compared to that in R3C under stable performance is attributed to biomass loss during the replacement of titanium collectors. At 2.0 V, although no obvious biogas upgrading was observed in R3C compared to R3B at 2.0 V, the net CH₄ production increased without detecting H₂ and any pH increase as a result of water electrolysis. Thus, with titanium anode and cathode collectors, instead of an enhanced CH₄ production through hydrogenotrophic methanogenesis utilizing H₂ from water electrolysis, CH₄ production might have been improved through electromethanogenesis associated with direct electron transfer to electrorophic methanogens. Although electromethanogenesis is able to convert CO₂ into CH₄ thus increasing the biogas CH₄ content, the extracellularly transfer of electrons to be used by electrorophic methanogens at the cathode is limited by several factors, such as availability and diffusion of substrates, electron transfer capacity of electroactive bacteria attached on the anode, and electron capture efficiency at the cathode. Therefore, the extent of biogas upgrading through electromethanogenesis is confined to a certain level.

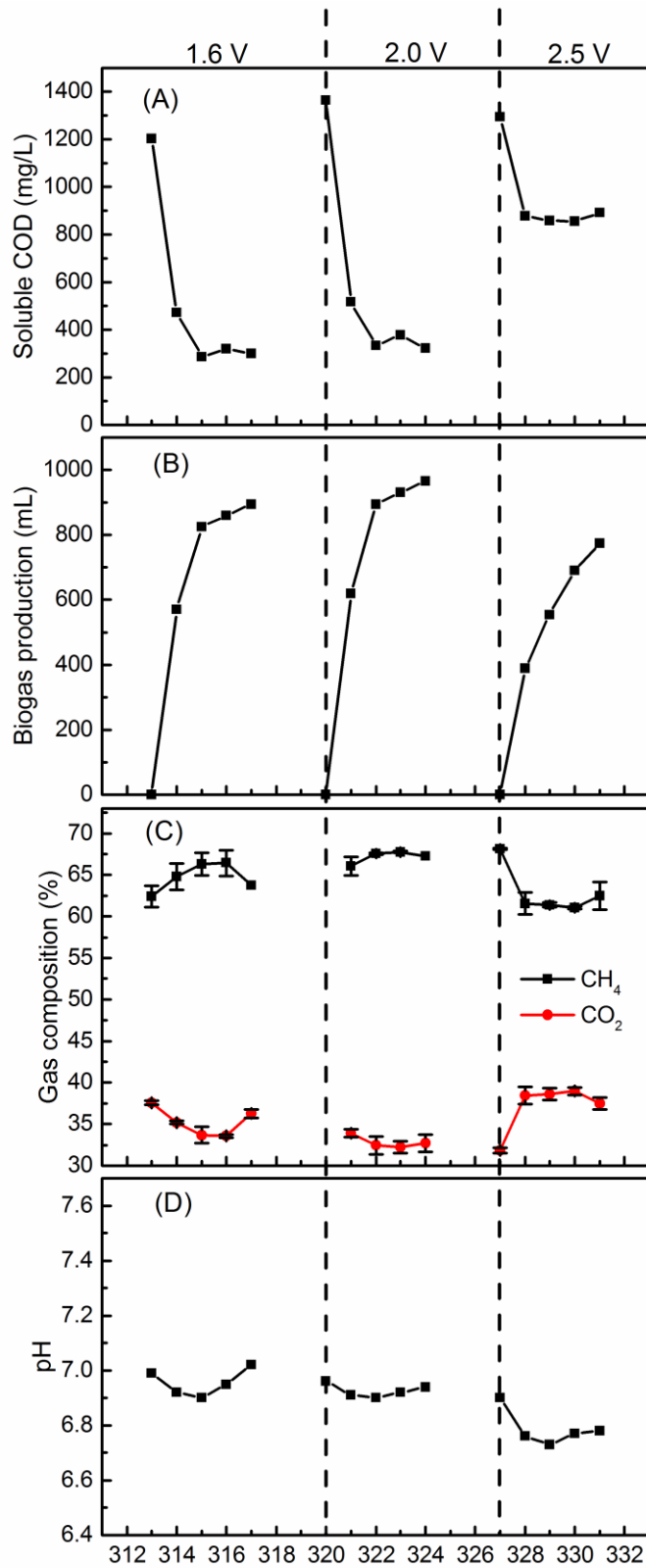


Figure 5.27. Soluble COD (A), biogas production (B), biogas CH_4 and CO_2 content (C), and pH (D) in R3C at 1.6, 2.0, and 2.5 V. Error bars represent mean values \pm one standard deviation, $n = 3$. Standard deviations less than 1% were not shown

Only acetate and propionate were detected in R3C at 1.6, 2.0, and 2.5 V. Before the application of 2.5 V, the VFAs were consumed within two days of feeding. The total VFAs concentration at the end of the feeding cycles increased from less than 100 mg COD/L to around 600 mg COD/L over the 4-day feeding cycle at 2.5 V (**Figure 5.28**). Therefore, it was again shown that 2.5 V was inhibitive to the metabolism of the mixed anaerobic microbial community developed and maintained in R3C. However, in contrast to R3A at 2.5 V, anodic corrosion and a high pH increase were not observed in R3C with titanium collectors. The oxide layer of the titanium collector protected it from corrosion, while water electrolysis was also prevented in R3C. Current surge on the second day of the feeding cycles was observed at both 1.6 and 2.0 V. The current in R3C changed irregularly at 2.5 V (**Figure 5.29**). Current surges indicate electrons transferred through the circuit at 1.6 and 2.0 V. Due to the high initial current upon applying a higher voltage, the current rise was less noticeable on the second day at 2.0 V.

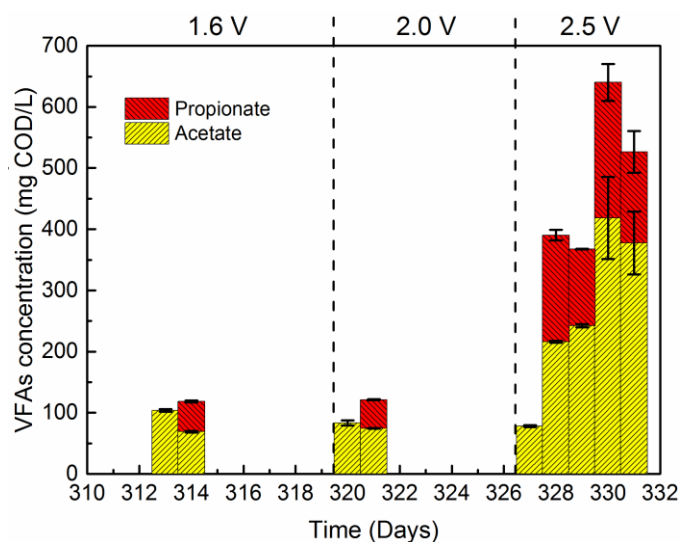


Figure 5.28. VFAs in R3C at 1.6, 2.0, and 2.5 V. Error bars represent mean values \pm one standard deviation, $n = 3$ (no VFA was detected in days 315-317 and 322-324)

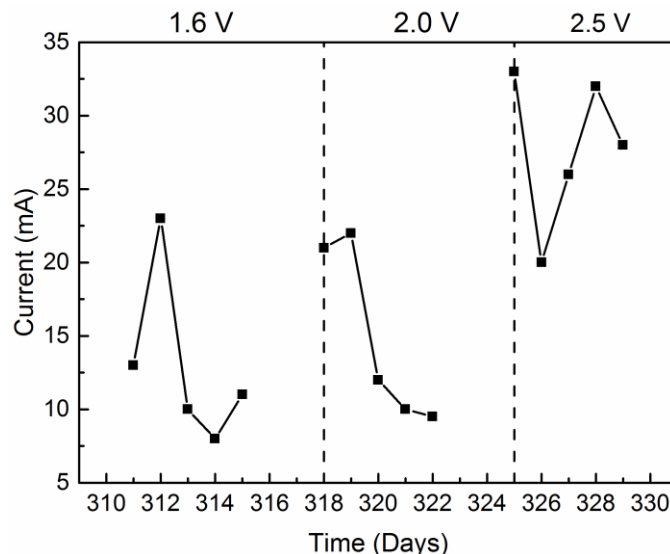


Figure 5.29. Current profile of R3C at 1.6 V (from day 311 to 315), 2.0 V (from day 318 to 322), and 2.5 V (from day 325 to 329)

In the light of the results of the abiotic tests described in Section 4.3, above, and the data summarized above, the cathode collector in R3C was replaced with stainless steel and the reactor was operated at 2.0 V. Similarly to R2, suspended biomass was transferred out of R3C, and gas recirculation, as well as 2X and 4X organic loadings were applied to R3C.

High extent of soluble COD removal was observed over the 4-day feeding cycles, even under 2X and 4X organic loading. About 80% of the soluble COD was removed within 4 days after feeding at 2X and 4X. On the 9th day after feeding at 4X, 86% of the soluble COD was removed. The total biogas production over 4 days decreased from 1180 to 710 mL after transferring out the suspended biomass, due to the loss of suspended biomass. A decrease of 40 mL in the produced total biogas at the end of the feeding cycle

under gas recirculation was observed, which is attributed to CO₂ dissolution (see Section 5.3.3, above). Given the higher organic loading, a correspondingly higher volume of biogas was produced over the feeding cycle under 2X and 4X organic loading. Due to CO₂ equilibrium between the gas and liquid phase, the biogas CO₂ content profile, representing the CO₂ partial pressure, was consistent with the pH profile corresponding to dissolved CO₂ over the feeding cycles. Nevertheless, the pattern of gas composition was mainly attributed to the sequential nature of fermentation, acidogenesis and methanogenesis. Under gas recirculation, the biogas CH₄ content increased from 68.1 ± 1 to $77.4 \pm 0.8\%$ (**Figure 5.30 A, B&C**). The pH in R3C was generally stable at around 7 before increasing the organic loading. At the 2X and 4X organic loading, the pH profile followed the pattern of first dropping during the first day, then bouncing back in the following three days. As discussed above for all other cases where higher organic loading was tested, the initial pH decrease and then increase is related to the sequential fermentation, acidogenesis, and methanogenesis for these batch-fed reactors. The exception from this pH pattern was when only biofilm was left in R3C, in which the pH did not decrease due to the efficient substrate transfer and consumption promoted by the cooperation between fermenters and methanogens residing in close affiliation in the biofilm (see Section 5.3.2, above). However, an initial acidification was observed under conditions of shock, high organic loading (**Figure 5.30 D**).

Based on the measured gas composition and the total headspace volume of R3C (1400 mL), 786, 568, 641, 1408, and 2610 mL of CH₄ was produced over the 4-day feeding cycles under I, II, III, IV, and V operational conditions, respectively. Compared to the net CH₄ production in R3C with a titanium cathode collector, the net CH₄ production over a

4-day feeding cycle increased by 19.1% in the R3C with a stainless steel cathode collector, which might be due to the elimination of competition for electrons between the titanium oxide layer and methanogens. Accordingly, more CH_4 was produced through electromethanogenesis by hydrogenotrophic methanogens directly accepting electrons from the cathode (Cheng et al., 2009). Although the net CH_4 production was improved, biogas upgrading was not observed in R3C with a titanium anode collector at 2.0 V, which might be attributed to the absence of water electrolysis and H_2 production in the biotic system. The main difference between R3C and R3B, in which both increased net CH_4 production and biogas upgrading were observed at 2.0 V, were the anodic corrosion and the alkaline pH representing water electrolysis. As described in Section 5.3.5.2 above, corrosion of the stainless steel collector at the anode might be beneficial to CH_4 production and biogas upgrading in BES-AD systems. In addition, water electrolysis continuously producing H_2 was essential to biogas upgrading in the BES-AD system used in this study. Moreover, it has been reported that hydrogenotrophic methanogenesis is responsible for most of the observed enhancement in CH_4 production in a microbial electrolysis AD reactor (Liu et al., 2016b). Besides the continuous H_2 supply, the micro-aerobic conditions created by an applied voltage of 2.8-3.5 V through water electrolysis was asserted as beneficial for the hydrolysis of a synthetic wastewater in a BES-AD system (Tartakovsky et al., 2011). Therefore, for the purpose of simultaneous CH_4 production enhancement and biogas upgrading, non-corroding anode collector material, such as graphite, capable of sustaining water electrolysis is a direction for further study.

In contrast to R2, after transferring out the suspended biomass in R3C, the net CH_4 production over the 4-day feeding cycle decreased significantly, which is attributed to the

lower biomass in the biofilm developed constantly under voltage in R3C compared to the biofilm developed before voltage was applied in R3B. Similarly to R2, under gas recirculation the CH_4 production was improved in R3C by 12.9%, which is attributed to the enhanced CO_2 transport and thus an increased concentration of HCO_3^- available for hydrogenotrophic methanogens to convert it to CH_4 (Geppert et al., 2016). The potential contribution of the voltage applied to R3C to the CH_4 production improvement under gas recirculation is discussed below in conjunction with the external CO_2 addition to R3C.

The concentration of VFAs remained low at the end of the feeding cycles, showing the resilience of R3C to shock organic loading. Acetate and propionate were the main VFA species detected during this part of the study (**Figure 5.31**). The current increased to a much higher level on the second day of the feeding cycle following transferring out the suspended biomass in R3C compared to the cycle with both suspended and biofilm biomass. Over the next feeding cycles under different operational conditions (i.e., gas recirculation, 2X and 4X organic loading), the peak current remained stable (**Figure 5.32**). Transferring out the suspended biomass excluded a possible substrate competition between fermentative bacteria in the biofilm and the suspended phase. Consequently, all oxidation of the substrates took place within the biofilm through syntrophic interactions between fermentative and electroactive bacteria transferring electrons through the external circuit to the cathode, which led to a higher current increase after feeding. The relatively stable current peak under the higher organic loading, implying a continuous electron source, indicates the finite electron transfer capacity of the bioanode. Thus, in order to promote electromethanogenesis at the cathode, an anode more compatible to the development and

attachment of exoelectroactive bacteria, thus resulting in a higher electron transfer efficiency, needs to be developed.

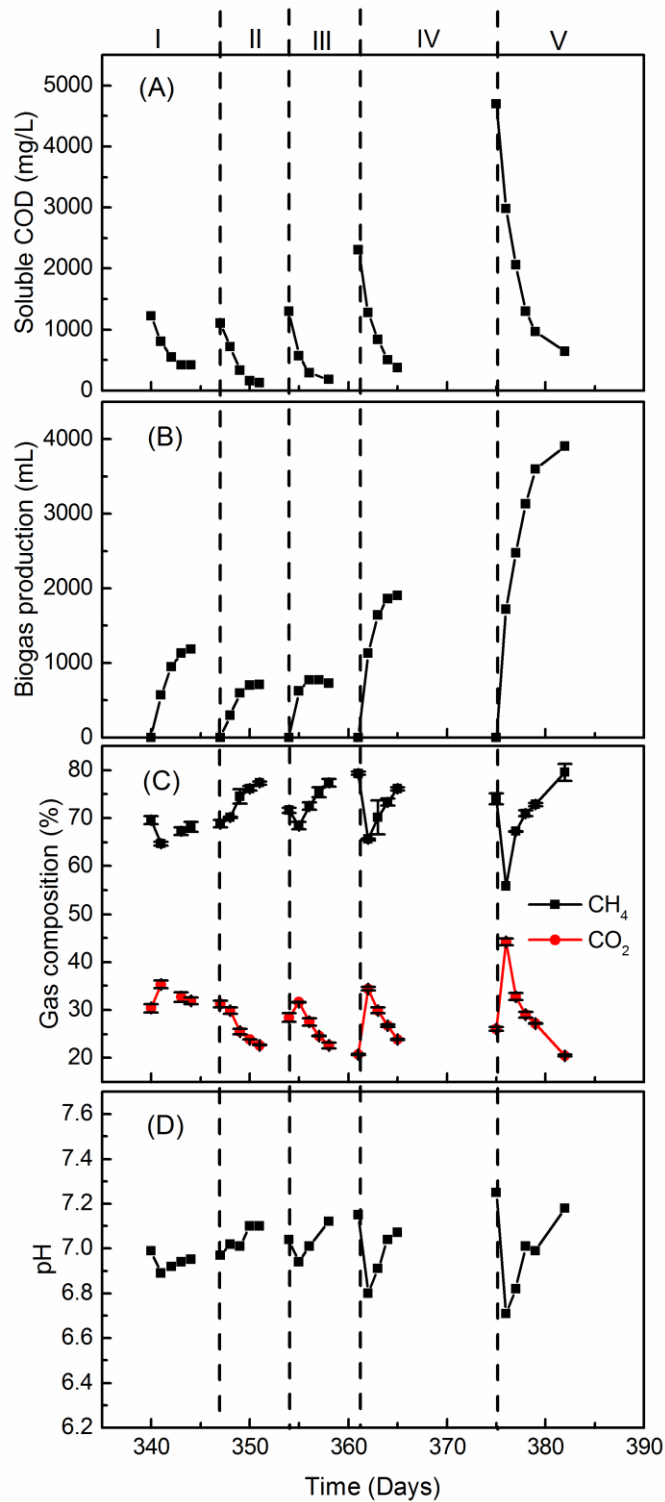


Figure 5.30. Soluble COD (A), biogas production (B), gas composition (C), and pH (D) in R3C before (I) and after (II) transferring out the suspended biomass, under gas recirculation (III), 2X (IV), and 4X (V) organic loading. Error bars represent mean values \pm one standard deviation, $n = 3$. Standard deviations less than 1% were not shown

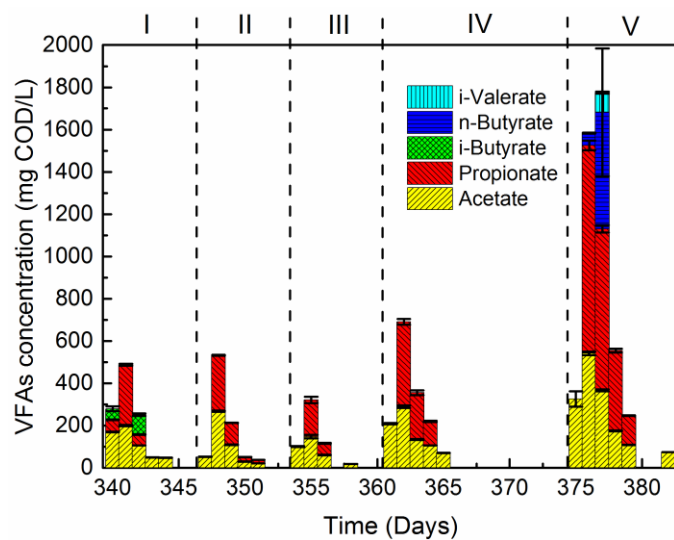


Figure 5.31. VFAs before (I) and after (II) transferring out the suspended biomass, under gas recirculation (III), 2X (IV), and 4X organic loading (V). Error bars represent mean values \pm one standard deviation, $n = 3$

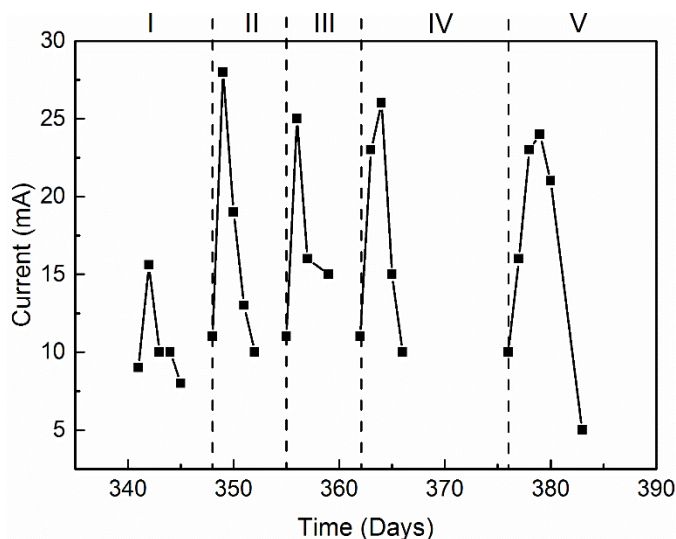


Figure 5.32. Current before (I) and after (II) transferring out the suspended biomass, under gas recirculation (III), 2X (IV), and 4X organic loading (V)

After the addition of 650 mL of CO₂ to the headspace of R3C at 2.0 V, no increase in the CH₄ volume was observed over the next two days, while 511 mL of CO₂ was dissolved (**Figure 5.33**). Thus, the external voltage did not contribute to the observed

increase in CH_4 production in R3C with enhanced CO_2 transport under gas recirculation during the operational condition III (**Figure 5.30**). R3C, unlike R2, did not produce CH_4 from the dissolved CO_2 under starvation conditions, which might be attributed to compromised biofilm in R3C developed at a constant voltage of 1.1 V. Consequently, biofilm was the essential part related to the CH_4 production improvement observed under biogas recirculation in the reactors used in this study.

Given the performance of R3C, the biofilm developed under the condition of constant voltage application was less advantageous than the biofilm developed on the electrodes of R3B before applying voltage. Accordingly, the preferable pathway to a successful start-up of BES-AD systems is applying voltage after a robust biofilm is developed on the electrodes under open circuit conditions and the system has reached a stable performance or using pre-inoculated, enriched bioelectrodes.

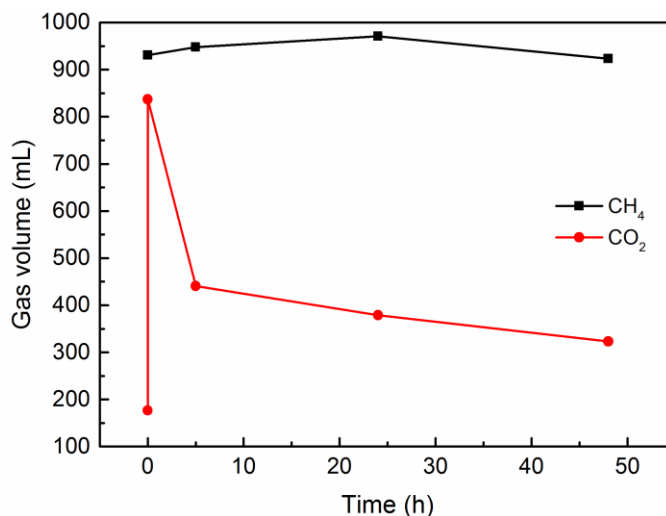


Figure 5.33. CH_4 and CO_2 in the headspace of R3C under starvation over two days after 650 mL of CO_2 was introduced to its headspace

Daily CV tests were run on R3C fed with a normal (i.e., 1X) organic loading during the initial three days of the feeding cycle and results are shown in **Figure 5.34**. On the first day, an oxidation peak at around -0.2 V was observed. Over the next two days, the peak current decreased from 0.62 mA to 0.3 mA and the peak shifted from -0.2 to -0.4 V. Due to the diminishing current and shift of the first oxidation peak, another oxidation peak at around 0.2 V was observed. A small reduction peak at around -0.6 V was observed in the initial two days (**Figure 5.34**). The initial intense oxidation peak corresponds to substrate(s) in its(their) reduced oxidation state. The oxidation peak declined over the feeding cycle along with the depletion (i.e., oxidation of the substrate(s)) by the mixed culture. The small reduction peak might represent the reduction of oxidized chemical species in the medium. As CO_2 , the end product of oxidation of organic substrates, escaped into the gas phase, a significant reduction peak was not observed. The difference between the CV tests run on abiotic (see Section 4.2.2, above) and biotic systems shows the oxidation of substrates occurring mainly during the first two days of the feeding cycle.

At the end of the operation of R3C, the biomass in the suspended phase, anode, and cathode was quantified separately through VS measurement. The VS in the suspended phase, anode, and cathode was 4.6 , 2.2 , and 1.9 g, respectively, corresponding to 53, 25, and 22% of the total biomass in R3C, respectively. However, an exchange of biomass between the suspended phase and the biofilm during the long-term operation of R3 cannot be excluded. Molecular characterization through 16S RNA sequencing of the suspended biomass, as well as anode and cathode biofilm microbial communities is pending.

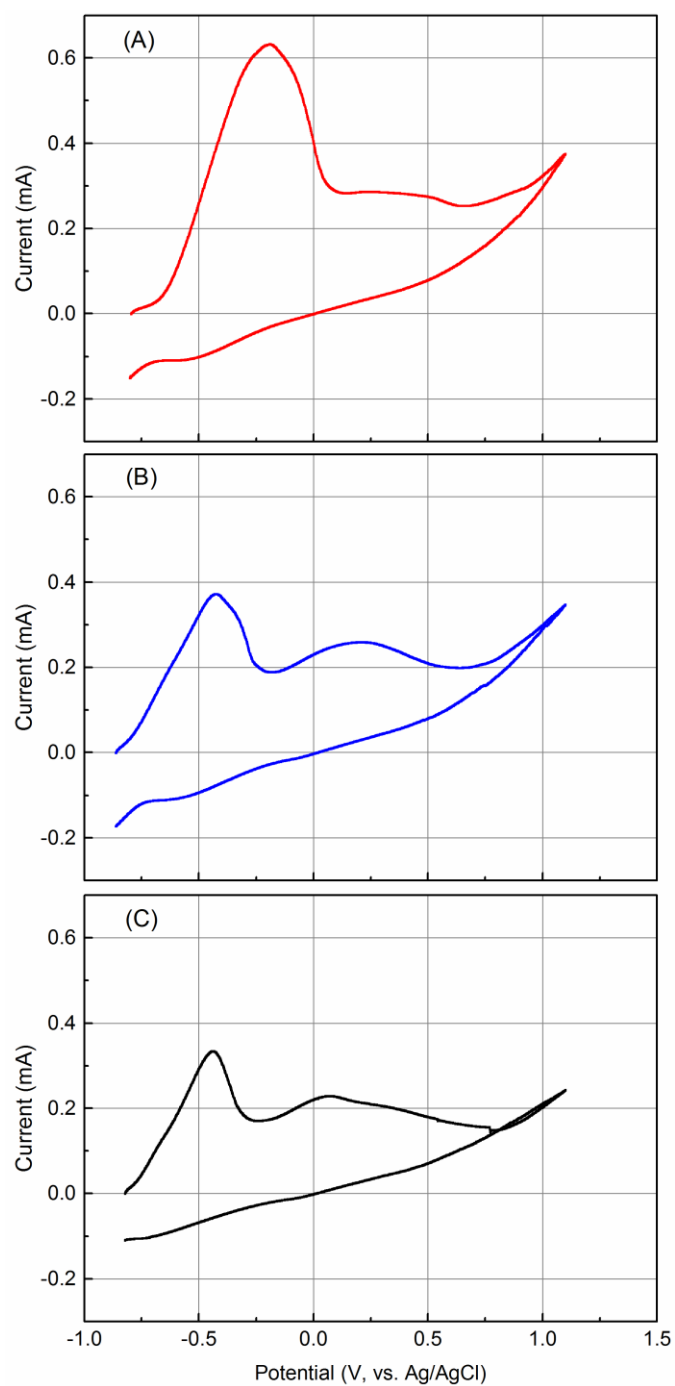


Figure 5.34. CV runs on R3C after 1 (A), 2 (B), and 3 (C) days of incubation under conditions of normal (i.e., 1X) organic loading

5.4 Summary

Biomass retention on the carbon felt electrodes is beneficial to anaerobic digestion producing CH_4 , as shown by a comparison between the performance of a conventional, suspended biomass anaerobic digester (R1) and a hybrid reactor having both suspended biomass and biofilm developed on two electrodes (R2), maintained under different operational conditions. Biofilm formation facilitates the acclimation of mesophilic mixed methanogenic cultures at room temperature and shortens the lag phase. Along with the development of the biofilm attached on the electrodes, the initial soluble COD consumption and CH_4 production rate were significantly higher in R2 than in R1. Biogas recirculation improves CO_2 dissolution and transport, which results in biogas upgrading by converting CO_2 to CH_4 . In contrast to suspended biomass anaerobic digesters, biofilm-bearing anaerobic digesters can withstand shock, high organic loadings without experiencing accumulation of VFAs leading to acidification.

The level and timing for voltage application are critical for the successful start-up and operation of a BES-AD integrated bioreactor. Water electrolysis and CV tests indicated that 2.0 V was the optimal voltage for the reactors with titanium anode collector and stainless steel cathode collector used in this study. Based on the performance of the two integrated reactors, applying voltage after the development of a robust biofilm on the electrodes under open circuit conditions and the reactor has reached a stable performance, results in a BES-AD integrated system which achieves a higher CH_4 production compared to applying the voltage from the beginning of biofilm development. Biogas upgrading and enhanced CH_4 production were achieved in a BES-AD reactor benefited from water electrolysis and electromethanogenesis. The relative portion of the extra CH_4 produced

directly from electrons and indirectly from H_2 remains unknown. Further investigation is needed to better understand the effect of iron on anaerobic digestion taking place in bioelectrochemical systems. Optimization of the bioelectrodes configuration in the BES-AD system for the simultaneous CH_4 production enhancement and biogas upgrading should be further investigated.

CHAPTER 6

CONCLUSIONS AND RECOMMENDATIONS

Biogas, as an energy-rich product resulting from the anaerobic digestion of concentrated waste streams, is a well-established and essential organic waste treatment process, receiving increasing attention in the pursuit of sustainable, carbon-neutral, zero net energy WWTP. Bioelectrochemical systems utilizing a small electrical energy input and electroactive microorganisms to convert CO_2 to CH_4 represent a promising technology for enhanced CH_4 production and in situ biogas upgrading. BES-AD integrated reactors were developed and operated in this study to: 1) improve CH_4 production from anaerobic digestion under various operational conditions; 2) demonstrate the biofilm contribution to CH_4 production; 3) investigate the significance of CO_2 mass transfer for biogas upgrading in BES; 4) investigate the relation between applied voltage and biofilm development; and 5) assess the resilience of biofilm/voltage integrated digesters to shock, high organic loading.

Carbon felt electrodes, with a high porosity and specific surface area, resulted in the development of robust biofilm. Along with the development of biofilm, the COD consumption and CH_4 production were improved in the anaerobic digester with suspended biomass and biofilm on the electrodes (R2) compared to the reactor with only suspended biomass (R1). Besides the higher rate and extent of substrate degradation, under gas recirculation conditions the biofilm brought about an increased CH_4 production from HCO_3^- made available for hydrogenotrophic methanogens within the network of

fermenters and acidogens through enhanced CO_2 mass transfer between gas and liquid phase and within the medium. The biofilm contributed significantly to high resilience of the integrated anaerobic digester to shock, high organic loading. The advantages of biofilm are attributed to the efficient interspecies substrate and electron transfer promoted by syntrophic interactions through the network of diverse microbial species in close association within the biofilm.

Given the benefits of the biofilm and the fact that voltage could be inhibitive to biofilm development, the successful start-up and operation of BES-AD integrated system was examined through applying various voltages on the integrated reactor at different times relative to biofilm development. The optimal voltage for a BES-AD system depends on many factors, such as material of the electrodes and collectors, conductivity of the medium and external circuit, and the electrodes configuration. Voltage at 2.5 V severely inhibited both fermentative bacteria and methanogens, leading to a high pH increase through triggering continuous water electrolysis. Due to the limited electron capture efficiency and low current density, low voltages in the range from 0.5 to 1.1 V failed to exert a noticeable effect on the anaerobic digestion taking place in the integrated BES-AD system. A voltage of 2.0 V, the starting point of water electrolysis occurring in the abiotic reactor, stimulated enhanced CH_4 production and biogas upgrading simultaneously in the BES-AD reactor. Nevertheless, corrosion and creation of alkaline conditions with pH values in excess of 8.0 were also observed in the system. The sacrificial corrosion of the stainless steel anode collector may introduce ferric iron acting as an electron acceptor, which could contribute to enhanced acidogenesis and H_2 evolution. Applying voltage on the reactor after biofilm is developed is preferable for a successful start-up and operation of BES-AD systems,

considering the performance of the BES-AD reactors initiated with and without voltage application. Given the results from abiotic tests and the characterization of the biotic reactors, application of 2.0 V to a reactor with titanium anode collector and stainless steel cathode collector was optimal for the integrated reactor used in this study. In BES-AD systems, voltage stimulates water electrolysis providing H_2 for hydrogenotrophic methanogenesis and promotes electromethanogenesis directly utilizing electrons and CO_2 to produce CH_4 leading to in situ biogas upgrading. Meanwhile, the biofilm attached on the conductive electrodes provides effective interspecies substrate and electron transfer through syntrophic interactions between fermenters and electroactive bacteria stimulated by the voltage, enhancing both the rate and extent of fermentation and acidogenesis, as well as interspecies H_2 transfer, ultimately resulting in enhanced CH_4 production. Consequently, the combination of voltage and electrodes capable of sustaining water electrolysis without causing sacrificial anode corrosion and exerting an inhibitory effect on the mixed microbial community would be optimal for a BES-AD system used for the simultaneous enhancement of CH_4 production and biogas upgrading.

Characterization and quantification of the BES-AD biomass, both suspended and in the biofilm through microbial community analysis is needed to better understand the relation between voltage and biofilm function. In addition to the mass transfer of gaseous CO_2 , the diffusion and transfer of substrate to and within the biofilm are of particular importance needed to be studied, especially when high strength and/or particulate substrates (e.g., municipal sludge) are used as the electron donor for BES-AD systems. Optimization of electrode configuration is needed to avoid sacrificial anode corrosion, biofouling causing clogging and limited mass transfer, and low current density attributed

to high internal resistance in the systems containing a complex medium and mixed cultures. Additional research is also needed to understand the role of zero valent iron and ferric iron in bioelectrochemically-assisted anaerobic digestion, which would result in superior biogas upgrading in situ through BES-AD technology utilizing an electron shuttle mechanism.

REFERENCES

- Andriani, D., Wresta, A., Atmaja, T.D. and Saepudin, A. (2014) A review on optimization production and upgrading biogas through CO₂ removal using various techniques. *Applied Biochemistry and Biotechnology* 172(4), 1909-1928.
- Appels, L., Baeyens, J., Degrève, J. and Dewil, R. (2008) Principles and potential of the anaerobic digestion of waste-activated sludge. *Progress in Energy and Combustion Science* 34(6), 755-781.
- Atkins, P. (1997) *Physical Chemistry*, Freeman & Company, W. H., New York.
- Azo Materials (<http://www.azom.com/article.aspx?ArticleID=1298>) (accessed on November 4th, 2016).
- Bajracharya, S., Sharma, M., Mohanakrishna, G., Dominguez Benneton, X., Strik, D.P.B.T.B., Sarma, P.M. and Pant, D. (2016) An overview on emerging bioelectrochemical systems (BESs): technology for sustainable electricity, waste remediation, resource recovery, chemical production and beyond. *Renewable Energy* 98, 153-170.
- Batstone, D.J., Keller, J., Angelidaki, I., Kalyuzhnyi, S.V., Pavlostathis, S.G., Rozzi, A., Sanders, W.T.M., Siegrist, H. and Vavilin, V.A. (2002) The IWA anaerobic digestion model No 1 (ADM1). *Water Science and Technology* 45(10), 65-73.
- Bauer, F., Hulteberg, C., Persson, T. and Tamm, D. (2013) Biogas upgrading - review of commercial technologies. SGC rapport 270, Svenskt Gastekniskt Center AB, Sweden.
- Beydilli, M. I. and Pavlostathis, S.G. (2005) Decolorization kinetics of the azo dye Reactive Red 2 under methanogenic conditions: effect of long-term culture acclimation. *Biodegradation* 16(2), 135-146.
- Bo, T., Zhu, X., Zhang, L., Tao, Y., He, X., Li, D. and Yan, Z. (2014) A new upgraded biogas production process: coupling microbial electrolysis cell and anaerobic digestion in single-chamber, barrel-shape stainless steel reactor. *Electrochemistry Communications* 45, 67-70.

- Canstein, H. V., Ogawa, J., Shimizu, S. and Lloyd, J.R. (2008) Secretion of flavins by *Shewanella* species and their role in extracellular electron transfer. *Applied and Environmental Microbiology* 74(3), 615-623.
- Chen, Y., Cheng, J.J. and Creamer, K.S. (2008) Inhibition of anaerobic digestion process: A review. *Bioresource Technology* 99(10), 4044-4064.
- Cheng, S., Xing, D., Call, D.F. and Logan, B.E. (2009) Direct biological conversion of electrical current into methane by electromethanogenesis. *Environmental Science & Technology* 43(10), 3953-3958.
- Choi, O., Um, Y. and Sang, B.-I. (2012) Butyrate production enhancement by *Clostridium tyrobutyricum* using electron mediators and a cathodic electron donor. *Biotechnology and Bioengineering* 109(10), 2494-2502.
- Clauwaert, P. and Verstraete, W. (2009) Methanogenesis in membraneless microbial electrolysis cells. *Applied Microbiology and Biotechnology* 82(5), 829-836.
- De Vrieze, J., Gildemyn, S., Arends, J.B.A., Vanwonterghem, I., Verbeken, K., Boon, N., Verstraete, W., Tyson, G.W., Hennebel, T. and Rabaey, K. (2014) Biomass retention on electrodes rather than electrical current enhances stability in anaerobic digestion. *Water Research* 54, 211-221.
- Dennis, P.G., Harnisch, F., Yeoh, Y.K., Tyson, G.W. and Rabaey, K. (2013) Dynamics of cathode-associated microbial communities and metabolite profiles in a glycerol-fed bioelectrochemical system. *Applied and Environmental Microbiology* 79(13), 4008-4014.
- Dykstra, C.M. and Pavlostathis, S.G. (2017) Evaluation of gas and carbon transport in a methanogenic bioelectrochemical system (BES). *Biotechnology and Bioengineering* 114(5), 961-969.
- Geppert, F., Liu, D., van Eerten-Jansen, M., Weidner, E., Buisman, C. and ter Heijne, A. (2016) Bioelectrochemical power-to-gas: state of the art and future perspectives. *Trends in Biotechnology* 34(11), 879-894.
- Gil-Carrera, L., Escapa, A., Mehta, P., Santoyo, G., Guiot, S.R., Morán, A. and Tartakovsky, B. (2013) Microbial electrolysis cell scale-up for combined wastewater treatment and hydrogen production. *Bioresource Technology* 130, 584-591.

- Gorby, Y.A., Yanina, S., McLean, J.S., Rosso, K.M., Moyles, D., Dohnalkova, A., Beveridge, T.J., Chang, I.S., Kim, B.H., Kim, K.S., Culley, D.E., Reed, S.B., Romine, M.F., Saffarini, D.A., Hill, E.A., Shi, L., Elias, D.A., Kennedy, D.W., Pinchuk, G., Watanabe, K., Ishii, S.i., Logan, B., Nealson, K.H. and Fredrickson, J.K. (2006) Electrically conductive bacterial nanowires produced by *Shewanella oneidensis* strain MR-1 and other microorganisms. *Proceedings of the National Academy of Sciences* 103(30), 11358-11363.
- Gregory, K.B., Bond, D.R. and Lovley, D.R. (2004) Graphite electrodes as electron donors for anaerobic respiration. *Environmental Microbiology* 6(6), 596-604.
- Gujer, W. and Zehnder, A.J.B. (1983) Conversion processes in anaerobic digestion. *Water Science and Technology* 15(8-9), 127-167.
- Henze, M., Loosdrecht, M.C.M.v., Ekama, G.A. and Brdjanovic, D. (2008) Biological wastewater treatment - principles, modeling, and design. IWA Publishing, London, UK Chapter 16.
- Ishii, S.i., Suzuki, S., Tenney, A., Norden-Krichmar, T.M., Nealson, K.H. and Bretschger, O. (2015) Microbial metabolic networks in a complex electrogenic biofilm recovered from a stimulus-induced metatranscriptomics approach. *Scientific Reports* 5, 14840.
- Jeremiasse, A.W., Hamelers, H.V.M. and Buisman, C.J.N. (2010) Microbial electrolysis cell with a microbial biocathode. *Bioelectrochemistry* 78(1), 39-43.
- Ju, D.-H., Shin, J.-H., Lee, H.-K., Kong, S.-H., Kim, J.-I. and Sang, B.-I. (2008) Effects of pH conditions on the biological conversion of carbon dioxide to methane in a hollow-fiber membrane biofilm reactor (Hf-MBfR). *Desalination* 234(1), 409-415.
- Kiely, P.D., Regan, J.M. and Logan, B.E. (2011) The electric picnic: synergistic requirements for exoelectrogenic microbial communities. *Current Opinion in Biotechnology* 22(3), 378-385.
- Kim, S., Choi, K. and Chung, J. (2013) Reduction in carbon dioxide and production of methane by biological reaction in the electronics industry. *International Journal of Hydrogen Energy* 38(8), 3488-3496.

- Kougias, P.G., Treu, L., Benavente, D.P., Boe, K., Campanaro, S. and Angelidaki, I. (2017) Ex-situ biogas upgrading and enhancement in different reactor systems. *Bioresource Technology* 225, 429-437.
- Kouzuma, A., Kato, S. and Watanabe, K. (2015) Microbial interspecies interactions: recent findings in syntrophic consortia. *Frontiers in Microbiology* 6, 477.
- López, J.C., Quijano, G., Souza, T.S.O., Estrada, J.M., Lebrero, R. and Muñoz, R. (2013) Biotechnologies for greenhouse gases (CH₄, N₂O, and CO₂) abatement: state of the art and challenges. *Applied Microbiology and Biotechnology* 97(6), 2277-2303.
- Li, N., He, L., Lu, Y.-Z., Zeng, R.J. and Sheng, G.-P. (2017) Robust performance of a novel anaerobic biofilm membrane bioreactor with mesh filter and carbon fiber (ABMBR) for low to high strength wastewater treatment. *Chemical Engineering Journal* 313, 56-64.
- Liu, D., Zhang, L., Chen, S., Buisman, C. and ter Heijne, A. (2016a) Bioelectrochemical enhancement of methane production in low temperature anaerobic digestion at 10°C. *Water Research* 99, 281-287.
- Liu, F., Rotaru, A.-E., Shrestha, P.M., Malvankar, N.S., Nevin, K.P. and Lovley, D.R. (2012) Promoting direct interspecies electron transfer with activated carbon. *Energy & Environmental Science* 5(10), 8982-8989.
- Liu, W., Cai, W., Guo, Z., Wang, L., Yang, C., Varrone, C. and Wang, A. (2016b) Microbial electrolysis contribution to anaerobic digestion of waste activated sludge, leading to accelerated methane production. *Renewable Energy* 91, 334-339.
- Liu, W., He, Z., Yang, C., Zhou, A., Guo, Z., Liang, B., Varrone, C. and Wang, A.-J. (2016c) Microbial network for waste activated sludge cascade utilization in an integrated system of microbial electrolysis and anaerobic fermentation. *Biotechnology for Biofuels* 9(1), 1-15.
- Logan, B.E. and Elimelech, M. (2012) Membrane-based processes for sustainable power generation using water. *Nature* 488(7411), 313-319.

- Logan, B.E., Hamelers, B., Rozendal, R., Schröder, U., Keller, J., Freguia, S., Aelterman, P., Verstraete, W. and Rabaey, K. (2006) Microbial fuel cells: methodology and technology. *Environmental Science & Technology* 40(17), 5181-5192.
- Logan, B.E. and Rabaey, K. (2012) Conversion of wastes into bioelectricity and chemicals by using microbial electrochemical technologies. *Science* 337(6095), 686-690.
- Lovley, D.R. and Phillips, E.J.P. (1988) Novel mode of microbial energy metabolism: organic carbon oxidation coupled to dissimilatory reduction of iron or manganese. *Applied and Environmental Microbiology* 54(6), 1472-1480.
- Marshall, C.W., Ross, D.E., Fichot, E.B., Norman, R.S. and May, H.D. (2013) Long-term operation of microbial electrosynthesis systems improves acetate production by autotrophic microbiomes. *Environmental Science & Technology* 47(11), 6023-6029.
- Marsili, E., Baron, D.B., Shikhare, I.D., Coursolle, D., Gralnick, J.A. and Bond, D.R. (2008) *Shewanella* secretes flavins that mediate extracellular electron transfer. *Proceedings of the National Academy of Sciences* 105(10), 3968-3973.
- McAllister, S., Chen, J.Y. and Fernandez-Pello, A.C. (2013) *Fundamentals of Combustion Processes*, Springer New York.
- Misiti, T., Tandukar, M., Tezel, U. and Pavlostathis, S.G. (2013) Inhibition and biotransformation potential of naphthenic acids under different electron accepting conditions. *Water Research* 47(1), 406-418.
- Moreno, R., San-Martín, M.I., Escapa, A. and Morán, A. (2016) Domestic wastewater treatment in parallel with methane production in a microbial electrolysis cell. *Renewable Energy* 93, 442-448.
- Morita, M., Malvankar, N.S., Franks, A.E., Summers, Z.M., Giloteaux, L., Rotaru, A.E., Rotaru, C. and Lovley, D.R. (2011) Potential for direct interspecies electron transfer in methanogenic wastewater digester aggregates. *mBio* 2(4), e00159-00111.
- Moscoviz, R., Toledo-Alarcón, J., Trably, E. and Bernet, N. (2016) Electro-fermentation: how to drive fermentation using electrochemical systems. *Trends in Biotechnology* 34(11), 856-865.

- Muñoz, R., Meier, L., Diaz, I. and Jeison, D. (2015) A review on the state-of-the-art of physical/chemical and biological technologies for biogas upgrading. *Reviews in Environmental Science and Bio/Technology* 14(4), 727-759.
- Myers, C.R. and Nealson, K.H. (1988) Bacterial manganese reduction and growth with manganese oxide as the sole electron acceptor. *Science* 240(4857), 1319.
- Myers, J.M. and Myers, C.R. (2001) Role for outer membrane cytochromes OmcA and OmcB of *Shewanella putrefaciens* MR-1 in reduction of manganese dioxide. *Applied and Environmental Microbiology* 67(1), 260-269.
- Nevin, K.P., Woodard, T.L., Franks, A.E., Summers, Z.M. and Lovley, D.R. (2010) Microbial electrosynthesis: feeding microbes electricity to convert carbon dioxide and water to multicarbon extracellular organic compounds. *mBio* 1(2), e00103-10.
- Parameswaran, P., Torres, C.I., Lee, H. S., Krajmalnik-Brown, R. and Rittmann, B.E. (2009) Syntrophic interactions among anode respiring bacteria (ARB) and Non-ARB in a biofilm anode: electron balances. *Biotechnology and Bioengineering* 103(3), 513-523.
- Patterson, T., Esteves, S., Dinsdale, R. and Guwy, A. (2011) An evaluation of the policy and techno-economic factors affecting the potential for biogas upgrading for transport fuel use in the UK. *Energy Policy* 39(3), 1806-1816.
- Pavlostathis, S.G. (2011) *Comprehensive Biotechnology (Second Edition)*, pp. 385-397, Academic Press, Burlington. Pavlostathis, S. G. 2011. Kinetics and Modeling of Anaerobic Treatment and Biotransformation Process. In *Comprehensive Biotechnology*, 2nd Edition, M. Moo-Young (Editor-in-Chief); Volume 6: Environmental Biotechnology and Safety, S. Agathos (Ed.), Elsevier, Amsterdam, The Netherlands.
- Pavlostathis, S.G. and Giraldo-Gomez, E. (1991) Kinetics of anaerobic treatment: a critical review. *Critical Reviews in Environmental Control* 21(5-6), 411-490.
- Pham, T.H., Boon, N., Aelterman, P., Clauwaert, P., De Schamphelaire, L., Vanhaecke, L., De Maeyer, K., Höfte, M., Verstraete, W. and Rabaey, K. (2008) Metabolites produced by *Pseudomonas* sp. enable a Gram-positive bacterium to achieve extracellular electron transfer. *Applied Microbiology and Biotechnology* 77(5), 1119-1129.

- Premier, G.C., Kim, J.R., Massanet-Nicolau, J., Kyazze, G., Esteves, S.R.R., Penumathsa, B.K.V., Rodríguez, J., Maddy, J., Dinsdale, R.M. and Guwy, A.J. (2013) Integration of biohydrogen, biomethane and bioelectrochemical systems. *Renewable Energy* 49, 188-192.
- Refaey, S.A.M., Taha, F. and El-Malak, A.M.A. (2005) Corrosion and inhibition of stainless steel pitting corrosion in alkaline medium and the effect of Cl^- and Br^- anions. *Applied Surface Science* 242(1–2), 114-120.
- Reguera, G., McCarthy, K. D., Mehta, T., Nicoll, J. S., Tuominen, M. T., Lovley, D. R. (2005) Extracellular electron transfer via microbial nanowires. *Nature* 435, 1098-1101.
- Rittmann, B.E. and McCarty, P.L. (2001) *Environmental Biotechnology: Principles and Applications*, McGraw-Hill, Boston.
- Rotaru, A.-E., Shrestha, P.M., Liu, F., Markovaite, B., Chen, S., Nevin, K. and Lovley, D. (2014) Direct interspecies electron transfer between *Geobacter metallireducens* and *Methanosarcina barkeri*. *Applied and Environmental Microbiology* 80(15), 4599-4605.
- Rozendal, R.A., Jeremiasse, A.W., Hamelers, H.V.M. and Buisman, C.J.N. (2008) Hydrogen production with a microbial biocathode. *Environmental Science & Technology* 42(2), 629-634.
- Schievano, A., Pepé Sciarria, T., Vanbroekhoven, K., De Wever, H., Puig, S., Andersen, S.J., Rabaey, K. and Pant, D. (2016) Electro-fermentation – merging electrochemistry with fermentation in industrial applications. *Trends in Biotechnology* 34(11), 866-878.
- Steinbusch, K.J.J., Hamelers, H.V.M., Schaap, J.D., Kampman, C. and Buisman, C.J.N. (2010) Bioelectrochemical ethanol production through mediated acetate reduction by mixed cultures. *Environmental Science & Technology* 44(1), 513-517.
- Tartakovsky, B., Mehta, P., Bourque, J.-S. and Guiot, S.R. (2011) Electrolysis-enhanced anaerobic digestion of wastewater. *Bioresource Technology* 102, 5685-5691.

- Tezel, U., Tandukar, M. and Pavlostathis, S.G. (2011) Comprehensive Biotechnology (Second Edition), pp. 447-461, Academic Press, Burlington. Tezel, U., M Tandukar, and S. G. Pavlostathis. 2011. Anaerobic Biotreatment of Municipal Sewage Sludge. In Comprehensive Biotechnology, 2nd Edition, M Moo-Young (Editor-in-Chief); Volume 6: Environmental Biotechnology and safety, S. Agathos (Ed.), Elsevier, Amsterdam, The Netherlands.
- Thran, D., Persson, T., Daniel-Gromke, J., Ponitka, J., Seiffert, M., Baldwin, J., Kranzl, L., Schipfer, F., Matzenberger, J., Devriendt, N., Dumont, M., Dahl, J. and Bochmann, G. (2014) Biomethane: status and factors affecting market development and trade. IEA Task 40 and Task 37 Joint Study <http://publications.jrc.ec.europa.eu/repository/handle/JRC91580>.
- Tock, L., Gassner, M. and Maréchal, F. (2010) Thermochemical production of liquid fuels from biomass: Thermo-economic modeling, process design and process integration analysis. Biomass and Bioenergy 34(12), 1838-1854.
- Tugtas, A.E. (2007) Effect of Nitrate Reduction on the Methanogenic Fermentation: Process interactions and Modeling. Ph.D. Dissertation, Georgia Institute of Technology.
- Van Eerten-Jansen, M.C.A.A., Heijne, A.T., Buisman, C.J.N. and Hamelers, H.V.M. (2012) Microbial electrolysis cells for production of methane from CO₂: long-term performance and perspectives. International Journal of Energy Research 36(6), 809-819.
- Villano, M., Scardala, S., Aulenta, F. and Majone, M. (2013) Carbon and nitrogen removal and enhanced methane production in a microbial electrolysis cell. Bioresource Technology 130, 366-371.
- Werner, C.M., Katuri, K.P., Hari, A.R., Chen, W., Lai, Z., Logan, B.E., Amy, G.L. and Saikaly, P.E. (2016) Graphene-coated hollow fiber membrane as the cathode in anaerobic electrochemical membrane bioreactors – effect of configuration and applied voltage on performance and membrane fouling. Environmental Science & Technology 50(8), 4439-4447.
- Xafenias, N., Anunobi, M.O. and Mapelli, V. (2015) Electrochemical startup increases 1,3-propanediol titers in mixed-culture glycerol fermentations. Process Biochemistry 50(10), 1499-1508.

- Zamalloa, C., Arends, J.B.A., Boon, N. and Verstraete, W. (2013) Performance of a lab-scale bio-electrochemical assisted septic tank for the anaerobic treatment of black water. *New Biotechnology* 30(5), 573-580.
- Zeng, X., Borole, A.P. and Pavlostathis, S.G. (2015) Biotransformation of furanic and phenolic compounds with hydrogen gas production in a microbial electrolysis cell. *Environmental Science & Technology* 49(22), 13667-13675.
- Zhang, J., Zhang, Y., Quan, X. and Chen, S. (2013) Effects of ferric iron on the anaerobic treatment and microbial biodiversity in a coupled microbial electrolysis cell (MEC) – Anaerobic reactor. *Water Research* 47(15), 5719-5728.
- Zhao, Z., Zhang, Y., Holmes, D.E., Dang, Y., Woodard, T.L., Nevin, K.P. and Lovley, D.R. (2016) Potential enhancement of direct interspecies electron transfer for syntrophic metabolism of propionate and butyrate with biochar in up-flow anaerobic sludge blanket reactors. *Bioresource Technology* 209, 148-156.
- Zhao, Z., Zhang, Y., Wang, L. and Quan, X. (2015) Potential for direct interspecies electron transfer in an electric-anaerobic system to increase methane production from sludge digestion. *Scientific Reports* 5, 11094.
- Zhou, M., Freguia, S., Dennis, P.G., Keller, J. and Rabaey, K. (2015) Development of bioelectrocatalytic activity stimulates mixed-culture reduction of glycerol in a bioelectrochemical system. *Microbial Biotechnology* 8(3), 483-489.